

WETTING FILMS STABILIZED
BY BLOCK-COPOLYMERS

Promotor: Prof. Dr. M.A. Cohen Stuart,
hoogleraar fysische chemie
met bijzondere aandacht voor de kolloidchemie

Copromotoren Dr. ir. N.A. M. Besseling
universitair docent
bij de leerstoelgroep fysische chemie en kolloidkunde
Dr. ir. L. K. Koopal
universitair docent
bij de leerstoelgroep fysische chemie en kolloidkunde

Samenstelling promotiecommissie:

Prof. Dr. ir. R.M. Boom (Wageningen Universiteit)

Prof. Dr. B. Mulder (AMOLF, Wageningen Universiteit)

Prof. Dr. F. Mugele (Universiteit Twente)

Dr. J. Laven (Technische Universiteit Eindhoven)

Dit onderzoek is uitgevoerd binnen de onderzoekschool PTN

WETTING FILMS STABILIZED
BY BLOCK-COPOLYMERS

Olga V. Eliseeva

Proefschrift
Ter verkrijging van de graad van doctor
op gezag van de rector magnificus
van Wageningen Universiteit,
prof. dr. M. J. Kropff
in het openbaar te verdedigen
op maandag 2 oktober 2006
des namiddags te 13.30 in de Aula

Olga V. Eliseeva

Wetting films stabilized by block copolymers

Thesis Wageningen University, the Netherlands 2006

ISBN 90-8504-494-4

A word is dead
When it is said,
Some say...
I say it just
Begins to live
That day...

Мысль умирает,
говорят,
Лишь произнесена...
А я скажу,
Что в этот миг
Рождается она...

Emily Dickinson

to Alexey Pamyatnykh
Алексею Памятных посвящается

Contents

Chapter 1 General introduction.....	4
1.1 Wetting Films.....	4
1.2 Motivation: wetting films in paint systems.....	4
1.3 Choice of the system and aim of the thesis.....	5
1.4 Non-ionic triblock copolymer surfactants	6
1.6 Disjoining pressure	6
1.7 Interaction forces in wetting films	7
1.7.1 Long-range forces	7
1.7.2 Short-range forces.....	8
1.7.3 Surface forces coming from adsorbed layers of polymeric surfactants	8
1.8 Film thickness measurements: thin film balance technique	9
1.9 Film drainage	12
1.9.1 Drainage of foam films	13
1.9.2 Drainage of wetting films	13
1.10 Foam films stabilized by non-ionic surfactants: surprising salt effect.	14
1.11 Wetting films stabilized by non-ionic surfactants	15
1.12 Outline of the thesis	15
References.....	16
Chapter 2 Polyethylene oxide-polypropylene oxide ABA copolymer in aqueous solution, at interfaces, and in wetting films	19
1 Introduction.....	20
1.1 Solution behaviour of block copolymer surfactants	20
1.2 Block copolymer surfactants at the air-water interface	22
1.3 Block copolymer surfactants at the silica-water interface	22
1.4 Foam and wetting thin films stabilized by block copolymer surfactants.....	23
2 Materials and Methods.....	24
2.1 Materials	24
2.2 Light scattering	24
2.3 The surface tension	25
2.4 Ellipsometry.....	25
2.5 Thin liquid film pressure balance (TFB)	27
3 Results.....	28
3.1 Static and dynamic light scattering	28
3.2 Adsorption of the surfactant at the air-water interface	30
3.3 Adsorption of the surfactant at the silica-water interface	32
3.4 Disjoining pressure isotherms.....	33
4 Discussion	35
4.1 Solution properties of the surfactant.....	35
4.2 Adsorption of the surfactant at the air-water interface	36
4.3 Adsorption of the surfactant at the silica-water interface	36
4.4 Interaction forces within the film stabilized by the surfactant.....	37
Conclusions.....	40

References.....	42
Chapter 3 Thinning of wetting films stabilized by a non-ionic surfactant	44
1 Introduction.....	45
2 Experimental section.....	45
2.1. Materials	45
2.2. Thin Film Balance (TFB).....	46
2.3 Ellipsometry.....	47
2.4 Ellipsometric imaging.....	48
3 Results.....	48
3.1 Surfactant F127 at interfaces of the film and in aqueous solutions	48
3.2 Thinning of wetting films	50
4 Discussion.....	54
4.1 The possible role of micelle-like aggregates in the thinning phenomena.....	54
4.2 Local and transient increase of the concentration of the surfactant within the films	55
4.3 Gel formation within the film	55
5 Summary and Remarks for futures study.....	56
Chapter 4 Equilibrium and transient thicknesses of wetting films	58
1 Introduction.....	59
2 Experimental.....	59
2.1 Materials	59
2.2 Preparation and saturation of silica.....	60
2.3 Formation and measurements of wetting films.....	60
2.3.1 Thin Film Balance (TFB).....	60
2.3.2 Formation and manipulation of wetting film	60
2.3.3 Measurements of the thickness of wetting films.....	61
2.4 Ellipsometric measurements of layers adsorbed at the silica-water interface. ...	62
2.5 Drop Tensiometry	63
3 Results and Discussion	63
3.1 NaCl effect on the kinetics of adsorption of surfactant at solid-water and air- water interfaces	63
3.2 Kinetics of wetting films: transient and equilibrium thicknesses	65
3.3 Comparison between final thicknesses of films attained with or without transient maxima.....	68
References.....	71
Chapter 5 Effects of pH and additives on aqueous wetting films stabilized by a triblock copolymer	72
1 Introduction.....	73
2 Experimental.....	74
2.1 Materials	74
2.2 Thin Film Balance (TFB).....	74
2.3 Ellipsometry.....	75
2.4 Static Light scattering	76
2.5 Contact angle goniometry	76
3 Result and discussion.....	76
3.1 Effects of additives on the properties of the surfactant in aqueous solutions	76

3.2 Effects of pH and additives on the adsorption of the surfactant at silica-water and air-water interfaces.....	77
3.3 Effects of pH and additives in wetting films: polymer-induced forces and drainage behavior.....	81
3.3.1 Polymer-induced forces in wetting films.....	81
3.3.2 Effects of pH and additives on drainage of wetting films	85
3.3.3 Wetting.....	88
4 Conclusions.....	88
References.....	89
Chapter 6 Interaction forces between surfaces immersed in solutions of a polyethylene oxide-polypropylene oxide copolymer	91
1 Introduction.....	92
2 Experimental.....	93
2.1 Apparatus.....	93
2.2 Materials	93
2.3 Technique and Procedure.....	94
2.3.1 Colloidal probe AFM.....	94
2.3.2 Procedure	95
3 Results.....	95
3.1 Hydrophilic silica surface and silica probe (phil/phil).....	95
3.2 Hydrophobized silica surface and hydrophilic silica probe (phob/phil).....	99
4 Discussion.....	103
4.1 F127 adsorption and adsorbed layer thicknesses at hydrophilic and hydrophobic surfaces.	103
4.2 Interactions between phil/ phil surfaces.....	104
4.3 Interactions between phob/ phil surfaces.....	105
5 Conclusions.....	105
References.....	107
Summary	108
Samenvatting.....	110
Краткое содержание для всех	111
Acknowledgements.....	115
List of publications	118
Curriculum vitae	119

CHAPTER 1 GENERAL INTRODUCTION

1.1 Wetting Films

When an air phase (1) approaches a solid phase (3) in a water phase (2), a wetting film with a thickness h may be formed (fig. 1).



Figure 1 Definition of wetting film.

In contrast to symmetric films (air/water/air or solid/water/solid systems), these films are asymmetric (solid and air are different materials). They are typical representatives of systems determined by hetero interaction (1).

Wetting films are related to the surface science fields of adhesion, spreading and colloidal stability. The rupture of aqueous wetting films on solid surfaces is an important step in a variety of coagulation processes. Whether or not film rupture takes place during the short contact time between a particle and a bubble is of decisive consequence for flotation success and yield. Another example of the importance of wetting films is paint systems. As of the motivation of the current study comes from the paint industry, we will first discuss the connection between wetting films and paint.

1.2 Motivation: wetting films in paint systems.

A solvent-born paint usually contains pigments, binder, and additives in a solvent. Pigments provide colour and hiding; binder “binds” the pigment together; solvent provides desired consistency and make it possible to apply the pigment and the binder to the surface being paint; and additives are low-level ingredients that provide specific paint properties such as resistance to fungi, de-foaming and good flow and levelling. Central issues in the paint industry are controlling the stability of such dispersions and the film formation.

The overall stability of paint dispersions relies on the stability of the thin films separating the dispersed particles. In the absence of stabilizing forces flocculation can occur which effectively will increase particle

sizes, leading to a corresponding loss in optical performance. At the same time, complete stability is not desirable either. In fact, a weakly flocculated system is preferred. The first reason is that this avoids the formation of a hard sediment when the paint is stored for a long time. Secondly, a weak network structure is resistant to gravitational forces but breaks down under the shear stress imposed when the paint is brushed on to a surface (2).

Many interactions are concerned within the paint dispersions, i.e. pigment-pigment, pigment-binder, pigment-solvent, pigment-additives, binder-binder, binder-solvent, binder-additives, solvent-additives. Dispersion stabilization in coatings is achieved mainly by one or two basic mechanisms: steric stabilization or charge stabilization (3). Steric stability is usually dominant in non-polar solvent-based systems and is achieved through the adsorption of solvated binders onto the pigment particle surfaces. Charge and steric stabilization is common method of achieving stable dispersions in water-based systems. It involves the adsorption of an ionized species (for charge stabilization) onto the pigment surface, or pH-dependent charging of oxidic pigments (adsorption of H^+ , OH^-). Pigment particles with similar electrical charges will repel each other and thus resist coagulation. Steric stabilization in water-borne paint is achieved via the adsorption of polymers (additives) onto the pigment or the binder particles.

Nowadays, the paint industry is progressively trying to avoid the use of non-polar solvent for environmental, health and safety considerations. Water-based paints are a good alternative. The majority of water-borne paints are so-called synthetic latex paints, i.e. aqueous dispersions of water-insoluble polymers. In other words, the binder in water-borne paints is a solid, plastic like synthetic polymeric material that is dispersed as microscopic particles in water. This dispersion is milky-white liquid called “latex” because it is reminiscent of natural latex from the rubber tree. This latex is then mixed with pigments and other ingredients to produce “latex paint”. In order to stabilize these dispersions, surface-active compounds are usually employed.

Film formation occurs when applying the paint on the surface. As the last vestiges of water evaporate, capillary action draws the binder particle together, causing them to fuse and bind the pigment into the continuous, flexible film that will be water resistant. This process is called coalescence. As the film is formed, the nature of the system changes rather radically from a hydrophilic environment to a hydrophobic one. At this point the use of surfactants can lead to a number of significant problems in the properties of films obtained from water-borne binder dispersions.

Important problems that still need to be solved are (i) the sensitivity of the formed films towards water and (ii) the attachment of binder particles to each other, to dispersed pigment and to the substrate.

1.3 Choice of the system and aim of the thesis

In the present study we considered studying film formation between particles possessing different physical and chemical properties. As a model system for our study, we have chosen wetting films stabilized by a non-ionic surfactant. It should be noted that wetting films formed from aqueous solutions of non-ionic

surfactants is a relatively “young” area, as compared to that of foam films. Therefore, many phenomena are still remaining unknown.

In order not to be confused, it is important to note that we did not study the films formed from the water-borne paint. These films contain all compounds of the paint, and have thicknesses of ~ 100 micrometers (μm). The subjects of the present work are water films (which might occur within the water-born paint) separating the dispersed particles. The thickness of these films is three orders of magnitude smaller as compared to paint films and ranges from a few to 100 nanometres (nm).

The main topic of the current work is the experimental study of the interactions within thin films stabilized by non-ionic polymeric surfactant, Pluronic F127 at a silica surface. The variable parameters in the experiment are the surfactant concentration, the pH, the nature and the concentration of additives. Another issue is the comparison of the surface forces in wetting films and those of hydrophilic and hydrophobic surfaces.

1.4 Non-ionic triblock copolymer surfactants

Water-soluble triblock copolymers of poly-(ethylene oxide) PEO and poly-(propylene oxide), with block sequence PEO-PPO-PEO, are non-ionic macromolecular surface-active agents, commercially available under the names Pluronics and Poloxamers. Variation of the molecular characteristics (PPO/PEO ratio, molecular weight) of the copolymer during the synthesis allows the production of molecules with optimum properties that meet specific requirements in different areas. These surfactants are an important class of surfactants and find widespread industrial application in detergency, dispersion stabilization, foaming and emulsification. They are also commonly used as stabilizers of thin films including wetting films.

An interesting property of these block copolymers is that they form micelles above a critical concentration. The driving force of aggregation is hydrophobic binding between the PPO blocks. Micellization of non-ionic block copolymers is very sensitive to the temperature and slightly to the presence of electrolytes (4-10).

One more interesting feature is their adsorption at hydrophilic (11-14) and hydrophobic surfaces (15-18). It is thought that at hydrophobic surfaces the hydrophobic PPO block drives the adsorption; while at hydrophilic surfaces the driving force is attachment through the hydrophilic moiety (PEO). Details will be discussed in the second and fourth chapter.

We have chosen one of the Pluronic surfactants as our model material because of their distinguishing properties discussed above. In addition, some experimental and theoretical studies are available on their micellization, adsorption solubilization and phase behaviour.

1.6 Disjoining pressure

An important concept in the study of interaction forces in thin liquid films is the so-called *disjoining pressure*, Π . Derjaguin and Obukhov introduce this concept in 1936 (19). Π is a pressure, which develops

when the two surfaces are brought to each other from infinity to a distance h (20). In other words, *the disjoining pressure* is the force between surfaces per unit area. The Gibbs energy of interaction per unit area between the surfaces can be associated with the process of isothermally bringing two surfaces together (20):

$$G(h) = - \int_{\infty}^h \Pi(h) dh \quad (2)$$

Positive disjoining pressure resists film thinning, while a negative pressure promotes film thinning. A variety of interaction forces contribute to $\Pi(h)$, each with its own sign, magnitude and typical decay as function of h . In the next section we discuss the components of the disjoining pressure.

1.7 Interaction forces in wetting films

Different kinds of forces are presented within the film and are depended on its thickness. Short-range forces (e.g. hydrogen bonds) control ‘*ultra-thin*’ films, which have a thickness of a few nanometres. Long-range forces (Van der Waals, electrostatic) govern ‘*thin*’ films having thicknesses of 2-100 nm. ‘*Thick*’ films have thicknesses of micrometers and higher. They have a negligible disjoining pressure and behave as bulk systems.

1.7.1 Long-range forces

Van der Waals interactions and electrostatic repulsion in ionic systems are the main long-range forces. Both interactions are taken into the account by the DLVO theory.

Van der Waals forces are always attractive between two like materials, and they are sometimes repulsive in wetting films. For a film of medium 2 between media 1 and 3 (fig.1), Van der Waals force of the disjoining pressure $\Pi(h)$ is written:

$$\Pi(h) = - A_{132}/6\pi h^3 \quad (3)$$

Here A_{132} is the Hamaker constant, and can be obtained from the h (Π) measurements, or deduced from force measurements for symmetrical systems by using some combining relation (21-23). Values of A are collected in the books (20-23). They are sometimes negative for the wetting films.

Electrostatic repulsion appears when the surfaces carry a charge. For an electrolyte solution of monovalent ions with bulk concentration of C_{∞} the disjoining pressure between two surfaces with a constant surface potential ψ_0 (typical values of $|\psi_0|$ around 100 mV) can be written as:

$$\Pi(h) = 64 C_{\infty} k T \tanh^2(e\psi_0/4kT) \exp(-2\kappa z) \quad (4)$$

Here, e is the elementary charge and κ^{-1} the Debye screening length defined as:

$$\kappa^2 = 2 C_{\infty} e^2 / \epsilon_0 \epsilon_r kT \quad (5)$$

and, $\epsilon_0 \epsilon_r$ is the solvent permittivity. In 10^{-3} M electrolyte the Debye length is of the order of 10 nm. For thicknesses smaller than the Debye length, the surface potential ψ_0 does no longer remain constant upon thinning and the expression (4) for $\Pi(h)$ underestimates the interactions (21-23).

1.7.2 Short-range forces

Short-range forces operate on molecular distances. They are induced by molecular ordering near the interacting surfaces and include hard core, hydrophobic interactions and hydrogen-bonding (22, 23). As far as this type of forces is determined by the solvent structure they might have an oscillatory behaviour, being alternately repulsive and attractive (23). Such solvation or structural forces arise whenever the liquid molecules adjacent to a hard wall are induced to order into quasi-discrete layers between two surfaces. When the medium is water, these forces are called hydration forces. In practice such forces can sometimes be described as an exponentially decaying function.

1.7.3 Surface forces coming from adsorbed layers of polymeric surfactants

When liquid films are formed from solutions containing adsorbing polymeric surfactant, so-called steric forces might come into play. They are of short range for small molecules and long range for macromolecules. These forces can be attractive or repulsive, which depends on many parameters, such as type of polymer, surface coverage, solvent quality, the type of interacting surfaces. Details are given elsewhere (23-25).

When two polymer-covered surfaces approach each other they experience a force once the outer segments begin to overlap, i.e. when the separation is smaller than a few times the radius of gyration, R_g . This interaction usually leads to a repulsive force due to unfavourable entropy associated with confining the chains between the surfaces. This repulsion is usually referred to as the steric or overlap repulsion.

Furthermore, *bridging* between two surfaces can occur whereby different segments from the same polymer coil can be simultaneously bound to both surfaces. Bridging takes place when the polymer is attracted to both surfaces, the coverage of which is not too high and not too low. Under suitable conditions attractive bridging forces can be strong and of long range, far exceeding Van der Waals attraction between two surfaces. Details are given (23, 26).

In the present case we consider the forces between a solid-liquid and a liquid-gas interface, both bearing adsorbed polymers. It is important to note that for stabilization of the films, polymer must be strongly

anchored to the surface. In addition, the final force will be also depending on extension of tails and on the quality of the solvent.

1.8 Film thickness measurements: thin film balance technique

One of the ways of obtaining information about the films is to apply an external pressure and to measure the corresponding thickness via interferometric ($h \geq 10$ nm) or ellipsometric techniques ($0.01 \text{ nm} \leq h \leq 100$ nm). The force in the film can be balanced by an applied pressure, hence the name “Thin Film Balance” (TFB).

As in our work the TFB technique was used, we briefly touch on the history of this technique. Details of the method will be discussed in chapters 2, 3, 4. Detailed reviews are given elsewhere (27-31). The idea of balancing the forces in thin films was first realized by Derjaguin and Obuchov (19) when they trapped air-bubbles underneath a glass slide which has been horizontally submerged in an aqueous solution. Buoyancy forces from the bubble created a pressure drop across the film between the bubble and the solid interface, which then drained. Eventually, drainage stopped when the disjoining pressure balanced the forces due to buoyancy, thus leaving a thin film, which prevented the air from contacting the solid. Following these pioneers, various apparatuses were constructed to directly manipulate the pressure imposed on a thin-liquid film. One of them was the so-called “Sheludko cell”(32) (fig. 2), later modified by Platikanov (33) and Manev (34) to investigate emulsion and wetting films (fig. 3).

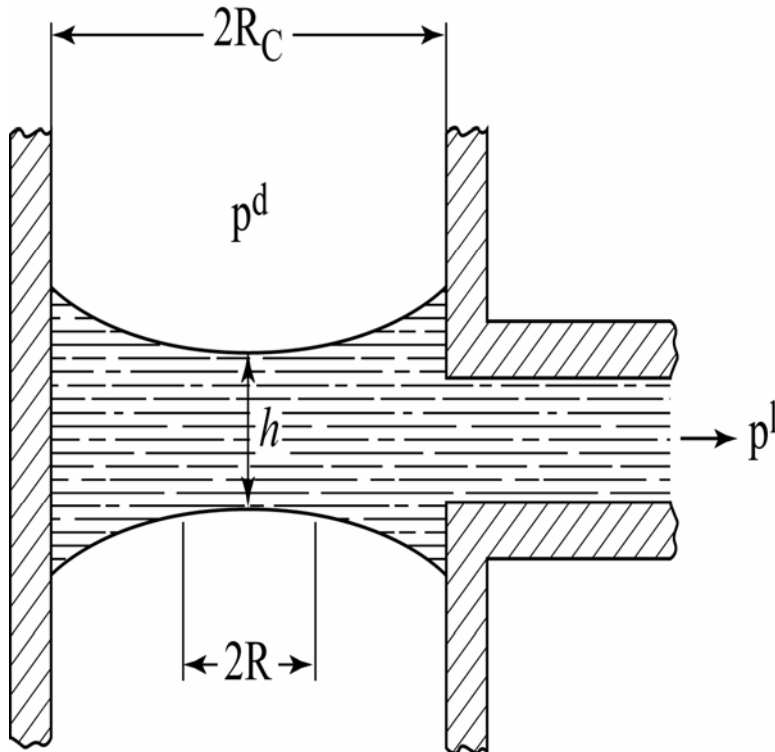


Figure 2 Scheludko cell: the film is formed by sucking out, by use of a piston, the liquid from a biconcave meniscus formed in a glass capillary. Here $2R_c$ – capillary diameter, $2R$ – film diameter, h – film thickness. p^d – equilibrium pressure in the drops; p^l – equilibrium pressure in the bulk liquid.

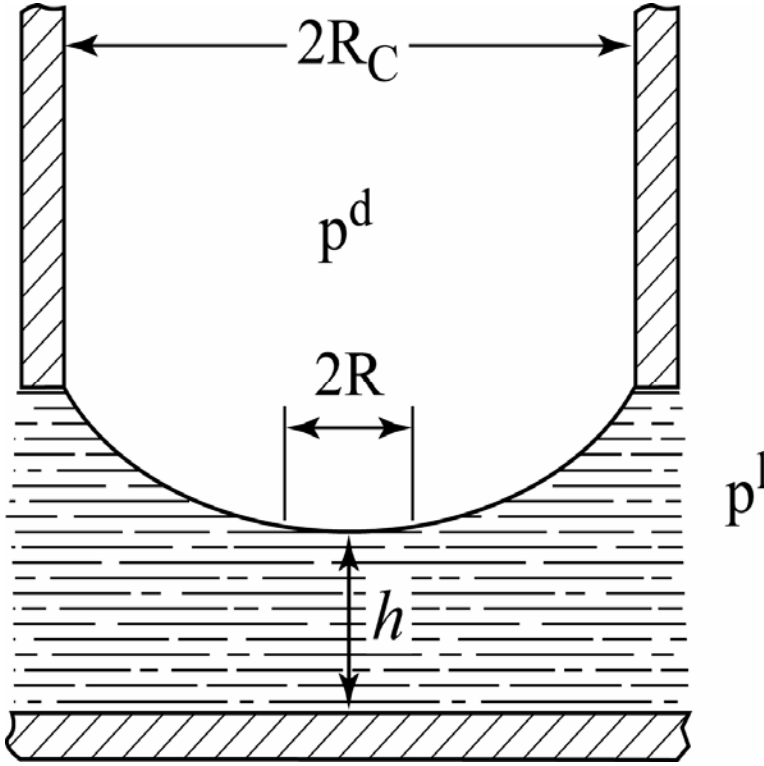


Figure 3 Formation of a wetting film by blowing out a bubble from a capillary against a flat solid surface. Here R_c – capillary diameter, $2R$ – film diameter, h – film thickness. p^d – equilibrium pressure in the drops; p^l – equilibrium pressure in the bulk liquid.

One of the limitations of the Scheludko cell and its variant is that it eliminates the low-pressure restriction. Mysels and Jones overcame this restriction by introducing a porous porcelain disc with a circular hole, instead of a capillary tube (27) (fig. 4). Shortly after that, Exerowa and Scheludko improved upon Mysels' original porous-plate design by welding a porous glass filter to the end of a tube.

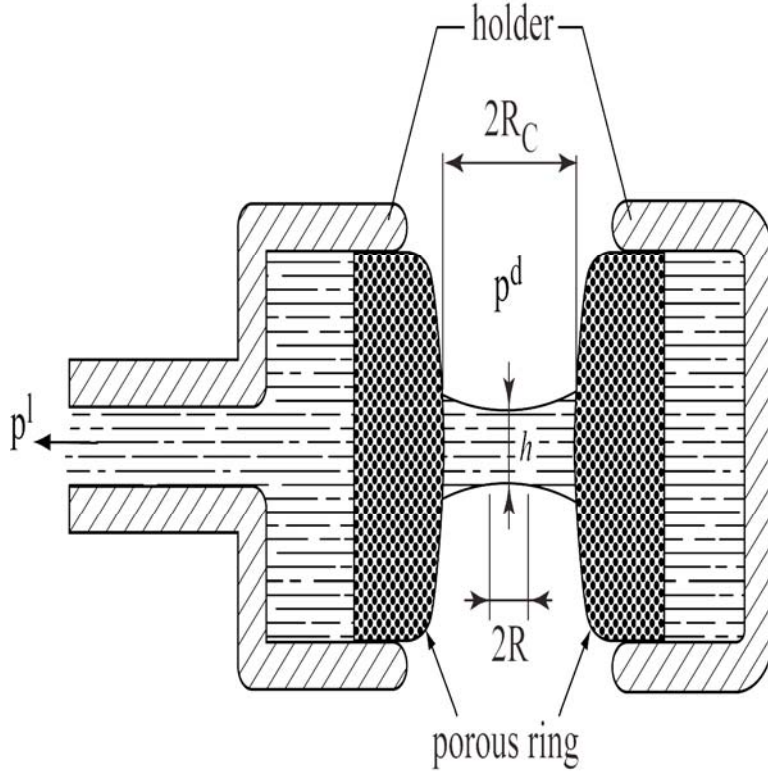


Figure 4 Scheludko cell with a porous ring. Here R_c - effective radius, $2R$ - film diameter, h - film thickness, p^d - equilibrium pressure in the drops; p^l - equilibrium pressure in the bulk liquid.

Later Shishin et al and Derjaguin et al (28, 29) described the application of this device to wetting films. More recently Zorin et al (35) have qualitatively applied the technique to measure the disjoining pressure isotherm between quartz and air in cationic surfactant solutions. Figure 5 illustrates the set-up used in the present study: a thin film (2) is formed on a silica surface (1), in a hole drilled in a porous glass disc (3), which is fused to the end of a glass tube (5). The latter is connected to a glass vessel (7), via a flexible tube (6). The film holder is placed inside a covered Plexiglas cell (4).

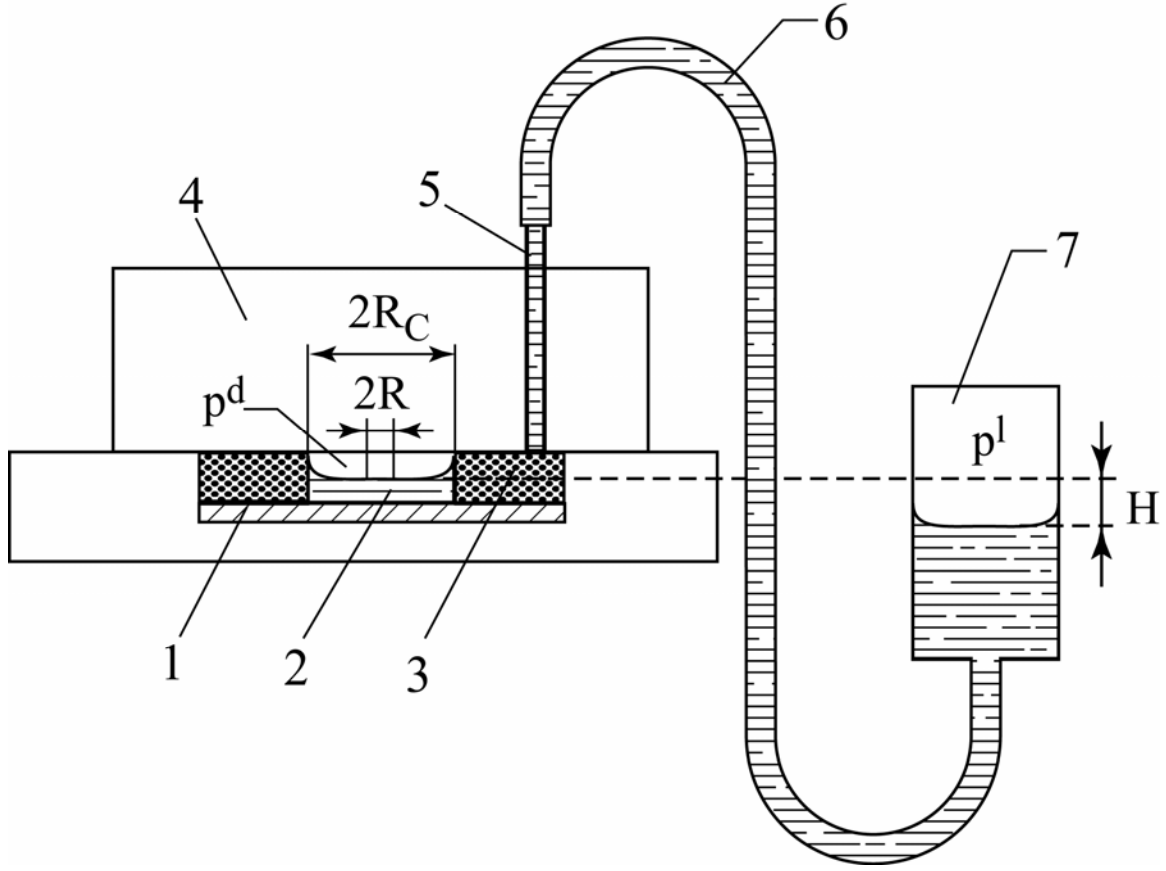


Figure 5 Set-up for formation of wetting film (2) at silica (1) used in the present study.

Here 3 - a porous disc, 5 - a glass tube, 4 - a Plexiglas cell, 6 - a flexible tube, 7 - glass reservoir with the solution studied, R_c - effective radius of the hole (0.25 cm), R - film radius (0.075 cm), h - film thickness, p^d - equilibrium pressure in the drops; $p^l = p_H$ - equilibrium pressure in the bulk liquid.

At equilibrium Π within the wetting film is opposite in sign and equal in magnitude to the hydrostatic pressure difference Δp_H . The hydrostatic pressure difference is given by $\Delta p_H = \rho g H$, where ρ is the liquid density, g is the gravitational acceleration and H the height difference between the silica surface (1) and the reservoir (7). H has negative values as the level in the vessel is below the silica surface.

1.9 Film drainage

Initially the formed film is thick. However, it becomes thinner under applied pressure (31). The processes of film thinning and film rupture comprise the most important non-equilibrium properties of thin films (31). As the drainage of foam film is extensively studied as compared to that of wetting films, we will first discuss the drainage behaviour of foam films.

1.9.1 Drainage of foam films

Draining foam films are generally of non-uniform thickness. Mostly, the central part of such films is thicker than its periphery. A thickening in the centre of the films, known as a dimple (thicker lens-like patch) which is surrounded by a thinner, almost plane-parallel, barrier ring (fig. 6) (31, 36).

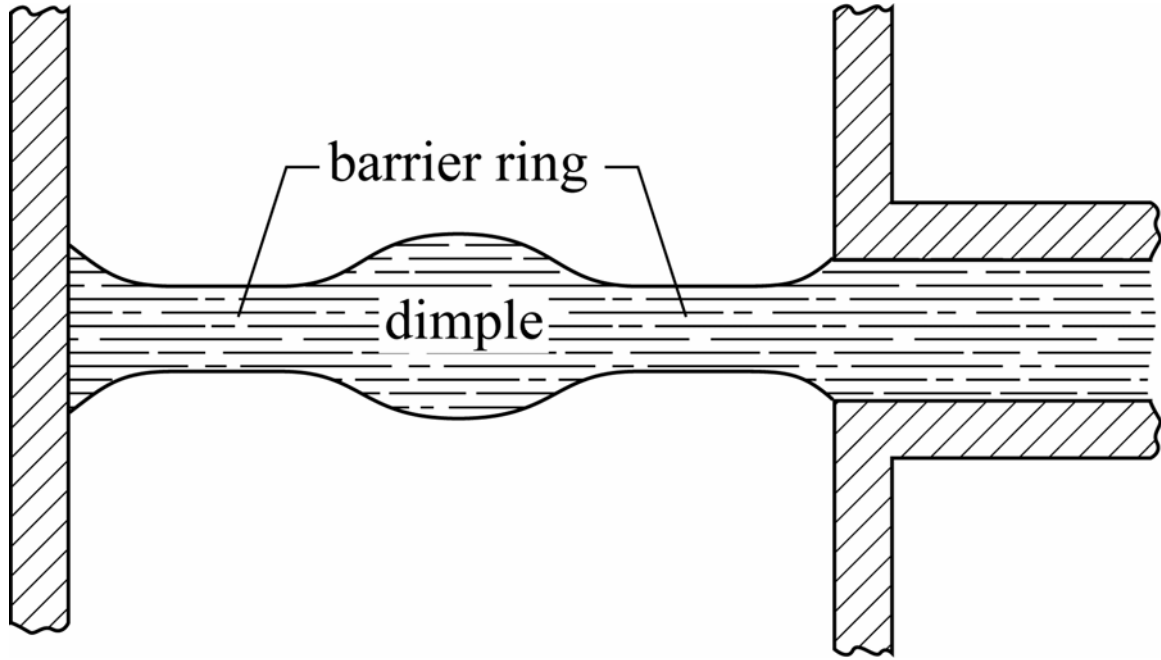


Figure 6 Dimple formation in foam films.

Dimples are transient structures. In later stages of drainage dimples relax.

For foam films it is known that Π influences the film drainage (31, 33, 36, 37). The extent and the onset of this influence depend on the controlling component of Π . At low electrolyte concentration the repulsive electrostatic component of the disjoining pressure is dominant. It inhibits the formation of a thin barrier ring and of the dimple itself. The film drains rapidly to its equilibrium thickness, and the drainage is faster than in the absence of the disjoining pressure, because the barrier ring is not formed (36). For high electrolyte concentration, the disjoining pressure is dominated by the Van der Waals attraction. Early in the drainage process, the barrier ring thins very quickly due to these attractions. When the short-range repulsive forces become dominant, a very thin annular (ring shape) film forms that forces the dimple into a lens. The drainage of the lens is then very slow because of the high resistance to flow in the thin annular film. Details have been discussed in (36).

1.9.2 Drainage of wetting films

Several distinct stages can be distinguished in the thinning process in wetting films. Since the drainage near the film border is initially faster than that in the films centre, the thickness at the barrier rim reaches quickly a value close to the equilibrium one. Thus, a dimple in wetting films might also be generated. Tsekov et al developed a simulation procedure for the dimple relaxation in aqueous wetting films on a glass surface (38), and compared the theory with experimental results. They generated films from 1 mM KCl solution in water, and the thickness in the centre of the film versus time was measured by a light interference method. During 1 minute the thickness was decreased from ~ 170 nm until 40 nm. Their results support the assumption that OH^- ions adsorb on the water-air surfaces. They have proposed that a coupling between the disjoining pressure and adsorption of OH^- ions (which leads to an increase of the thinning rate at the end stages of drainage) is playing an important role. However, relaxation on a longer time scale (> 2 minutes) was not considered.

Since experimental work on the drainage of aqueous films at solid surfaces is scarce, we have studied the drainage of aqueous films stabilized by triblock copolymers (chapters 3, 4). The drainage of wetting films was driven by a hydrostatic suction, which is counterbalanced by a disjoining pressure. Dimple formation might occur when there is no sufficient long ranged repulsion between the interfaces.

1.10 Foam films stabilized by non-ionic surfactants: surprising salt effect.

Foam films formed from aqueous solutions of non-ionic surfactant have been studied in detail (18, 31, 39-46). The stability of these films is attributed either to electrostatic or to steric interactions. Electrostatic interactions are described within the DLVO theory (van der Waals force is also present). For that reason increasing of the ionic strength can screen the repulsion. It is thought that the air-water interface carries the charge and the origin of the charge is explained by the adsorption of OH^- ions (31, 43).

In the absence of electrostatics non-DLVO forces are responsible for the stability of the films. When the films are thin, brush-to-brush repulsion governs the stability of the film. However, at low pressure a 'soft' steric repulsion is proposed to stabilize the film. The explanation given by Exerowa and co-workers (18, 31, 43) is that the film thickness is governed by the longest, and not by the average polymer tail.

An interesting effect of the salt concentration on the thickness of foam films stabilized by non-ionic surfactants was found by Van den Boomgaard and Lyklema (47). They observed a maximum in the film thickness when increasing the concentration of salt. This phenomenon was attributed to the influence of electrolytes on the conformation of the hydrophobic moiety, besides the hydrophilic one. Later, Müller and Rheinländer gave another view on this phenomenon (42). They suggested that at a certain concentration of salt specific interactions might occur between the ethylene oxide groups and the salt cations. This would lead to a change in the configuration of the hydrophilic chains, a redistribution of ions, and as a result a more extended double layer repulsion.

The two mechanisms of this phenomenon are still under discussion.

In our work we were interested in finding out whether a similar effect also occurs in wetting films.

1.11 Wetting films stabilized by non-ionic surfactants

Foam films of non-ionic surfactants are studied in detail, but the corresponding wetting films are less studied. Recently, a number of studies on wetting films formed from aqueous solutions of triblock copolymers have been reported by a number of groups (46, 48-53). As for foam films, the interactions within these films were explained by either electrostatic or steric repulsion. Namely, at low ionic strength the stability of films is governed by electrostatic repulsion. At constant Π a decrease of the film thickness is measured when increasing the pH or the ionic strength, like for foam films. This decrease is classically explained by a modification of the DLVO model (46).

An interesting feature is that at higher ionic strengths some additional repulsive forces are also detected in wetting films. Analogous to foam films, it is proposed that these forces are steric in origin, and changes of the pH do not influence dramatically the film thicknesses (46, 49-53).

1.12 Outline of the thesis

We will describe our results in six chapters, of which the present introduction is the first. In the second chapter we consider the effects of NaCl on the behaviour of a triblock copolymer surfactant, F127 in aqueous solution, at different interfaces and in wetting films. The third chapter is devoted to the drainage behaviour of wetting films stabilized by a surfactant. The time-dependent thickness of wetting films formed from aqueous solutions of NaCl on silica modified with a surfactant is discussed in the fourth chapter. In the fifth chapter we discuss the effects of the nature of additives and the pH on the interaction forces in wetting films stabilized by a surfactant. The sixth chapter is devoted to the interactions between a modified and a native silica surface immersed in the solution of a surfactant.

References

1. J. Lyklema, *Fundamentals of Interfaces and Colloid Science: liquid-fluid interfaces*, FICS (Academic Press, London, 2000), vol. III.
2. J. Clayton, *Pigment&Resin Technology* **27**, 231-239 (1998).
3. K. Holmberg, D. O. Shah, M. J. Schwuger, *Handbook of applied surface and colloid chemistry* (Wiley, 2002).
4. P. Alexandridis, V. Athanassiou, S. Fukuda, T. A. Hatton, *Langmuir* **10**, 2604-2612 (1994).
5. P. Alexandridis, V. Athanassiou, T. A. Hatton, *Langmuir*, 2442-2450 (1995).
6. P. Alexandridis, J. F. Holzwarth, *Langmuir* **13**, 6074-6082 (1997).
7. P. Alexandridis, J. F. Holzwarth, T. A. Hatton, *Macromolecules* **27**, 2414-2425 (1994).
8. J. K. Armstrong, B. Z. Chowdhry, M. J. Snowden, S. A. Leharne, *Langmuir* **14**, 2004-2010 (1998).
9. E. Florin, R. Kjellander, J. C. Eriksson, *J. Chem. Soc. Faraday Trans.* **80**, 2889 (1984).
10. M. Malmsten, B. Lindman, *Macromolecules* **25**, 5440-5445 (1992).
11. J. Lyklema, *Fundamentals of Interface and Colloid Science: solid-liquid interfaces* (Academic press, 1995), vol. II.
12. M. Malmsten, P. Linse, T. Cosgrove, *Macromolecules*, 2474-2481 (1992).
13. S. Partuka, S. Zaini, M. Lindeheimer, B. Bruin, *Colloid and Surfaces* **12**, 255-270 (1984).
14. J. Rubio, J. A. Kitchener, *J. Colloid Interface Sci.* **57**, 132-142 (1976).
15. R. Sedev, R. Steitz, G. H. Findenegg, *Physica B* **315**, 267-272 (2002).
16. R. Sedev, *Colloids and Surfaces* **156**, 65-70 (1999).
17. A. Nelson, T. Cosgrove, *Langmuir* **21**, 9176-9182 (2005).
18. D. Exerowa, R. Sedev, R. Ivanova, T. Kolarov, T. F. Tadros, *Colloid and Surfaces A:Physicochem.Eng. Aspects* **123-124**, 277-282 (05.01.2005, 1997).
19. B. V. Derjaguin, E. Obukhov, *Zhur. Fiz. Khim.* **7**, 297 (1936).
20. J. Lyklema, *Fundamentals of Interfaces and Colloid Science*, FICS (Academic press, London, 1991), vol. I, A 9.4.
21. B. V. Derjaguin, N. V. Churaev, V. M. Muller, *Surface Forces* (Consultants Bureau N.Y., 1987).
22. A. M. Cazabat, *Les Houches 1988, Session XLVIII, Liquids at interfaces*. J. Charvolin, J. F. Joanny, J. Zinn-Justin, Eds. (North-Holland, Elsevier Science Publishers B.V., Amsterdam, 1990).
23. J. N. Israelachvili, *Intermolecular and surface forces* (Academic press, San Diego, 1992).
24. J. Klein, *Les Houches 1988, Session XLVIII, Liquids at interfaces*. J. Charvolin, J. F. Joanny, J. Zinn-Justin, Eds. (North-Holland, Elsevier, Amsterdam, 1990).
25. D. H. Napper, *Polymeric stabilization of colloidal dispersions* (Academic Press, London, 1983).

26. G. J. Fleer, M. A. Cohen Stuart, F. Leermakers, *Effect of polymers on the interaction between colloidal particles in Fundamentals of Interface and Colloid Science*. J. Lyklema, Ed., FICS (Elsevier, Amsterdam, 2005), vol. V.
27. K. J. Mysels, M. N. Jones, *Discuss. Faraday Soc.* **42**, 42 (1966).
28. B. V. Derjaguin, Z. M. Zorin, N. V. Churaev, V. A. Shishin, *Wetting, Spreading and Adhesion*. J. F. Padday, Ed. (Academic Press, London, 1977).
29. V. A. Shishin, Z. M. Zorin, N. V. Churaev, *Kolloidnyi Zhurnal (English transl.)* **39**, 351 (1977).
30. P. M. Claesson, T. Ederth, V. Bergeron, M. Rutland, *Advances in Colloid and Interface Science* **67**, 119-183 (1996).
31. D. Platikanov, D. Exerowa, *Thin Liquid Films in Fundamentals of Interface and Colloid Science*. J. Lyklema, Ed., FICS (Elsevier, Amsterdam, 2005), vol. V, 6.1 - 6.91.
32. A. Scheludko, D. Exerowa, *Kolloidnyi Zhurnal (English edition)* **155**, 39 (1957).
33. D. Platikanov, *Journal of Physical Chemistry* **68**, 3619-3624 (1964).
34. E. Manev, S. V. Sazdanova, D. T. Wasan, *J. Dispersion Sci. Tech.* **5**, 111 (1984).
35. Z. M. Zorin *et al.*, *Journal of Colloid and Interface Science* **152**, 170-182 (1992).
36. J. L. Joye, G. J. Hirasaki, C. A. Miller, *Journal of Colloid and Interface Science* **177**, 542-552 (1996).
37. K. Danov, *Effect of Surfactants on Drop Stability and Thin Film Drainage*. V. M. Starov, Ivanov, I.B., Ed., Fluid Mechanics of Surfactant and Polymer Solutions (Springer, 2004).
38. R. Tsekov, Letocart, P., Schulze, H. J., *Langmuir* **16**, 8206-8209 (2000).
39. T. Van den.Boomgaard, J. Lyklema, *Langmuir* **5**, 245 (1989).
40. A. D. Nikolov, D. T. Wasan, N. D. Denkov, P. A. Kralchevsky, I. B. Ivanov, *Progr Colloid Polym Sci* **82**, 87-98 (20.01.2005, 1990).
41. P. A. Barneveld, J. M. H. M. Scheutjens, J. Lyklema, *Colloid Surfaces* **52**, 107 (1991).
42. H. J. Müller, T. Rheinländer, *Langmuir* **12**, 2334-2339 (1996).
43. D. Exerowa, P. Kruglyakov, *Foam and Foam Films* (Elsevier, 1998).
44. K. Khristov, B. Jachimska, K. Malysa, D. Exerowa, *Colloid and Surfaces A:Physicochem.Eng. Aspects* **186**, 93-101 (20.01.2005, 2001).
45. N. V. C. D. Exerowa, T. Kolarov, N. E. Esipova, N. Panchev and Z. M. Zorin, *Advances in Colloid and Interfaces Science* **104**, 1-24 (2003).
46. D. Exerowa, N. V. Churaev, T. Kolarov, N. E. Esipova, S. V. Itskov, *Colloid Journal* **68**, 155-161 (2006).
47. T. Boomgaard, J. Lyklema, *Langmuir* **5**, 245 (1989).
48. N. V. Churaev, *Colloid Journal* **62**, 517-525 (21.01.2005, 2000).
49. N. V. Churaev, *Colloid Journal* **65**, 263-274 (20.01.2005, 2002).
50. B. Diakova, C. Filiatre, D. Platikanov, A. Foissy, M. Kaisheva, *Advances in Colloid and Interface Science* **96**, 193-211 (20.01.2005, 2002).

51. B. Diakova, M. Kaisheva, D. Platikanov, *Colloids and Surfaces A:Physicochem.Eng. Aspects* **190**, 61-70 (2001).
52. B. Diakova, D. Platikanov, R. Atanassov, M. Kaisheva, *Advances in Colloid and Interface Science* **104**, 25-36 (20.01.2005, 2003).
53. N. E. Esipova, S. V. Itskov, N. V. Churaev, *Colloid Journal* **64**, 699-705 (2002).

Chapter 2 Polyethylene oxide-polypropylene oxide ABA copolymer in aqueous solution, at interfaces, and in wetting films

ABSTRACT

The solution behaviour of the polymeric surfactant Pluronic F127 and its adsorption on silica-water and air-water interfaces, as well as the disjoining pressure isotherms of asymmetric films (silica/aqueous solution/air) containing this surfactant are studied. Pluronic F127 is a co-polymeric surfactant, composed of two hydrophilic polyethylene oxide (PEO) blocks and a hydrophobic polypropylene oxide (PPO) block. It has an average molecular composition $\text{PEO}_{99}\text{PPO}_{65}\text{PEO}_{99}$. The interfacial properties of adsorbed surfactant layers (the surface concentration Γ and the thickness h) and the aqueous wetting film properties (film thickness h_{film}) are studied via ellipsometry. The solution properties of surfactant are investigated using surface tensiometry and light scattering. The interactions between the air-water and silica-water interfaces are measured with a thin film pressure balance technique (TFB) and interpreted in terms of disjoining pressure as a function of the film thickness. The relations between the behaviours of the asymmetric films, adsorption at air-water and silica-water interfaces and the solution behaviour of the polymeric surfactant is discussed. Special attention is paid to the influence of the concentrations of surfactant and NaCl. It was found that addition of electrolyte lowers the cmc, diminishes adsorption of surfactant on silica, and increases the thickness of the asymmetric film.

1 Introduction

It is generally accepted that several types of forces operate between surfaces across thin liquid films. The net effect of these forces can be experimentally measured and is often discussed in terms of the disjoining pressure Π , the force between two surfaces per unit area. The different contributions to Π are often assumed to be additive:

$$\Pi(h) = \Pi_{vdW} + \Pi_{edl} + \Pi_{st} + \Pi_{solv} + \Pi_{supra} + \dots \quad [1]$$

The subscripts in [1] indicate the following contributions: vdW = London-van der Waals dispersion forces, edl = electrostatic double layer forces, st = steric forces, $solv$ = solvation forces and $supra$ = ‘supra-molecular’ forces. The well-known dispersion forces and electrostatic forces are long range and are well described by the classical DLVO theory. The steric forces occur upon approach of two surfaces covered with polymers. In this case the protrusions of these polymers become confined into a small space, and in the absence of any other interactions, repulsive forces arise associated with the unfavourable entropy of this confinement. The solvation forces, or hydration forces in aqueous systems, originate from interfacial perturbation of solvent structure and the supra-molecular forces are due to molecular assemblies that may be present in thin films. For more details we refer to reviews by Bergeron (1) and Israelachvili (2). Positive disjoining pressures resist film thinning and negative pressures lead to film instability.

Interesting components for the study of the steric forces are triblock copolymer surfactants of the type $PEO_nPPO_mPEO_n$, where PEO is polyethylene oxide, which is hydrophilic, and PPO is polypropylene oxide, which is hydrophobic. It is known that a change of temperature or addition of simple electrolytes can affect their behaviour in solution (3-5).

The main purpose of the present study is to investigate the interactions across an aqueous film formed between an air-water and a silica-water interface in the presence of a surfactant Pluronic F127 ($PEO_{99}PPO_{65}PEO_{99}$). Extensive studies of this compound and closely related ones are reported in the literature (6-9), but there are still controversies with respect to their behaviour in thin films, and the role that added electrolytes play is not fully clear. We will therefore focus on the roles of the concentration of both the surfactant and NaCl. Because the solution properties of surfactants like Pluronic F127 and their adsorption at air-water and silica-water interfaces are crucial for the behaviour of thin films containing such compounds, we will briefly review what is known about these phenomena.

1.1 Solution behaviour of block copolymer surfactants

Aggregation behaviour of amphiphilic $PEO_nPPO_mPEO_n$ polymeric surfactants in aqueous solution has been studied in some detail (6-14). For a single-component surfactant the cmc (critical micelle concentration) can be easily determined from the break in the surface tension isotherm, and the adsorbed amount is found by applying the Gibbs equation to $\gamma(c)$ for $c < \text{cmc}$:

$$\Gamma \approx -d\gamma/RTd\ln c \quad [2]$$

Here Γ is the surface excess, γ the surface tension, R the gas constant, T the temperature, and c the bulk concentration. However, with a polymeric surfactant sample the situation is more complex because such samples contain a range of components that may differ both in molar mass and composition. For such a system it is not obvious that the Gibbs equation in its simple form [2] can be applied. In general, in γ vs. $\ln c$ plots of triblock copolymers the appearance of two breaks instead of one is characteristic (13). Alexandridis et al (13) propose that the low-concentration break originates from rearrangement of the copolymer molecules on the surface at complete coverage of the air-water interface and that the high concentration break can be used to determine the cmc. Chen et al (15) found evidence for a change in the molecular conformation of the methyl groups of the PPO blocks on the air-water interface at the low-concentration break. Alternatively, a theoretical study by Linse and Hatton (16) suggests that the low-concentration break is most likely the effect of depletion of the solution of surfactant components due to the low value of the concentration times the volume-to-surface ratio. Due to these complications many different values of the cmc for a polymeric surfactant F127 are found in the literature. We collected the main results in Table 1.

Table 1 Reported cmc values of a triblock copolymer surfactant F127 determined by different methods (surface tension (ST), dye solubilization (DS))

Cmc		$T / ^\circ\text{C}$	Conditions	Method	Reference
μM	wt %				
2000	2.5	20	H ₂ O (or 100 mM NaCl)	ST	26
555	0.7	25	H ₂ O	DS	9
3174	4	20	H ₂ O	DS	9
3.2*	0.004*	25	H ₂ O	ST	10
240**	0.3**	25			
1600/2000	2/2.5	25	H ₂ O		8
720/800	0.9/1	25	0.5 M NaCl	ST/DS	8
480/640	0.6/0.8	25	1 M NaCl	ST/DS	8
160/160	0.2	25	2 M NaCl	ST/DS	8

**The authors obtained these values from the first kink of $\gamma - \ln C$*

***We took these values from the second kink of $\gamma - \ln C$ data given in reference 10*

It is found that the micellization of Pluronic type surfactants in aqueous solutions is strongly temperature and slightly salt dependent, and that the salt type is important as well (3-5, 8). It is observed that the nature of anions is more important than that of cations, and that the magnitude of the changes depends on the size of the anion (3).

1.2 Block copolymer surfactants at the air-water interface

The behaviour of $\text{PEO}_n\text{PPO}_m\text{PEO}_n$ surfactants at the air-water interface has been studied by means of surface tension, ellipsometry and neutron reflectivity(13, 15, 17-20). It was found that PPO blocks tend to form a dense non-hydrated layer at the interface, while PEO blocks tend to form a hydrated layer protruding in the solution (15). Sedev et al.(18) determined the adsorbed layer thickness of a series of triblock co-polymeric surfactants at the air-water interface by means of neutron reflectivity. They found that the thickness of the adsorbed layer increased linearly with the EO chain length. For the copolymers with two blocks of 100 EO units (as used in our study) the layer thickness is approximately 7.8 nm. Phipps et al. (21) performed neutron reflection experiments on surfactant F127 adsorbed at the hexane-water interface for concentrations above the cmc (0.5 wt %). The volume fraction profile of surfactant (F127) at the interface shows that the PEO segments protrude 9 nm into the aqueous sub-phase and the PPO segments 4 nm into hexane (the adsorbed amount is estimated to be around $2.9 \pm 0.5 \text{ mg/m}^2$).

1.3 Block copolymer surfactants at the silica-water interface

Malmsten et al (22) found that $\text{PEO}_n\text{PPO}_m\text{PEO}_n$ block co-polymeric surfactants adsorb from aqueous solution at silica surfaces with their PEO moieties on the surface, similarly to PEO homo-polymers of comparable molecular weight. The adsorbed amount was independent of the PPO content in the range 0-30% and found to be rather low ($0.35\text{-}0.4 \text{ mg/m}^2$, without salt, $\text{pH} \approx 6$). The hydrodynamic thickness of the adsorbed layer was found in the range 2-5 nm. These results were explained by the fact that the surface is unsaturated with respect to the polymer, which reduced the tendency for tail formation. Using a mean-field theory Malmsten et al argue that the PPO segments are preferentially located in the middle region of the adsorbed layer. From the temperature dependence of the adsorbed amount they also concluded that surface association at the untreated hydrophilic silica surface takes place at a concentration just below the solution cmc. Similarly Schar et al. (23) inferred a flat configuration adopted by these copolymers from the estimated thickness of adsorbed layers ($< 4 \text{ nm}$) for many Pluronics. They concluded that the structure of the adsorbed layer of non-ionic copolymers on hydrophilic surfaces is determined by the interactions of hydrophilic PEO block with the silica surface. However, Eskilsson and Tiberg (24) reported larger surfactant (F127) layer thickness at silica. They found an increase in the thickness from 4 to 13 nm with increasing c at $T = 25^\circ \text{C}$ in the same range of concentrations as studied by Malmsten et al (0.1 – 0.5 wt %).

This brought them to the conclusion that adsorbed F127 surfactants tend to form micelle-like aggregates at the silica surface. Surface aggregates are first observed at a concentration range 0.14-0.4 wt %. The observed variation in adsorption behaviour at silica may be due to the differences in silica surfaces.

In conclusion, the structure of surfactant Pluronic F127 on silica depends on many parameters such as the electrolyte concentration, the pH as well as on the treatment of the silica surface.

1.4 Foam and wetting thin films stabilized by block copolymer surfactants

Sedev et al (19) measured disjoining pressure isotherms for foam films (air/aqueous solution/air) containing Pluronic F108 (PEO₁₂₂PPO₅₆PEO₁₂₂) at 0.1 M of NaCl. Under this condition the electrostatic interactions are largely screened and steric forces stabilize the liquid film. The authors proposed that at low pressures (< 300 Pa) a soft steric repulsion is governed thicknesses of foam films (which are about 30-60 nm). Sedev et al speculated that the surfactant unimer molecules were trapped in the film core. At higher pressures the thickness is found to be in the range where brush-to-brush contacts govern the stability of the film ($h_{\text{total}} \approx 30$ nm). For symmetric films made of block copolymers an unexpected influence of electrolyte concentration upon the film thickness was reported in the literature (25-27). Van den Boomgaard and Lyklema (25) were the first to report that for free films stabilized by non-ionic block copolymer the equilibrium thickness as a function of electrolyte concentration passes through a maximum for high electrolyte concentrations typically at 2 M for NaCl. The Synperonic copolymers they used have similar hydrophobic and hydrophilic parts as Pluronics. Later, Barneveld et al. (26) found the same effect with non-ionic surfactants (C_nEO_m). More recently Müller and Rheinländer (27) studied the influence of salt (NaCl, KCl) on the thickness of foam films made of non-ionic surfactants (C₁₂EO_m). First they found a decrease of film thickness at low salt concentration (below 0.02 M) and at higher salt concentration an increase of film thickness, similarly, as found by Van den Boomgaard et al and Barneveld et al. The authors of reference(27) found that increase of the film thickness starts at a relatively well-defined critical salt concentration. For all investigations the film thickness reached values near double that of combined layer thickness at the surfaces of the film. So far no convincing explanation has been given.

The interaction forces in asymmetric liquid films (silica/aqueous solution/air) stabilized by surfactants F108 and F127 have been studied recently (28-31). It was found that at a constant disjoining pressure the thickness of aqueous films containing these surfactants decreases with increasing electrolyte concentration up to certain plateau level. The transition from electrostatic to steric film stability is measured at about 0.01 M NaCl. Surprisingly, at this electrolyte concentration a film thickness is found to be much larger than the twice the adsorbed layer thickness. According to the authors (31) such a thick film is metastable.

In our work we probe higher pressures (up to 4 kPa) and investigate the effect of variation of surfactant and electrolyte concentration.

2 Materials and Methods

2.1 Materials

Pluronic F127 (average molecular composition $\text{PEO}_{99}\text{PPO}_{65}\text{PEO}_{99}$) was obtained from Sigma- Aldrich CO., USA and used without further purification. Pluronic F127 has an average molecular weight of 12600 and PEO content of 70%. Aqueous solutions of F127 were prepared by dissolving the polymers in distilled water with gentle agitation. Sodium chloride, NaCl (purity min 99.99% supplied by J.T. Baker Chemicals B.V., Holland) was used without further purification. The water used was purified in two demineralization steps: a first and a second ion exchange treatment followed by running the water through an active carbon column and an ultra-filtration membrane.

Polished silicon wafers (p-type, boron-doped, oriented $\langle 1-0-0 \rangle$, resistivity 12-18 Ωcm) were purchased from Wafer Net, Germany. The thickness of the natural oxide layer was about 2 nm. Wafers were cut into small strips and boiled for 5 min at 80° in a mixture of 25 % NH_3 , 30 % H_2O_2 and H_2O (1:1:5 by volume). Then the strips were rinsed with water and in ethanol (99.8 %). They were kept in a closed container under water until use. Before the strips were placed in the cell, they were dried in nitrogen and treated in a plasma cleaner (Anadis Instruments B.V., Model PDC-32 G) for 30 seconds. The plasma treatment was performed with air (10 Pa). The contact angle of water was always lower than 8°, indicating the hydrophilic nature of the silicon oxide surface. All measurements were done at pH \approx 6.

2.2 Light scattering

Static light Scattering (SLS) and Dynamic Light Scattering (DLS) were used for the characterization of the surfactant in solution. The light source was a Lexel 450 mW (max) multi line width Ar-laser ($\lambda=514.5$ nm). Light Scattering measurements were carried out with the static/dynamic compact goniometer System (ALV/DLS/SLS-5000), Langen, Germany using the ALV-5000/E/WIN software. The detection angle was 90°. The measurements were done in a thermostatic cell at a temperature of 294-295 K. For DLS measurements, the scattered intensity was recorded by means of a multi-channel digital correlator and converted to the intensity autocorrelation function $g^{(2)}(q, \tau)$ which is related to the field autocorrelation function $g^{(1)}(q, \tau)$ as:

$$g^{(2)}=1+A (g^{(1)})^2 \quad [3]$$

Here τ is the time delay, A is an instrument constant of order unity which depends on the geometry of the set-up and $q=4\pi n \sin(\theta/2)/\lambda$ is the norm of the scattering vector (n is the refractive index of the solvent, λ is the wave length in vacuum and θ is the angle between the detector and the direction of the incident light).

For mono-disperse, spherical particles, one can show that the field autocorrelation function can be written:

$$g^{(1)} = e^{-\Gamma\tau} \quad [4]$$

Here Γ is the relaxation rate, which is related to the diffusion coefficient D by $\Gamma = Dq^2$, and D is related to the hydrodynamic radius R_H via the Stokes-Einstein equation:

$$R_H = k_B T / 6\pi\eta D \quad [5]$$

Where k_B is the Boltzmann constant and η the solvent viscosity at temperature T .

For a hetero-disperse system one can write:

$$g^{(1)} = \int G(\Gamma) e^{-\Gamma\tau} d\Gamma \quad [6]$$

Here $G(\Gamma)$ is a distribution function to be evaluated. The CONTIN method for data analysis was used. Usually the normalized distribution function $\Gamma G(\Gamma)$ is presented. We will follow this convention and plot $\Gamma G(\Gamma)$ versus the hydrodynamic radius.

2.3 The surface tension

Surface tension measurements of air-aqueous solution interfaces were done with a Wilhelmy plate tensiometer (Sigma 70 KSV Instruments Ltd) at room temperature (294-295 K). As a check the surface tension of pure water (72.3 ± 0.5 mN/m) was measured.

2.4 Ellipsometry

The thickness of the film was determined via *in situ* null ellipsometry. To this aim a Multiskop (Optrel Gbr, Berlin), controlled by a computer was used for the measurements. The light source is a He-Ne laser with wavelength of 632.8 nm and angle of incidence was 70° , which is the Brewster angle for the air-silicon interface (75°). The technique measures the change of the polarization state (parameters Δ and ψ) of a light beam upon reflection at an interface and from these parameters the layer thickness and the refractive index of the film can be obtained (32, 33). The program 'Ellipsometry' (version 1.31 - for Windows) written by Plamen Petrov (1997) was used for the numerical evaluation of the film thickness (h) and the refractive index of the film (n).

A four-layer model (silicon/ silicon oxide/aqueous film/air) was considered for the computation of the film thicknesses (h_{film}). The values of 3.85 and -0.02 were used for the real (n_i) and imaginary (k_i) parts of the refractive index of silicon, respectively (33). The refractive index of 1.46 was used for the silicon oxide layer. The thickness of the oxide layer of approximately 2 nm was determined. Silicon oxide and the liquid film were considered to be transparent (i.e. the imaginary part of the refractive index k_i was chosen null).

Adsorption of surfactant on a silica-water interface was also investigated by means of *in situ* null ellipsometry. In this case a silicon oxide strip was placed in a Teflon cell with glass windows. The cell was filled with water (or salt solution) and after adding a known amount of surfactant solution and stirring, a measurement was started. The ellipsometric angles Δ and ψ were recorded as functions of time until they

were reached stable values. The time for reaching stable values of Δ and ψ for the silica-water interface depends on the surfactant concentration, ranging from a few minutes for the concentrations of surfactant lower than 100 μM to a few hours for the concentrations of that higher than 400 μM . The general trend is that the higher the surfactant concentration the longer it takes to reach stable values.

A four-layer model (silicon/silicon oxide/adsorbed surfactant layer/aqueous solution of surfactant) was used for the numerical evaluation of the refractive index n_{ads} , the mean thickness h_{ads} of adsorbed surfactant layer, and the surface concentration per unit area, Γ . In these calculations, the surface concentration per unit area, Γ (not to be confused with the relaxation rate in equations 4 and 6) on the silica-water interface was determined using the expression (34):

$$\Gamma = (n_{ads} - n_{sol}) h_{ads} / (dn_{sol}/dc) \quad [7]$$

Here n_{sol} is the refractive index of the solution; dn_{sol}/dc is the refractive index increment of surfactant in aqueous solution. The refractive index of solution n_{sol} for each concentration of surfactant was measured with an Abbe refractometer (21 °C, white light), and the dn/dc of 0.1276 ml/g was obtained from the $n_{sol}(c)$ dependence.

The adsorption of surfactant at the air-water interface is determined via ellipsometry by using a glass beaker instead of a Teflon cell. The angle of incidence used in this case is 50°, which is close to the Brewster angle of the water-air interface. The measurements of the parameters Δ and ψ were performed separately for series of pre-prepared solutions with known concentrations of surfactant. The equilibration time for air-water interfaces was a few minutes for each concentration. The investigation of kinetics of adsorption of surfactant at the air-water interface by means of ellipsometry is a difficult task due to the high evaporation rate. However, the values of Δ and ψ were stable and did not change in time during 10-20 minutes. A three-layer model is used for the numerical calculations of Γ and h_{ads} (aqueous solution/adsorbed surfactant layer/air).

For low values of Γ and h_{ads} ($\Gamma < 1 \text{ mg/m}^2$ and $h_{ads} < 5 \text{ nm}$), it is difficult to simultaneously obtain the refractive index of the adsorbed layer and its thickness from the ellipsometric parameters. The reason for that is the small contrast in refractive index between the adsorbed layer and the bulk solution (33). This is the case for some measurements of surfactant adsorption on the silica-water interface. Therefore, we used a fixed value of 1.38 for the refractive index of the adsorbed layer of surfactant in order to calculate Γ and h_{ads} on air-water and silica-water interfaces. This value was an estimation based on literature data on similar systems and our own results for the adsorbed layer at the air-water interface. The refractive index of adsorbed layer of a similar di-block copolymer (PEO₁₀₆ B₁₆, B is polybutylene oxide) at hydrophobized silica has been found to be between 1.38 and 1.39, depending on the concentration of di-block copolymers (17). Unfortunately, there were no data on the refractive index of di- or tri-block copolymer surfactant at the air-water interface. We calculated the refractive index of the adsorbed surfactant layer for different concentrations of copolymer on the air-water interface from our ellipsometric measurements and found values ranging from approximately 1.348 up to 1.382 (results is not shown). Our maximum value of the

refractive index was close to the literature values of a similar di-block copolymer at hydrophobic silica given above (17). The molecular orientation of surfactant at hydrophobic solid surfaces and at air-water interfaces should be similar due to the hydrophobic interactions between PPO blocks and interfaces: PPO blocks form a dense layer at the interface and PEO blocks protrudes into the solution. Supposing that the refractive index of surfactant layers at hydrophobic silica and air interfaces are similar, a value of 1.38 was used for the refractive indexes of surfactant adsorbed layer at the air-water interface. The value for h_{ads} depends somewhat on the value used for the refractive index of the adsorbed layer. However, Γ is much less sensitive to n_{ads} because of the errors in the thickness and the refractive index (in equation 7) are covariant in such way that they cancel out to a large degree.

2.5 Thin liquid film pressure balance (TFB)

The interactions across wetting films formed from aqueous solution of a surfactant F127 are studied by means of the thin liquid film pressure balance technique (TFB). A schematic drawing of our set-up is shown in Figure 1.

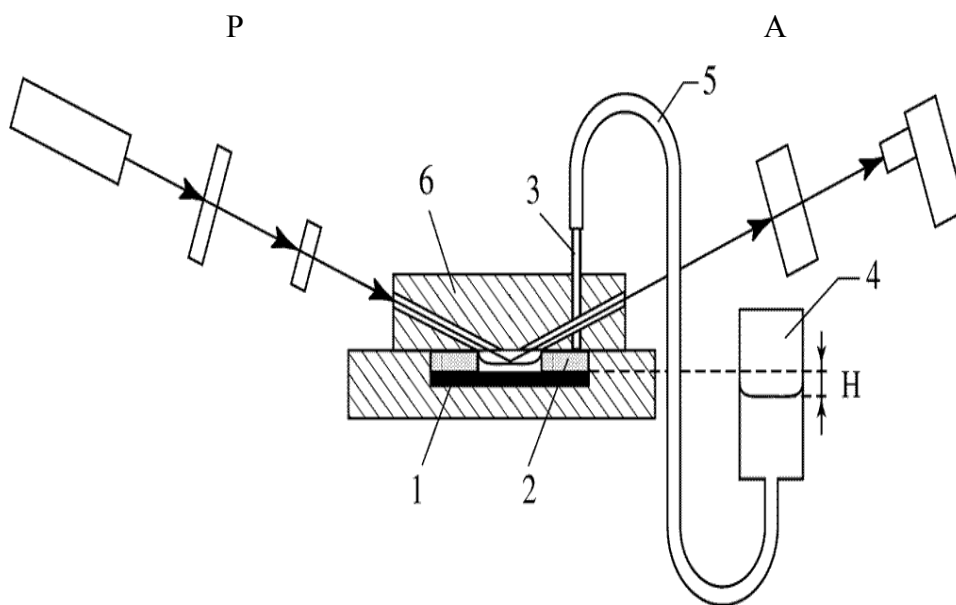


Figure 1 Thin-Film Balance. (1) silica sample plate, (2) porous glass disc, (3) glass tube, (4) glass vessel, (5) polyvinylchloride (Rauclair) tube, (6) plexiglas cell.

Arrows indicate the light beam; (A) analyzer, (P) polarizer.

A thin liquid film is formed on a silica surface (1) in a hole drilled in a porous glass disc (2) (Robu, Germany, pore size 4 μm), which is fused to the end of a glass tube (3) connected to a glass vessel (4) via a

polyvinylchlorid (Rauclair) tube (5). The film holder is enclosed in a covered Plexiglas cell (6) with narrow channels for the light beam. At equilibrium, the disjoining pressure is opposite and equal in magnitude to the hydrostatic pressure difference Δp_H :

$$\Pi(h) + p_H = 0 \quad [9]$$

The hydrostatic pressure difference is given by $\Delta p_H = \rho g H$, where ρ is the liquid density, g is the gravity acceleration and H is the height difference between the silica surface and the liquid in vessel (4) and has negative values as the level in the vessel is below the silica surface. H is measured with a cathetometer (Model AT11-N600, Japan). Repeating the procedure of increasing or decreasing the pressure (changing H) provides the data to map out the entire repulsive part of the disjoining pressure isotherm $\Pi(h)$; h is the film thickness. The typical waiting time between points of $\Pi(h)$ isotherm depends on the equilibration time. At low pressures (< 100 Pa) equilibration is very slow, and the waiting time can be a few hours (depending on the concentration of polymer). At higher pressures the thickness reaches a stable value more quickly (around 5-30 minutes).

3 Results

3.1 Static and dynamic light scattering

We used static light scattering (SLS) to determine the cmc values of surfactant in water and dynamic light scattering (DLS) to determine the size of the individual molecules of surfactants and micelles in the bulk solution. Upon increasing the concentration of surfactant we encountered a kink in the scattered intensity.

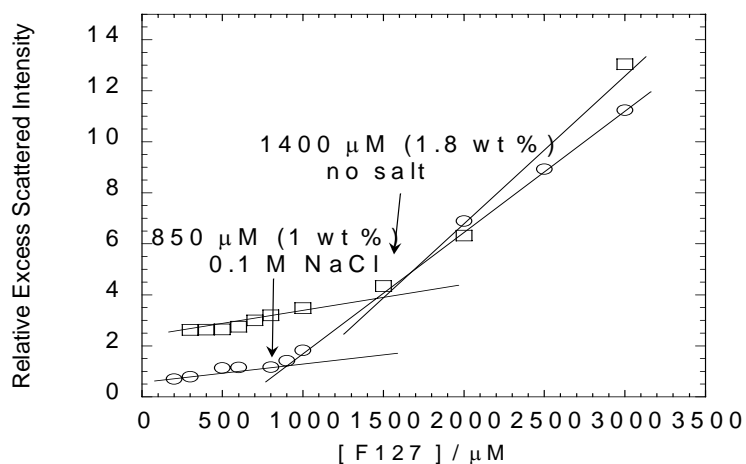


Figure 2 Relative excess scattered intensity at $\theta = 90^\circ$ vs. concentration of surfactant F127 at $T=22^\circ \text{C}$.

In Figure 2 the SLS results are shown. The critical micelle concentration of surfactant is determined from the intersection point of the two straight lines. The cmc equals 1400 μM (1.8 wt %) in a salt free solution and 850 μM (1 wt %) in 0.1 M NaCl. The relative excess scattered intensity was calculated as $(I - I_{\text{solvent}}) / I_{\text{toluene}}$, where I , I_{solvent} , I_{toluene} are scattered intensities of surfactant solution, water or NaCl solution, and toluene, respectively. Figure 3 represents plots of the distribution function $\Gamma G(\Gamma)$ versus the hydrodynamic radius R_H , as calculated from the correlation rate Γ using the Stokes-Einstein relation [5] for various concentrations of F127 at a background concentration of 0.1 M NaCl.

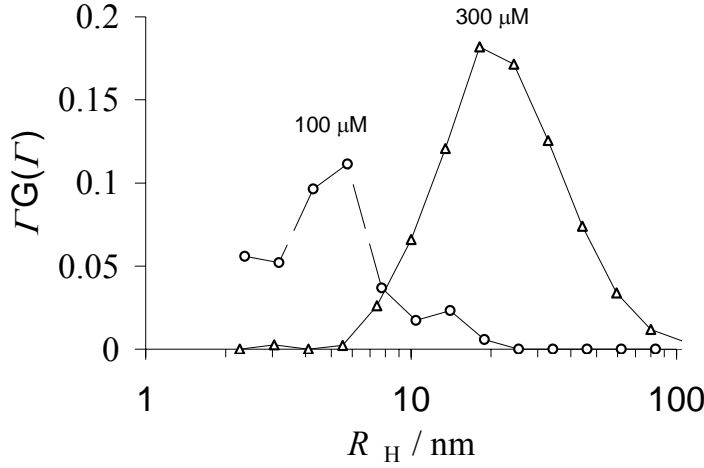


Figure 3 Distribution function $\Gamma G(\Gamma)$ versus hydrodynamic radius R_H different concentrations of F127 (shown on the figure) in 0.1 M NaCl at $T = 22^\circ\text{C}$.

For a 100 μM solution of F127 in 0.1 M of NaCl we observe unimers at $R_H \approx 5\text{-}6$ nm and a small peak at $R_H \approx 12\text{-}14$ nm presumably due to aggregates. The increase at small R_H ($\sim 1\text{-}2$ nm) is due to the numerical errors in the calculations. Increase of the surfactant concentration results in a more pronounced micellar peak ($R_H \approx 14\text{-}18$ nm).

Figure 4 shows the influence of salt on the size distribution of 100 μM surfactant.

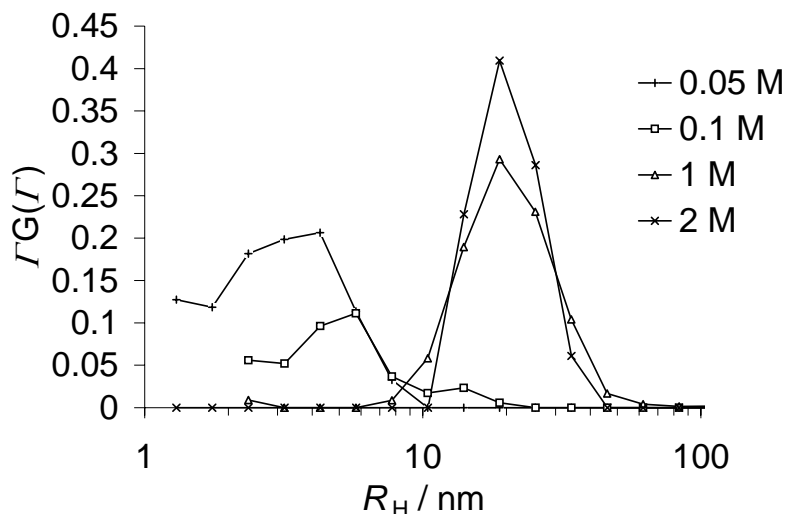


Figure 4 Distribution function $\Gamma G(I)$ versus hydrodynamic radius R_H of a 100 μM F127 solution at different concentrations of NaCl (shown on the figure) at $T = 22^\circ\text{C}$.

The unimer peak becomes smaller upon addition of salt. At a concentration of 0.05 M NaCl there is just a clear unimer peak with the maximum at $R_H \approx 3\text{-}4$ nm. At 0.1M NaCl the unimer peak becomes smaller with a maximum shifted to $R_H \approx 5\text{-}6$ nm, and a small peak at $R_H \approx 12\text{-}14$ nm appears which must be due to aggregates. The aggregate peak becomes more pronounced and the unimer peak vanishes completely at higher salt concentrations (1-2 M).

3.2 Adsorption of the surfactant at the air-water interface

Surface tension isotherms for the surfactant in water and in 0.1 M NaCl are presented in Figure 5. As found by others (see introduction), we obtain isotherms, which show two (not very clear) breaks. In the first and the third part of isotherm there is no significant difference between the solutions with and without 0.1 M NaCl. In the middle part, in the concentration range from about 1 until 100-200 μM , a decrease of γ is observed in the presence of 0.1 M NaCl. The concentration at which the second kink occurs (at 700-1000 μM) corresponds reasonably well with the SLS results.

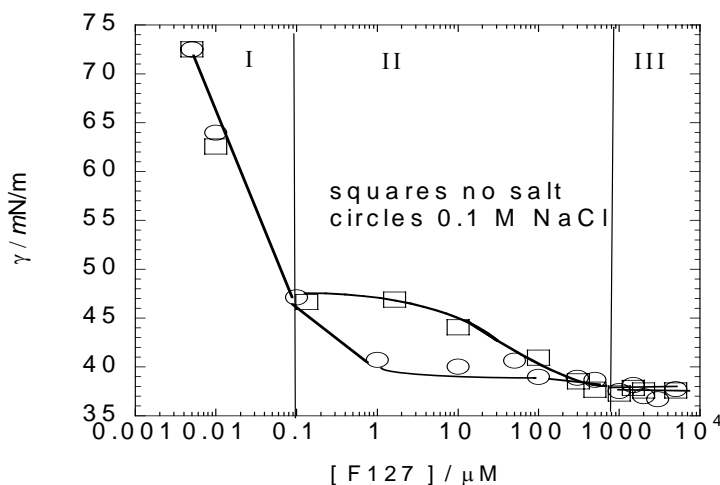


Figure 5 Surface tension as a function of the concentration of F127 at $T=22\text{ }^{\circ}\text{C}$.

The surface tension data are reported after 2 hours of equilibration, and this for each concentration of surfactant. However, we observed a slight decrease in surface tension after 2 hours for all concentrations. The decrease was about 1-2 % per hour of the nominal value measured at two hours. This decrease can be due to the polydisperse nature of the triblock copolymer sample. Our main criterion for establishing steady-state situation was the quasi constancy for values of the surface tension as obtained after 2 hours waiting time.

Figure 6 shows the thickness and the surface concentration of surfactant on the air-water interface obtained via the ellipsometric measurements. The h and Γ are given as a function of surfactant concentration in the absence and in the presence of 0.1 M NaCl.

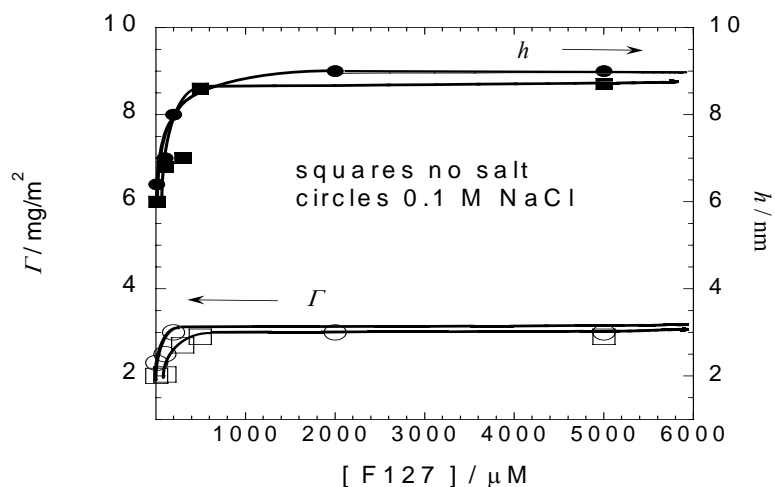


Figure 6 Surface concentration Γ (open symbols) and ellipsometric thickness h (black symbols) of surfactant on the air-water interface versus surfactant concentration at $T=22\text{ }^{\circ}\text{C}$.

We can see that the surface concentration increases up to a plateau value of 3 mg/m^2 . The plateau thickness is around 9 nm , which coincides with findings of Phipps et al. (21).

3.3 Adsorption of the surfactant at the silica-water interface

The adsorption of polymeric surfactant F127 on silica is studied by means of ellipsometry. In Figure 7 the surface concentration and the ellipsometric thickness of surfactant on the silica surface are shown.

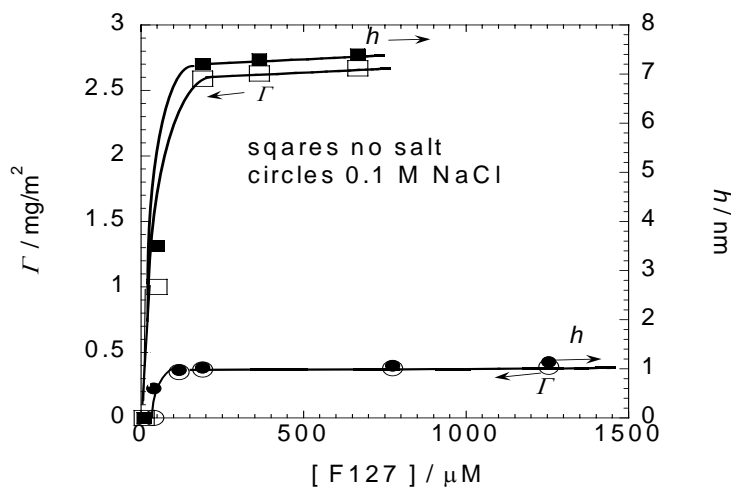


Figure 7 Surface concentration Γ (open symbols) and ellipsometric thickness h (black symbols) of surfactant at the silica-water interface versus surfactant concentration at $T=22\text{ }^{\circ}\text{C}$.

Both the layer thickness and the surfactant concentration are dramatically influenced by salt. Without salt the surface concentration of surfactant reaches a plateau value of 2.6 mg/m^2 and a layer thickness of 7.5

nm. In the presence of 0.1 M NaCl the surface concentration decreases almost sevenfold (0.4 mg/m^2) with a layer thickness of only 1 nm.

3.4 Disjoining pressure isotherms

Figure 8 displays the disjoining pressure isotherms for the films formed from 3 different concentrations of surfactant (100, 400, 1500 μM) in the presence of 10^{-4} M NaCl. We compare them with an isotherm measured for the film formed from only 10^{-4} M NaCl (without surfactant).

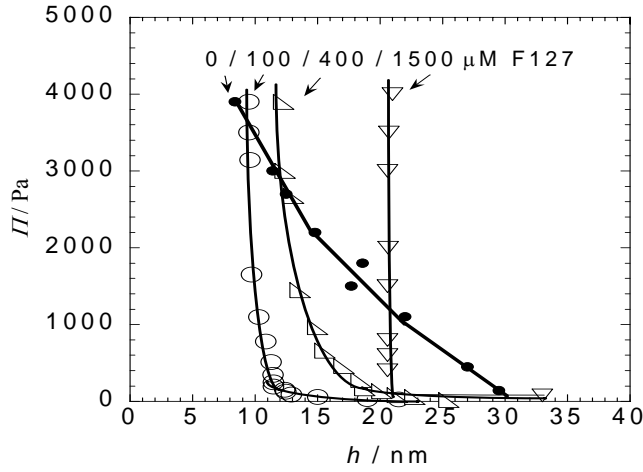


Figure 8 $\Pi(h)$ isotherms for asymmetric liquid films formed from surfactant solutions of different concentrations (100, 400, 1500 μM - open symbols) in 10^{-4} M NaCl in comparison with a film formed from only 10^{-4} M NaCl (black symbols) at $T=22^\circ\text{C}$.

For the latter case we observe a gradual repulsion between the interfaces ranging from 7 up to around 30 nm. This repulsion most likely has an electrostatic origin.

After subtracting the Van der Waals component ($\Pi_{\text{vdW}} = -A_H / 6\pi h^3$ with the Hamaker constant $A_H = -10^{-20}$ J for quartz/ aqueous film/ air (35)) from the measured disjoining pressure, we have plotted the resulting force curve obtained in the absence of polymer on a semi-logarithmic scale (results are not shown). A decay length of 10 nm was extracted from the slope ($\ln \Pi / h$) instead of the expected 30 nm for an electrolyte concentration of 10^{-4} M. The reason for this discrepancy between theoretically and experimentally obtained decay length can originate from the invalidity of the equation used for the electrostatic component of the disjoining pressure $\Pi = (\epsilon_o \epsilon \kappa^2 / 2\pi) \phi_1 \phi_2 e^{-\kappa h}$ for our system. Here ϵ_o is the vacuum permittivity, ϵ – the dielectric constant of solution, κ is the inverse of the Debye length, ϕ_1 and ϕ_2 are the potentials of the air-water and silica-water interfaces, respectively. The above equation is indeed based on the linear superposition approximation, which is not consistent with significant overlaps of the double layers as a-priori observed in the system investigated. Furthermore charge induced phenomena may

take place via surface charge regulation that may occur for distances well above κ^{-1} . In our case the surface of silica seems to have a very low surface charge and therefore very low surface potential at pH=6 (36, 37), whereas the surface potential at the air-water interface is shown to be around -30 mV (38, 39). This situation is very favourable for charge/ potential induction processes. One more reason can be our experimental uncertainty: for larger h and small Π where the exponential relation $\Pi \sim e^{-\kappa h}$ is expected to hold, it is extremely difficult to measure weak and slowly decaying interactions accurately.

By adding surfactant the behaviour of isotherms changed and they can be divided into 2 regions: the low pressure and the high-pressure regions. In the low-pressure region (< 300 Pa) we observe a gradual increase of the disjoining pressure with a decrease in the film thickness. In the high pressure region a steep increase in the disjoining pressure is seen, indicating strong repulsion between the surfaces. An increase in surfactant concentration shifts a steep part of isotherms to larger film thickness.

Figure 9 displays the disjoining pressure isotherms of four films formed from solutions of surfactant of different concentrations (50, 100, 200, and 300 μM) in 0.1 M.

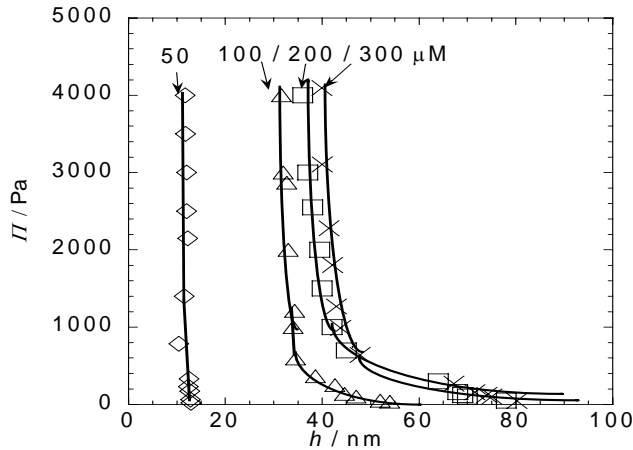


Figure 9 $\Pi(h)$ isotherms for asymmetric liquid films stabilized by a surfactant (50, 100, 200 and 300 μM) in 0.1 M NaCl at $T=22^\circ\text{C}$.

This salt concentration was chosen in order to suppress electrostatic contributions to the disjoining pressure ($\kappa^{-1} \approx 1$ nm for 0.1 M NaCl). A film formed from only 0.1 M NaCl without surfactant is not stable and breaks immediately. For all non-zero surfactant concentrations a steep increase in the disjoining pressure with decreasing distance is observed at high pressures. Similar fig. 8 an increase in surfactant concentration shifts a steep part of isotherms to larger film thickness. However a new feature is also observed: the thicknesses formed from 100, 200 and 300 μM have the values which are two time higher as compared to that of fig.8. This steep increase develops at various separations depending on the concentration of surfactant: 11 nm (50 μM), 32 nm (100 μM), 39 nm (200 μM), and 42 nm (300 μM).

Figure 10 shows the interactions in the asymmetric films formed from solutions of surfactant of fixed concentration (100 μ M) at different concentrations of NaCl.

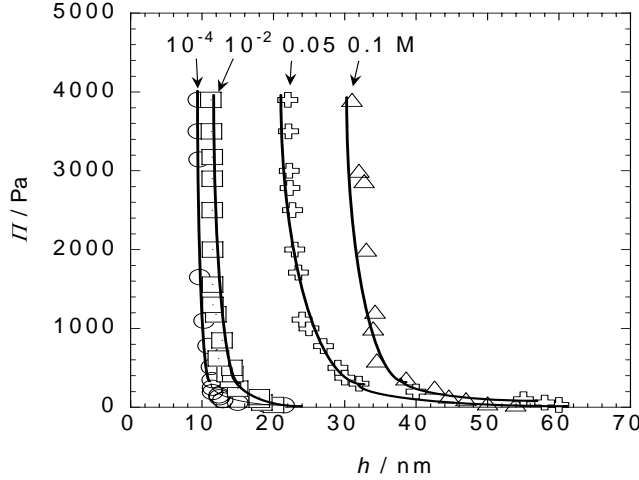


Figure 10 $\Pi(h)$ isotherms for asymmetric liquid films stabilized by a surfactant (100 μ M) in different concentrations of NaCl (10^{-4} , 10^{-2} , 5×10^{-2} , 10^{-1} M) at $T=22^\circ\text{C}$.

Repulsive forces are observed for all concentrations of NaCl. The addition of salt up to 0.01 M has almost no effect on the interactions in the films: a strong repulsion occurs at about 10 nm for 10^{-4} M NaCl and at 12 nm for 10^{-2} M NaCl. However, the repulsive curves shift to higher separations of 22 nm and 32 nm for 0.05 and 0.1 M, respectively. These ranges of the thicknesses are similar to that of fig. 9. At 1 M NaCl we could not obtain reproducible values of the thicknesses.

4 Discussion

4.1 Solution properties of the surfactant

From DLS and SLS results we have clear indication that the aggregation of surfactant molecules starts earlier in 0.1 M NaCl. This is in agreement with the reported data that the micellization of Pluronic type copolymers is salt dependent (see Introduction and Table 1). Our values are close to those of Desai et al (8) measured by surface tension and dye solubilization. Besides, from figures 3 and 4 it follows that the aggregates are observed at 100 μ M surfactant, which is 8 times below the cmc as found by SLS (in 0.1 M NaCl). For this concentration the distribution curve does not only show a pronounced unimer peak at $R_H \approx 5-6$ nm but also a small peak at $R_H \approx 12-14$ nm, which may indicate that some aggregates are formed. The micellar hydrodynamic radius was found to be 11-15 nm by others (8, 40). The number of aggregates is larger for 200 and 300 μ M surfactant. If we compare the $IG(I)$ distributions for surfactant in the presence of different concentrations of NaCl (fig.3), we can see the same trend as for increasing surfactant

concentration. The aggregation peak first occurs for 0.1 M NaCl and increases in size for higher salt concentrations. Taking into account that the Pluronic sample is polydisperse, these results are not surprising. A small but relatively hydrophobic fraction forms the first aggregates, and a true micellar solution develops gradually. Salt shifts all these effects to lower surfactant concentrations because NaCl decreases the solvent quality of the aqueous solution with respect to the EO blocks (salting-out effect (41)).

Clearly, the cmc of surfactant goes down with increasing electrolyte concentration. At fixed surfactant concentration we pass from $C_{F127} < \text{cmc}$ to $C_{F127} > \text{cmc}$ upon adding NaCl,

4.2 Adsorption of the surfactant at the air-water interface

As was already mentioned in the introduction it is problematic to obtain the adsorbed amount of surfactant at the air-water interface and the area per molecule from the surface tension isotherm. One of the reasons is the polydispersity, which makes the use of the Gibbs equation for the determination of the adsorbed amount rather dubious. Nevertheless procedures for that purpose can be found in the literature (skipping the first part of the isotherm). The authors of ref (29) obtained values for the adsorbed amount via the Gibbs equation [2]. The thickness of the adsorbed layer was estimated using De Gennes' scaling theory for polymer brushes (42, 43). Values of 5.95 mg/m² for the adsorbed amount and 14.6 nm for the layer thickness were obtained for surfactant in the absence and in the presence of salt. If we would use the same procedure we would find a value for the adsorbed amount which is 2.5 times higher than our ellipsometric finding, but similar to the value of reference (29). From the ellipsometric measurements we extracted a value for the plateau of the adsorbed amount of 3 mg/m² and a layer thickness of 9 nm with and without 0.1 M NaCl. A similar adsorbed amount of surfactant (2.9 mg/m²) was reported at the hexane-water interface (21). It is expected that the behaviour of F127 at air-water interfaces is similar as at hexane-water interface. Malmsten et al.(22) reported values of Γ_{F127} of around 2-2.3 mg/m² on hydrophobized silica, which is close to our Γ obtained via ellipsometry. We think that adsorbed amounts obtained from ellipsometric measurements are more reliable than results obtained from the surface tension. The initial increase in the adsorption isotherms (Figure 6) seems to be somewhat steeper in the presence of NaCl. This can be explained by a salting out effect, which is known for PEO molecules (41) as well as for PEO containing complexes (44).

4.3 Adsorption of the surfactant at the silica-water interface

It is commonly believed that the EO segments of the triblock copolymers have the highest surface affinity for a hydrophilic surface and that the triblock-copolymer adsorbs in a pancake conformation. In other words, the adsorption of PEO-PPO-PEO triblock surfactants is predominantly determined by interactions of PEO with silica: by hydrogen bridges between the surface silanol groups with the oxygen of the polyethylene oxide (-SiOH... (-OCH₂CH₂-)). In agreement with that, small layer thicknesses of surfactant at silica were found (23, 45). However, similar to Eskilsson and Tiberg (24) we found higher values of Γ and h at the silica-water interface without NaCl. The plateau value of the adsorbed amount at

silica is comparable with that at the air-water interface. The larger values of Γ and layer thickness at higher concentrations may be explained by micellar or bilayer structures. Such structures at silica may result from hydrophobic interactions between PPO groups. The authors of ref (24) found even a higher value for the plateau layer thickness of F127 (12-14 nm) but a lower adsorbed amount (1.5 mg/m^2) as compared with our data. The differences in the adsorbed amounts may be due to differences between the surfaces. Eskilsson and Tiberg used silicon wafers, which were oxidized thermally at 900°C . It is known that heating above 400°C leads to some irreversible dehydroxylation giving siloxane groups (46). In our experiment we used silicon wafers with the natural oxide layer, which probably has higher silanol content than the thermally oxidized layers.

Our experimental data on surfactant adsorption at the silica-water interfaces reveal a strong salt effect: 0.1 M NaCl clearly decreases the adsorbed amount. This is in contrast to the air-water interface. This finding is not surprising, taking into account the degree of dissociation of silanol groups on silica. It is a well-known fact that the degree of dissociation of silanol groups in aqueous solution increases with increasing pH and ionic strength (37, 47, 48). Hence, adsorption of surfactant decreases upon increasing pH or ionic strength due to a deprotonation of silanol binding sites. Van der Beek (47) and Tiberg (37) found that the adsorption of PEO and PEO-containing non-ionic surfactants (C_{12}EO_8) on silica decreases upon increasing pH or ionic strengths.

4.4 Interaction forces within the film stabilized by the surfactant

The disjoining pressure isotherms for asymmetric films containing 10^{-4} M NaCl and the surfactant show only repulsive forces between two surfaces. This repulsion can have an electrostatic and a steric origin. The electrostatic repulsion between interfaces might occur if the interfaces of the film carry charges.

It is under discussion that the air-water interface has a negative charge, which arises due to preferential adsorption of OH^- ions. The potential (-30 mV) at the air-water interface for foam films stabilized by non-ionic surfactant Pluronic F108 in 10^{-4} M NaCl was measured and discussed (49). However, the mechanism of OH^- adsorption is not fully clear. Some propositions are advanced in the literatures. Stubenrauch et al (50) considered that the adsorption of OH^- ions is driven by the specific dynamic water structure at the interface, and/or surface reactions. He proposed the interface charge is reduced by the adsorption of surfactant via switching off the surfaces reactions. Manev et al. (51) give a different explanation: he argues that a decrease in the diffuse electrical layer potential at the air-water interface in the presence of non-ionic surfactants is governed by a displacement of ions (H^+ and OH^-) from the surface, as species foreign to the adsorption layer structure.

The negative charges of silica stem from the deprotonation of silanol groups ($\text{SiOH} \rightleftharpoons \text{SiO}^- + \text{H}^+$) and are determined by the pH and by the ionic strength in the solution. The charge starts to increase strongly above $\text{pH} \sim 5$ (36, 52). It is measured that at pH 6 the surface potential changes from -25 mV in 0.001 M KCl up to -75 mV in 0.1 M NaCl (36). The decrease of the surface charge upon adsorption of non-ionic surfactant

might be attributed to the decrease in the dielectric constant of the molecular environment close to the silanol groups, which reduces the dissociation degree and thus the charge density (53).

Therefore, there are indications that an air-water and a silica-water interface are negatively charged and that the adsorption of non-ionic surfactants might lead to a decrease of the surface charge density at the interfaces of asymmetric film studied in the present work. This can explain a strong decrease of the repulsion at large thicknesses when the surfactant is added (fig. 8).

At higher pressures the double layer forces overcome but strong repulsion remains. This repulsive force most likely comes from the surfactant adsorbed at interfaces of the film. The film thickness obtained from the steep part of isotherms of fig. 8 reflects the combined thickness of the adsorbed layers on both interfaces. Indeed, at the air-water interface we observed an increase of the layer thickness up to 9 nm when increasing the concentration of surfactant (fig. 6). The surfactant adsorbed on the silica-water interface yields a thickness up to 7.5 nm depending on the concentration of surfactant (fig. 7). In figure 11 we plotted the thickness of the film measured at a constant Π (curve 1) together with the total thickness of adsorbed layers of surfactant at interfaces of the film (curve 3) versus the concentration of NaCl at a fixed surfactant concentration (100 μ M). It is seen that whereas the sum of the thicknesses of the adsorbed layers decreases slightly upon increasing the concentration of salt, the thickness of the film increases strongly.

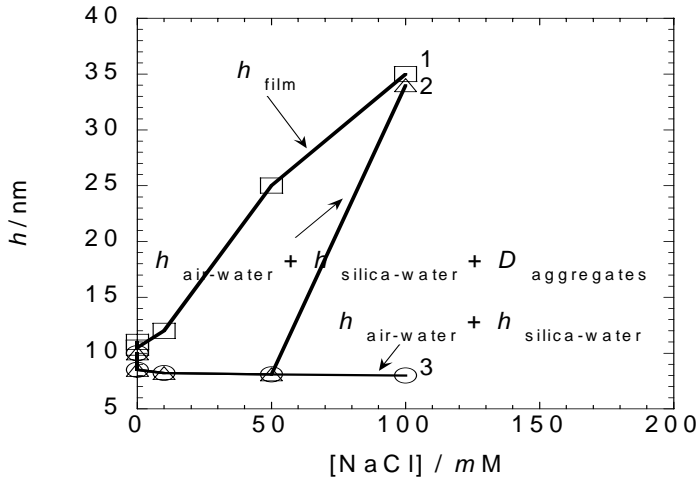


Figure 11 Thickness of the asymmetric film h_{film} at $\Pi = 1\text{kPa}$ (1) compared with the total thickness of adsorbed layers on both interfaces $h_{ads. layers}$ with (2) and without (3) aggregates in between (D is the diameter of aggregates measured by DLS) versus NaCl concentration. $C_{F127}=100\mu\text{M}$.

It is clear that the thickness of the film increases with salt concentration and only adsorbed layers cannot explain the larger film thicknesses observed upon increasing the concentration of NaCl. This effect of salt

on the thickness of the film may have a similar origin as in reported data of the unexpected salt effect in symmetric films made of non-ionic surfactants²³⁻²⁵. Our explanation of this phenomenon is based on the DLS measurements described in section 3.1. At 100 μM surfactant we observed aggregates of a diameter of 24-28 nm. The aggregates increase in size and in number upon increasing the surfactant or salt concentration. Probably, these aggregates play a role in the film structure, and the unexpected film thickness may be explained by the trapped aggregates (with salt-dependent sizes) between the two adsorbed layers. In fig.11 we are also plotted the thickness of two layers of surfactant adsorbed at interfaces of the film plus the diameter of the micelles (measured via DLS) in between them measured (curve 2). Indeed, in 0.1 M NaCl the thickness of the film coincides with the sum of the layers adsorbed together with the aggregates in between them.

This feature is even clearer in fig. 12, where we plotted the thicknesses versus the concentration of surfactant in 0.1 M NaCl. Here *curve 1* reflects the thickness of the film; *curve 3* shows the total thickness of the surfactant layers adsorbed on both interfaces and *curve 2* presents the thickness of adsorbed layers of surfactant on both interfaces plus trapped micelles (of the size measured by DLS) in between.

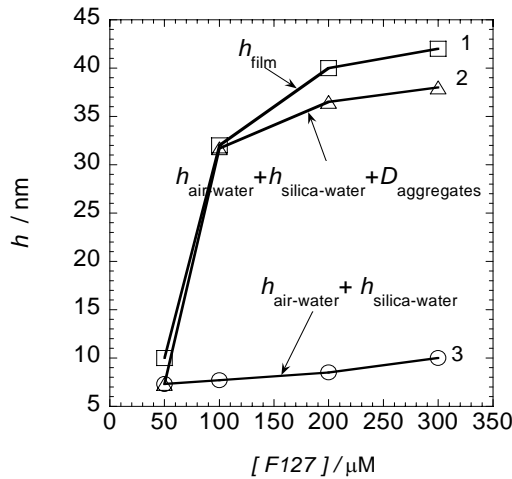


Figure 12 Thickness of the film h_{film} at $\Pi = 1\text{kPa}$ (1) compared with the total thickness of adsorbed layers on both interfaces $h_{\text{ads.layers}}$ with (2) and without (3) aggregates in between (D is the diameter of aggregates measured by DLS) versus the concentration of surfactant at 0.1 M NaCl.

A large difference between the sum of the adsorbed layers thickness (*curve 3*) and the thickness of the film (*curve 1*) becomes less pronounced when we assume the film contains a layer of trapped micelles with a size $D_{\text{aggregates}}$ (*curve 2*).

In order to summarize our findings, we plotted possible structures of the films, which might form in different conditions (fig.13).



Figure 13 Possible structures of asymmetric liquid films stabilized by surfactant.

Case (a) reflects the structure of the film when the concentration of surfactant below the cmc ($< 850 \mu\text{M}$) and when the concentration of NaCl does not exceed 0.05 M. A flat conformation of surfactant on silica is most probable in these conditions. Case (b) reflects the possible structure of the film when the concentration of surfactant is higher than the cmc and the concentration of salt smaller than 0.05 M. Bi-layer or micelle-like structure of surfactant on silica is very possible in these conditions. Therefore, the films have higher thicknesses as compared to that case (a). Case (c) reflects the possible structure of the film when the concentration of surfactant is higher than the cmc and the concentration of NaCl is higher 0.05 M. In these conditions aggregates are trapped between the interfaces of the film and as a result of that govern the interactions in the films. Expected thicknesses are higher as compared to cases (a) and (b).

Yet, an unexplained point is observed in Figure 11 at 0.05 M NaCl. From the DLS measurements we observed an increase of a micellar peak upon increase of the NaCl concentration at a given surfactant concentration. Nevertheless, aggregates are not yet seen for 0.05 M of NaCl (fig. 4). One therefore expects values of the thickness of the film are close to the values of the thickness of the adsorbed layers without aggregates in between. A tentative explanation is that the structure of surfactant inside a film is more complex than just adsorbed layers and trapped aggregates between them. The structure of adsorbed layers inside thin films might be different from the structure of separately measured adsorbed layers of surfactant.

Conclusions

We studied the behaviour of triblock copolymer surfactant F127 in solution, at air-water and silica-water interfaces and in thin aqueous films on a silica surface. The cmc of the surfactant in aqueous solution, its adsorption on silica-water interface and the thickness of the films formed from this surfactant are strongly influenced by the salt concentration. Presence of 0.1 M NaCl decreases the cmc by a factor of

two, the adsorbed amount at silica by a factor of seven, and increases the thickness of the films by a factor of three.

Stable films are formed for all studied ranges of the surfactant concentration and the salt concentration. The thicknesses of the films stabilized by the surfactant can be explained by steric interactions when the concentrations of NaCl concentrations smaller than 0.05 M. The range of these interactions increases with the concentration of the surfactant. This is explained by an increased adsorbed amount of the surfactant on both interfaces of the film.

A pronounced increase in the thicknesses of the film stabilized by the surfactant is measured when increasing the concentration of NaCl. This is similar to what was found in several investigations on symmetric films stabilized by various types of non-ionic surfactants. We proposed that the trapped aggregates between the two adsorbed layers could explain the thickness of these films.

References

1. V. Bergeron, *Condens. Matter* **11**, R215-R238 (1999).
2. J. N. Israelachvili, *Intermolecular and surface forces* (Academic press, San Diego, 1992).
3. V. K. Aswal, R. S. G. Kohlbrecher, P. Bahadur, *P. Chem. Phys. Lett.* **349** (2000).
4. Y. Su, H. Liu, Q. Wang, J. Chen, *Langmuir* **18**, 865-871 (2002).
5. Y. Su, X. Wei, H. Liu, *J. Colloid Interface Sci.* **264**, 526-531 (2003).
6. C. Wu, H. Liu, B. Chu, *Macromolecules* **30**, 4574-4578 (1997).
7. N. Pandit, T. Trygstad, S. Croy, M. Bohorguez, C. J. Koch, *J. Colloid Interface Sci.* **222**, 213-220 (2000).
8. P. R. Desai, N. J. Jain, R. K. Sharma, P. Bahadur, *Colloids Surf.:A* **178**, 57-69 (2001).
9. P. Alexandridis, J. F. Holtzwarth, T. A. Hatton, *Macromolecules* **27**, 2414 (1994).
10. G. Wanka, H. Hoffman, W. Ulbricht, *Colloid Polym. Sci.* **268**, 101 (1990).
11. G. Wanka, H. Hoffman, W. Ulbricht, *Macromolecules* **27**, 4145-4159 (1994).
12. P. Linse, M. Malmsten, *Macromolecules* **25**, 5434 (1992).
13. P. Alexandridis, V. Athanassiou, S. Fukuda, T. A. Hatton, *Langmuir* **10**, 2604-2612 (1994).
14. P. Alexandridis, J. F. Holtzwarth, T. A. Hatton, *Macromolecules* **27**, 2414-2425 (1994).
15. J. Chen, M. Even, Z. Chen, *Macromolecules* **36**, 4478-4484 (2003).
16. P. Linse, T. A. Hatton, *Langmuir* **13**, 4066 (1997).
17. B. Rippner, K. Boschkova, P. M. Claesson, T. Arnebrant, *Langmuir* **18**, 5213-5221 (2002).
18. R. Sedev, R. Steitz, G. H. Findenegg, *Physica B* **315**, 267-272 (2002).
19. R. Sedev, D. Exerowa, G. H. Findenegg, *Colloid Polym. Sci.* **278**, 119-123 (2000).
20. M. Munoz, F. Monroy, F. Ortega, J. Rubio, D. Langevin, **16**, 1083-1093 (2000).
21. J. S. Phipps, R. M. Richardson, T. Cosgrove, A. Eaglesham, *Langmuir* **9**, 3530-3537 (1993).
22. M. Malmsten, P. Linse, T. Cosgrove, *Macromolecules*, 2474-2481 (1992).
23. J. A. Shar, T. M. Obey, T. Cosgrove, *Colloid and Surfaces A:Physicochem.Eng. Aspects* **150**, 15-23 (1999).
24. K. Eskilsson, F. Tiberg, *Macromolecules* **31**, 5075-5083 (1998).
25. T. Van den Boomgaard, J. Lyklema, *Langmuir* **5**, 245 (1989).
26. P. A. Barneveld, J. M. H. M. Scheutjens, J. Lyklema, *Colloid Surfaces* **52**, 107 (1991).
27. H. J. Müller, T. Rheinländer, *Langmuir* **12**, 2334-2339 (1996).
28. B. Diakova, C. Filiatre, D. Platikanov, A. Foissy, M. Kaisheva, *Advances in Colloid and Interface Science* **96**, 193-211 (20.01.2005, 2002).
29. B. Diakova, M. Kaisheva, D. Platikanov, *Colloids and Surfaces A:Physicochem.Eng. Aspects* **190**, 61-70 (2001).
30. B. Diakova, D. Platikanov, R. Atanassov, M. Kaisheva, *Advances in Colloid and Interface Science* **104**, 25-36 (20.01.2005, 2003).
31. D. Exerowa *et al.*, *Adv. Colloid and Interface Sci.* **104**, 1-24 (2003).

32. R. M. Azzam, N. M. Bashara, *Ellipsometry and Polarized Light* (Amsterdam, 1989), vol. North-Holland.
33. H. G. Tompkins, *A User's Guide to Ellipsometry* (Academic Press, Inc., San Diego, 1993).
34. J. A. De Feyter, J. Benjamins, F. A. Veer, *Biopolymers* **17**, 1759-1772 (1978).
35. J. Lyklema, *Fundamentals of Interfaces and Colloid Science*, FICS (Academic press, London, 1991), vol. I, A 9.4.
36. T. Goloub, L. K. Koopal, *Langmuir* **13**, 673-681 (1997).
37. F. Tiberg, University of Lund (1994).
38. P. K. D. Exerowa, *Foam and Foam Films* (Elsevier Science B.V., Amsterdam, 1998).
39. E. D. Manev, Pugh, R. J., *Langmuir*, 2253-2260 (1991).
40. T. Liu, V. Nace, B. Chu, *Langmuir* **15**, 3109-3117 (1999).
41. F. E. Beiley, J. V. Koleske, *Poly(ethylene oxide)* (Academic press., New York, 1976).
42. P. G. de Gennes, *Macromolecules* **13**, 1069 (1980).
43. S. Alexander, *J. Phys. (Paris)* **38**, 983 (1977).
44. S. V. Solomatin, T. K. Bronich, A. Eisenberg, V. A. Kabanov, A. V. Kabanov, *Langmuir* **20**, 2066-2068 (2004).
45. C. G. P. H. Schroën, M. A. Cohen Stuart, K. van der Voort Maarschalk, A. Van der Padt, K. Van't Riet, *Langmuir* **11**, 3068-3074 (1995).
46. J. Rubio, J. A. Kitchener, *J. Colloid Interface Sci.* **57**, 132-142 (1976).
47. G. P. Van der Beek, M. A. Cohen Stuart, *J. Phys. (Paris)* **49**, 1449 (1988).
48. B. H. Bijsterbosch, *J. Colloid Interface Sci.* **47**, 186-198 (1974).
49. D. Exerowa, P. Kruglyakov, *Foam and Foam Films* (Elsevier, 1998).
50. C. Stubenrauch, O. J. Rojas, J. Schlarmann, P. M. Claesson, *Langmuir* **20**, 4977-4988 (2004).
51. E. Manev, R. J. Pugh, *Langmuir* **7**, 2253-2260 (1991).
52. H. Shirahama, J. Lyklema, W. J. Noorde, *J. Colloid Interface Sci.* **139**, 177-187 (1990).
53. C. R. O. Stubenrauch, J.; Schlarmann, J.; Claesson Per M., *Langmuir*, 4977-4988 (2004).

Chapter 3 Thinning of wetting films stabilized by a non-ionic surfactant

ABSTRACT

We investigated the thinning of wetting films formed from aqueous solution of non-ionic triblock copolymer Pluronic F127 on the surface of silica using a home-made thin-film balance and time-resolved ellipsometry. Imaging ellipsometry was used to visualize the film structures at subsequent stages of their development. The results unambiguously show that the time required for the formation of steady films strongly depends on the electrolyte concentration. When increasing the latter from 10^{-4} to 0.1 M, this time typically increases with several orders of magnitude, from a few minutes to several hours. Moreover, for sufficiently large amounts of salt, two characteristic relaxation regimes can be clearly identified. After initial quick thinning, further thinning slows down enormously. These typical kinetic regimes are thought to result from the coupled dependencies of the bulk and interfacial properties of F127 on salt concentration. Possible explanations of the phenomenon are discussed.

1 Introduction

It is known that with polymer-mediated surface forces non-equilibrium effects are often important because of the sluggish adsorption and desorption of polymers. The interactions between interfaces with adsorbed polymer layers often exhibit hysteresis and/or time-dependence (1). The results presented in the current paper are in line with these effects. In our previous investigation (2) we found thick wetting films on silica formed from an aqueous solution of the triblock copolymer Pluronic F127 (PEO₉₉-PPO₆₅-PEO₉₉). In contrast with (3-5), we observed a pronounced increase of the thickness upon increasing of the NaCl concentration at a constant hydrostatic pressure (2). This observation was rather unexpected; firstly, because electrostatic repulsion diminishes upon increase electrolyte concentration, secondly, because the amount of adsorbed F127 at silica was shown to decrease with increasing NaCl concentration. Therefore, one would expect that the range of repulsion between the surfaces would decrease. The large film thickness observed at higher electrolyte concentrations was thought to be associated with the presence of trapped aggregates within the film. In the present paper we establish that this large thickness is not static but relaxes very slowly towards lower values. In order to obtain a more detailed picture of these features, we studied the thinning behavior of the films over time, at a fixed hydrostatic pressure and temperature. To either confirm or refute the effect of micelles on the kinetics of film thinning, different concentrations of F127 (below, at, above the critical micelle concentration) were considered.

2 Experimental section

2.1. Materials

The polymeric surfactant (triblock copolymer) Pluronic F127 (average molecular composition PEO₉₉PPO₆₅PEO₉₉, Sigma-Aldrich CO., USA) was used without further purification. Pluronic F127 has a number-average molar mass, M_n of 12600 and a PEO content of 70% by weight. Further in the text the term of ‘polymeric surfactant’, or ‘surfactant’, or ‘F127’ is used for the triblock copolymer. Aqueous solutions of F127 were prepared by dissolving the polymer in demineralised water under gentle agitation. Sodium chloride, NaCl (purity min 99.99% supplied by J.T. Baker Chemicals B.V., Holland) was used without further purification. The water used is purified using a two-stage deionization processes (ion exchanger/active carbon), supplied by a “Barnstead pure UV system” (USA). After deionization, the water is filtered through a 0.2-micron filter. It produces water with a resistivity of 18.3 Megohm-cm (MΩcm).

All measurements were carried out at pH \approx 6 and $T \approx$ 21-23°C.

Polished silicon plates, Si (p-type, boron-doped, oriented <1-0-0>, resistivity 12-18 Ωcm) were purchased from Wafer Net, Germany. The thickness of the natural silicon oxide SiO₂ layer on the surface was about 2 nm, as determined by ellipsometry. Wafers were cut into small slices and boiled for 5 min at 80°C in a

mixture of 25% NH_3 , 30% H_2O_2 and H_2O (1:1:5 by volume). The slices were then rinsed with water and ethanol (99.8%). They were kept in a closed container under water until use. Before the slices were placed in the cell, they were dried with a stream of nitrogen and treated for 30 seconds in a plasma cleaner (Harrick, Model PDC-32 G). The plasma treatment was performed with air (10 Pa). The contact angle of water was always lower than 10° , indicating the hydrophilic nature of the silicon oxide surface. All measurements were carried out at $\text{pH} \approx 6$ and $T \approx 21\text{-}23^\circ\text{C}$.

2.2. Thin Film Balance (TFB)

The TFB technique was used to measure the thinning of films. This technique, based on the original design of Mysels and Jones (6), was developed and described for wetting films by Shishin and Derjaguin et al (7, 8). A schematic drawing of the TFB used in the current study is given in Figure 1.

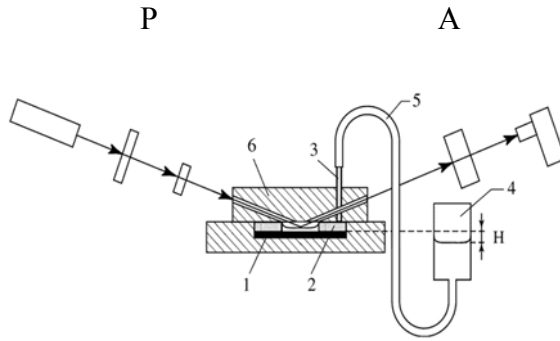


Figure 1 Thin-Film Balance. Explanation is given in the text.

A thin liquid film is formed on a silica surface (1), in a hole of 0.5 cm drilled in a porous glass disc (2) (Robu, Germany, pore size $4\mu\text{m}$), which is fused to the end of a glass tube (3). The latter is connected to a glass vessel (4), via a polyvinylchlorid (Rauclair) tube (5). The film holder is placed inside a covered Plexiglas cell (6). The Plexiglas cover and the porous discs have narrow channels and grooves for the incident and reflected light beams. The silica plates and porous glass disc were saturated for a night in a F127 solution before TFB measurements. Manipulation of the hydrostatic pressure changes the disjoining pressure in the film. At equilibrium, the disjoining pressure, Π is opposite and equal in magnitude to the hydrostatic pressure p_H :

$$\Pi(h) + p_H = 0$$

The hydrostatic pressure is given by $p_H = \rho g H$, where ρ is the liquid density, g is the gravitational acceleration and H is the height difference between the silica surface and the liquid in vessel (4) and has negative values as the level in the vessel is below the silica surface. H is measured with a cathetometer

(Mitutoyo, Model AT11-N600, Japan). In the film thickness relaxation experiments an applied hydrostatic pressure of -4.5 kPa (H is negative) was switched on after which thinning of the film was followed by ellipsometry.

2.3 Ellipsometry

Ellipsometry measures variations of the polarization state of light reflected from interfaces. The experimental data are expressed in terms of the ellipsometrical angles ψ (where $\tan \psi = |r^p|/|r^s|$ is the amplitude ratio of the parallel (p) and perpendicular (s) reflection coefficient,) and Δ (the change in the phase difference that occurs upon reflection). These are related to the Fresnel reflection coefficients r^p and r^s , for p- and s-polarized light as $r^p/r^s = \tan \psi e^{i\Delta}$. These coefficients are complex functions of the angle of incidence, the wavelength, the optical properties of the substrate, the ambient medium, the layers and the thickness of the layers. Details can be found elsewhere (9).

The ellipsometric angles were determined via *in situ* null ellipsometry. In null ellipsometry, the polarizing elements (P - stands for polarizer, A – stands for analyzer in Figure 1) are rotated until the signal at the photo-detector is minimized (“nulled”). A Multiskop instrument (Optrel Gbr, Berlin) controlled by a computer was used for the measurements. The light source was a He-Ne laser with wavelength of 632.8 nm. Because of some differences between the available porous discs, we measured at angles of incidence varying between 65° and 70°, which is close to the Brewster angle for an air-silicon interface (75°). The ellipsometric angles were recorded as a function of time until a steady state was reached.

A four-layer model {silicon/ silicon oxide/aqueous film/air} was considered for the computation of the film thickness, h_{film} . In the calculations of the film thickness, predetermined values for the refractive indices of silicon (3.85), silica (1.46), aqueous solution (n_{sol}) and air (1.00), as well as for the thickness of the silica layer (2 nm) were used. In this model the thickness of the film h_{film} is calculated under the assumption that the film is homogeneous and has the refractive index of the solution n_{sol} , which was measured with an Abbe refractometer for each polymer concentration (21° C, white light). It is also possible to compute the film thickness using the six layer model: silicon ($n=3.85$)/ silicon oxide ($n=1.46$, $h=2$ nm)/F127 adsorbed layer at the silica-water interface / aqueous film/ F127 adsorbed layer at the air-water interface /air. In this model the film is “divided” into sub-layers: F127 layer at the air-water interface ($n=1.38$, $h_1 \sim 7$ nm (2))/ aqueous core (n_{sol} depends on the C_{F127} , h_2 should be calculated) / F127 layer at the silica-water interface ($n=1.38$, h_3 is taken from our previous data (2)), where the h_{film} equal to the sum of these sublayers: $h_1 + h_2 + h_3$. In the beginning we calculated the h , using both models. However, the difference between the film thicknesses obtained from two models was always smaller than 2.5 %. For that reason, we used the first model (four layer) for the determinations of the film thickness in this work. While the accuracy of the calculated sample parameters such as the adsorbed layer thickness (h_{ads}) or the film thickness (h_{film}) as well as the index of refraction (n_{ads} or n_{film} , respectively) depends on the assumed model, trends in these parameters are even less sensitive to the model. It should be noted that the computation of thickness of the wetting film is more accurate than the thicknesses of the surfactant films at interfaces of the film. The

choice of the refractive indexes of the adsorbed polymer layer influences strongly the value obtained for the thickness of the adsorbed layer. We used the value 1.38 for the refractive index of the adsorbed layers at interfaces. This value was an estimation based on literature data for similar systems and our own results. More details are discussed in our previous publication (2).

2.4 Ellipsometric imaging

By adding an objective and a detector, e.g. a sensitive CCD (charge-coupled device) camera to an ellipsometer, one can obtain an image of the surface. The objective images the illuminated area of the sample onto the camera. Areas that have different optical properties cause a different signal in the camera image. Especially those areas that are currently fulfilling the condition of the ellipsometric “null”, i.e. where the optical parameters are such that the light reflected is extinguished for the particular setting of polarizer, compensator and analyzer will appear dark in the image. With the nulling mode, the signal on an area of the sample surface can be minimized, while simultaneously patches that do not satisfy the ‘null’-conditions appear as bright areas. Hence, inhomogenities and/or microstructures can be detected and analyzed with high sensitivity. More details can be found elsewhere (10).

The imaging part consists of an objective with a large working distance (Mitutoyo, M Plan Apo 10×: 378-803-2, Japan) and a CCD camera (KAMO2, 480×640 pixel sensor, EHD Physikalische Technik, Germany). Before obtaining each image, the analyzer and polarizer were put in the nulling position. This implies that dark patches in the image have a thickness corresponding to the average ellipsometric thickness. Brighter patches are either thicker or thinner. Because contrast was optimized in the images, the images provide no information on the magnitude of the variation of the film thickness. The field of view is about 640×960 μm. To decrease a high intensity of the light reflected from some parts of the film, optical density filters (OD 0.60/OD 0.80, Newport corp., U.S.A) were mounted in front of the laser.

3 Results

3.1 Surfactant F127 at interfaces of the film and in aqueous solutions

Prior to the analysis of the kinetics of wetting films, we discuss the behaviour of F127 in aqueous solutions and at the two interfaces of the film. Tables 1 and 2 summarize the results pertaining to the solution properties of F127 and the thickness of the adsorbed layers at interfaces of the film (the thickness of wetting films is not shown here). Some of the results are taken from our previous work (2), some are new. Those pieces of information will be required for the interpretation of the thickness and the thinning behavior of wetting films.

Self-assembly occurs at lower F127 concentrations when NaCl is present. At 22°C the critical micelle concentration (cmc) of F127 in water, obtained from static light scattering (SLS), equals $1400 \pm 70 \mu\text{M}$ (~1.8 wt %) and $850 \pm 40 \mu\text{M}$ (~1 wt %) without salt and at 0.1 M NaCl, respectively (2). As documented in the literature the aggregation number and the radius of spherical aggregates of F127 increases when

increasing temperature (11). We found a similar trend when increasing the NaCl concentration: the hydrodynamic diameter of aggregates increases from 4.3 nm up to 25 nm when changing the NaCl concentration from 10^{-4} M up to 1 M, respectively (Table 1).

Table 1 The diameter (D) of objects in solutions of F127 measured by dynamic light scattering (DLS) and the combined thickness of adsorbed layers of F127 ($h_1 + h_2$) at silica-water (h_1) and air-water (h_2) interfaces obtained via ellipsometry at different salt concentrations, $c_{F127} = 400 \mu\text{M}$, $T = 22^\circ\text{C}$.

$C_{\text{NaCl}} / \text{M}$	D / nm	$h_1 + h_2 / \text{nm}$	h_1 / nm	h_2 / nm
0	-	15	7.5	7.5
10^{-4}	4.3	15	7.5	7.5
10^{-1}	12	9.5	1	8.5
1	25	9.2-9.5	0.2-0.5	9

Table 1 shows the results for a polymer concentration of 400 μM , which is below the cmc determined via SLS. The second column represents the sizes (hydrodynamic diameter) of unimer coils or aggregates of F127 as measured by dynamic light scattering (DLS). The measured diameter of 4.3 nm at 10^{-4} M NaCl most likely applies to unimer coils. The radius of gyration R_g of F127 macromolecule in a good solvent is around 5.7 nm as calculated by the Flory relationship $R_g = aN^{3/5}$ (12), where a (~ 0.2 nm) is an effective monomer size and the number $N = N_{\text{PO}} + 2N_{\text{EO}}$. The sensitivity of the set-up was not sufficient to obtain reproducible values of the hydrodynamic radius for the polymer solution (400 μM) without added salt. The measured diameter of 12 nm at 0.1 M NaCl probably belongs to aggregates formed from lower molecular mass polymers (diblock copolymers, which are most likely present in the sample (11)). F127 is a commercial surfactant, which has been reported to be rather polydisperse. The results of Wanka et al (11) show that the distribution of the molar mass of the samples is very broad and extends over an order of magnitude. The diameter of 25 nm at 1 M NaCl is probably the size of the micelle.

In the third column of Table 1 a change of the sum of thicknesses of adsorbed layers of F127 at the interfaces upon increasing NaCl concentration is shown. The fourth and the fifth columns stand for the thickness of adsorbed layers at silica-water h_1 and air-water interfaces h_2 .

The important messages of Table 1 are that upon increase of the NaCl concentration: i) aggregation occurs already below the cmc as measured by SLS; ii) the size of the aggregates increases upon increasing NaCl concentration; and iii) sum of the thicknesses of adsorbed layers of F127 at interfaces of the wetting film goes down with increasing NaCl concentration.

Table 2 collects similar information as Table 1 for polymer concentrations above the cmc.

Table 2 The diameter of aggregates (D) of the solution of F127 measured by dynamic light scattering (DLS) and the thickness of adsorbed layers of F127 at silica-water (h_1) and air-water (h_2) interfaces obtained via ellipsometry at different c_{F127} and c_{NaCl} , $T = 22^\circ C$.

C_{NaCl} /M	$C_{F127}/\mu M$	D/nm	$h_1 + h_2/\text{nm}$	h_1/nm	h_2/nm
0	2800	36	16	7.5	8.5
10^{-4}	1500	36	16	7.5	8.5
10^{-1}	800	36	10	1	9

We see that the size of aggregates (column 3) is the same for all polymer concentrations (column 2). Similarly, in $[NaCl] \leq 10^{-4}$ M the thickness of adsorbed F127 layers (column 4) of 16 nm is the same at and above the cmc. At 0.1 M NaCl the thickness of adsorbed layers is almost 2 times smaller (10 nm) in comparison with the aforementioned thickness due to a dramatic decrease of Γ at the silica-water interface upon increase of the electrolyte concentration (2).

3.2 Thinning of wetting films

Figures 2 a, b show the influence of salt on thinning behavior of films formed from 400 μM F127 at an applied, p_H of -4.5 kPa.

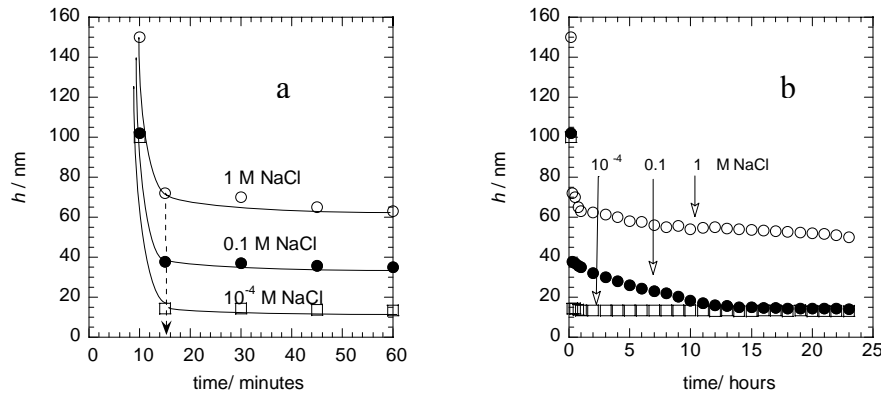


Figure 2 Influence of NaCl on the relaxation of wetting films at $T = 22^\circ C$, $p_H = -4.5$ kPa, $c_{F127} = 400 \mu M$.

Figure 2a emphasizes the relaxation of the film during the first hour after switching on an applied pressure of -4.5 kPa. It can be seen that within 15 minutes the films relax to a thickness, which seems to be constant in time. These ‘plateau’ values of the film thickness depend strongly on salt concentration, and are equal to 14, 38 to 70 nm at 10^{-4} , 0.1 and 1 M NaCl, respectively. However, when the observation time is

extended to many hours, further relaxation of the films was observed at 0.1 and 1 M NaCl (Fig. 2b). In the presence of 0.1 M NaCl it took 15 hours for the film to relax from 38 down to 14 nm. In 1 M NaCl the film relaxed from 70 down to 30 nm in 7 days at which time the thinning process is still not completed yet. For the last case the full relaxation is not shown. It is evident that these thinning processes exhibit two kinetic regimes if 0.1 and 1M NaCl is present in the solution: a *fast thinning regime* for the first 15 minutes and a much *slower thinning regime* for subsequent hours. At 10^{-4} M NaCl no significant slow thinning was observed. In our previous work (2), the film thickness after the ‘fast’ relaxation process was thought to be the final value. Further in the text, a film at the “onset” of a slow thinning process will be called a *non-equilibrium* film.

Figure 3 compares the thicknesses of *non-equilibrium* (1) and *equilibrium* (3) films together with: i) the combined thickness of adsorbed layers of F127 at silica-water and air-water interfaces (4); ii) the combined thickness of adsorbed layers of F127 at film interfaces with two layers of aggregates (2) in between.

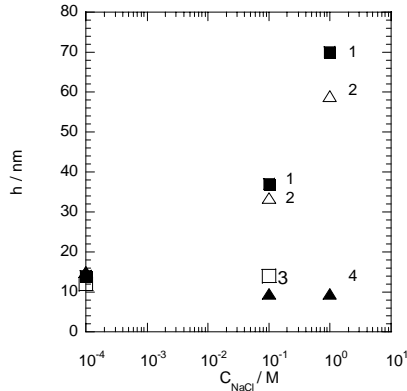


Figure 3. Non-equilibrium film thickness (1), equilibrium film thickness (3) at $p_H = -4.5$ kPa compared with the total thickness of adsorbed F127 layers (4) plus two layers of aggregates in between (2) versus NaCl concentration at $c_{F127} = 400 \mu M$ and $T = 22^\circ C$. The size of the aggregates are measured with DLS and taken from Table 1.

We see that the thickness of adsorbed layers (4) decreases slightly, while the thickness of the film (1) increases with increasing NaCl concentration. The thickness of *non-equilibrium* films (1) coincides with the total adsorbed layer thickness with two layers of aggregates in between (2) up to 0.1 M NaCl (at higher NaCl concentrations this does not hold), and the thickness of equilibrium films (3) is close to the thickness of adsorbed layers (4). The salient feature is that those non-equilibrium films relax to equilibrium films. One might think that the slow drainage is caused by micelles in the film. Therefore, the question is: will we observe different relaxation kinetics of films below, at and above the cmc if no NaCl is present?

Figures 4 a, b depict the relaxation of films for a polymer concentration below ($400 \mu M$), at ($1500 \mu M$), and above ($2800 \mu M$) the cmc at $p_H = -4.5$ kPa and $T = 22^\circ C$. Figure 4a focuses (as Figure 2a) on the relaxation during the first hour. The relaxation time slightly increases upon increasing F127 concentration. However, after 30 minutes all films reach a thickness that does not change anymore during the subsequent

hours (Fig. 4b). Passing the cmc does not mark a change in behavior. At a low NaCl concentration ($\leq 10^{-4}$ M) we observe fast thinning towards the equilibrium thickness for all cases that were examined.

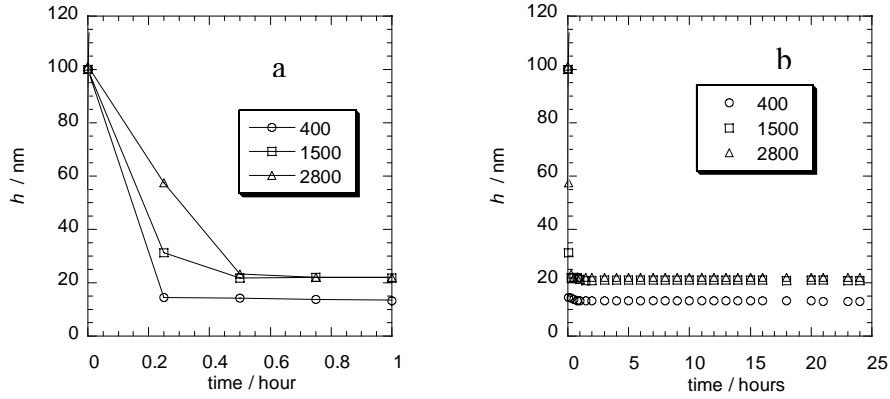


Figure 4 Influence of $[F127]$ on the relaxation of asymmetric F127 films. \circ — c_{F127} : 400 μM ($0.3 \times \text{cmc}$), \square —1500 μM (slightly higher the cmc) at $c_{\text{NaCl}} = 10^{-4}$ M; \triangle —2800 μM ($\sim 2 \times \text{cmc}$) without salt, $p_H = -4.5$ kPa, and $T = 22^\circ\text{C}$. Concentrations of F127 in μM are shown on the figures.

If we consider the relaxation of the film formed from a F127 solution (400, 800 μM) in 0.1 M NaCl, again ‘fast’ and ‘slow’ thinning processes can be distinguished (Figure 5). The relaxation time at 800 μM increases up to ~ 20 hours.

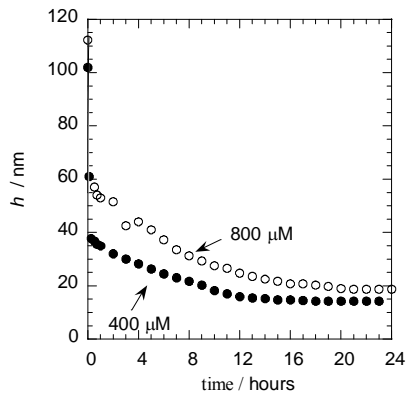


Figure 5 Relaxation of wetting films formed from aqueous solution of F127 in 0.1 M NaCl at $T = 22^\circ\text{C}$, $p_H = -4.5$ kPa. The F127 concentration is indicated in the figure.

If we estimate the non-equilibrium thickness of the film obtained from a F127 solution at 800 μM F127 and 0.1 M NaCl, we find that this value (~ 55 nm) is close (within experimental error) to the thickness of adsorbed layers at the film interfaces (10 nm) plus the size of trapped micelles (36 nm) in between. The film thickness of 20 nm, which is reached after 24 hours, is still much higher than the total adsorbed layers thickness (10 nm). Most likely, the film still did not reach an equilibrium thickness.

In conclusions, we observed increase of the larger relaxation (in hours!) upon rising c_{NaCl} , and smaller relaxation time (in minutes) upon increase of the polymer concentration c_{F127} . Hence, the presence of micelles in aqueous solution does not seem to play an important role in the slow film-thinning phenomenon, and the salt-induced slow relaxation must have a different origin.

In order to obtain further information about the process of film thinning, ellipsometric images of the films were made during relaxation. Figure 6 shows images of films formed from F127 aqueous solution (400 μM) at p_H of -4.5 kPa after different waiting times at two different NaCl concentrations. For dark patches the thickness is such that the settings of the polarizer and the analyzer correspond to the “null” setting. For bright patches the film is either thinner or thicker as explained in the experimental section. It is clear that the images of films with NaCl concentrations of 10^{-4} and 0.1 M NaCl M are different.

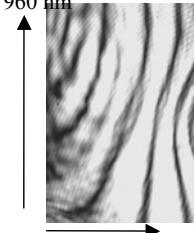



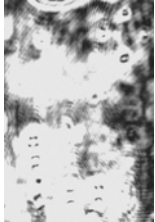
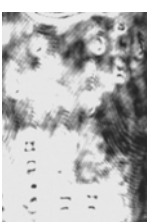
Solution / t	1 minutes	1 hour	18-20 hours
400 μM F127 + 0.1 mM NaCl	 a	 b	 c
400 μM F127 + 0.1 M NaCl	 d	 e	 f

Figure 6 Ellipsometric images of the film at $p_H = -4.5$ kPa, $T = 22^\circ\text{C}$, $c_{\text{F127}} = 400$ μM , $c_{\text{NaCl}} = 10^{-4}$ M (a, b, c) and 0.1 M (d, e, f),

Images of films formed at 10^{-4} M NaCl (Figure 6 a, b, c)

Because the equilibrium thickness of 11 nm was reached very quickly (Figure 2), identical images of the film were expected at least after 1 hour and 20 hours. However, different images were observed after 1 minute, 1 hour and 20 hours. The dark patches in the image correspond to the average ellipsometric

thickness. Bright patches are either thinner or thicker, but the difference might be very small. Unfortunately, we cannot extract the magnitude of the differences in thickness from these pictures; most probably they are small. Our interpretation of these images is that the films are still draining in time but that the changes in the thickness are extremely small.

Images of films at 0.1 M NaCl (Figure 6 d, e, f)

For the film formed at 0.1 M NaCl nearly the same pictures were observed after one minute, one hour and 18 hours. Moreover, these films seem to be heterogeneous: large structures (in lateral direction) of 50-100 μm are seen. The locations and the shapes of the structures do not change during the thinning of the film, indicating that they are stuck within the film. It is important to note that the average thickness of this film strongly decreases from d, to e, to f, as seen in Fig.2. As explained in the experimental section, the analyzer and polarizer were adjusted before new image was recorded. These images are very similar to the photographic images made by Monteux et al. (13) of foam films containing microgels formed from polymer/surfactant aggregates. Their films show also an extremely slow drainage. The formation of a viscous surface gel layer of polymer/surfactant aggregates, stuck to the surface was proposed as an interpretation of such images. If this is the case, the structure and the properties of such networks can be strongly influenced by the rate of film formation (14). Most probably, such immobile structures are present within the film if $[\text{NaCl}]$ increases.

4 Discussion

The drainage of films without salt or in 10^{-4} M NaCl is quick and the drainage time slightly increases upon increasing F127 concentration. This slight increase of the drainage time from 15 to 35 minutes upon increasing F127 concentration might be explained by a slight increase of the viscosity of the solution. It is well known that in general polymer mobility decreases and the viscosity increases with increasing polymer concentration. An increase of the NaCl concentration has a much stronger effect on the rate of film drainage: the relaxation time increases from 15 minutes to more than 150 hours upon increasing the NaCl concentration from 10^{-4} to 1 M, respectively. ‘Thick’ non-equilibrium films obtained in the presence of 0.1 and 1 M NaCl relax to a smaller thickness, but it takes hours, or even days. The effect of electrolyte concentration on the rate of film drainage is surprising and calls for an explanation. Let us discuss several possibilities.

4.1 The possible role of micelle-like aggregates in the thinning phenomena

One possibility is that aggregates of F127, which are present in the solution, slow down the film drainage. In Figure 3, the thickness of the *non-equilibrium* (1) films nicely coincides with the total thickness of adsorbed layers of polymer at film interfaces plus two layers of aggregates in between (2) if the NaCl concentration does not exceed 0.1 M. This brought us to the idea that the slowness of the relaxing non-equilibrium thickness might be due to trapped aggregates (2). The size of aggregates increases with NaCl concentration (Table1), and this is in line with the experimental finding that the non-equilibrium

thickness increases upon increasing NaCl concentration. However, in the absence of NaCl or at low NaCl concentrations ($\leq 10^{-4}$ M) slowly relaxing thick non-equilibrium films do not occur. Apparently, if there is no salt in the solution, micelles/ aggregates are not trapped within the film and flow out of the film quickly. We conclude that the mere presence of micelles in itself is not a sufficient condition for the occurrence of slowly relaxing thick non-equilibrium films.

4.2 Local and transient increase of the concentration of the surfactant within the films

Another contribution to an explanation may be a rising polymer concentration inside film during thinning. Van der Gucht et al (15) pointed out, that ‘if the diffusion of polymers between the gap and the bulk is too slow to maintain equilibrium, the amount of polymers in the gap is determined by the flow of fluid out of the gap’(15). Depending on the concentration profile of mobile polymer and on the flow profile, an increase of the concentration inside film may arise, leading to an osmotic repulsive contribution to the force between the surfaces of the film. When the flow profile overlaps with a depletion zone of mobile polymer (a zone where the concentration of mobile polymers is lower than in the bulk solution), the concentration inside the film increases during the film thinning. Such a mechanism may contribute to the occurrence of slowly relaxing thick non-equilibrium film. However, at present we cannot be sure because we do not know enough about the details of the concentration and the flow profiles.

4.3 Gel formation within the film

Perhaps, the most important factor might originate from the gelation of F127 in aqueous solution, which is strongly influenced by the presence of co-solutes. It is known that F127 form aggregates of different kinds, depending on the sizes of the blocks, the solvent properties, the temperature, and the co-solutes (11, 16). At low concentrations, it is generally observed that micelles are formed, while for higher concentrations, liquid crystalline phases may occur as well (11, 16). Malmsten’s work (16) on the phase behavior of F127 in water demonstrates that a gel region exists at higher concentration of F127 and at intermediate temperatures (~ 30 wt % F127 at 20°C). It is also established that NaCl displaces the whole gel region and cloud point (CP) to lower temperatures. The stability range of the gel phase is strongly dependent on the presence of co-solutes. NaCl, which is referred as a typical ‘salting-out’ co-solute displaces the whole gel region, as well as CP, to lower temperature (16). Indeed, the presence of 1 M NaCl shifts the gel region to lower concentration (17 wt% at 20°C) (16). Their experimental data suggest that the gel consists of a close-packed array of micelles of roughly the same size as those in dilute solution.

If we estimate for example, the overall ($C_{F127, \text{ film}}$) concentration of polymer inside films of 40 nm formed from 400 μM (0.5 wt %) of F127 without and in 0.1, 1 M NaCl (by summation of the bulk F127 concentration c^b and adsorbed amount of F127 at the air-water interface $\Gamma^{\text{air-water}}$ divided by the film thickness h_{film} : $C_{F127, \text{ film}} = c^b + \Gamma^{\text{air-water}} / h_{\text{film}}$) we find as average concentrations of polymer inside film 12.5, 6.25 to 9 wt %, respectively . Of course, the smaller the thickness, the higher the polymer concentration within the film: the concentration of polymer takes values around 24.5, 13, 18 wt %

if we decrease the film thickness to 20 nm. Taking into account that the presence of 0.1 M NaCl leads to a desorption of F127 from the silica surface (2), and that the concentration of polymer indeed is higher than in the solution, one might expect that the polymer concentration in the film will not be in equilibrium with the external solution. Hence, we think that a gel inside film (or at the air-water interface) might occur under the impact of NaCl and upon quick film formation. If gelation occurs within the film (or at one interface) this readily explains why films will drain very slowly (due to the slow diffusion of polymer within the gel network), and why they might be heterogeneous. Indeed, slow drainage of films was observed at 0.1 and 1 M NaCl; and heterogeneous patches along the film were observed in ellipsometric images at 0.1 M NaCl (Figure 6 d, e, f).

5 Summary and Remarks for futures study

In this study, we investigated the relaxation behaviour of thin wetting films formed from solutions of the polymeric surfactant F127 and NaCl. What was already anticipated in a previous publication (2) has now been confirmed: an increase of the NaCl concentration leads to the formation of non-equilibrium thick films. These films relax with time to a smaller equilibrium thickness. The non-equilibrium thickness and the relaxation time increase upon increase of the electrolyte concentration.

The presence of 10^{-4} M NaCl in the aqueous F127 solution has a negligible effect on the relaxation of wetting films: equilibrium films are formed very quickly. Although slight film drainage is probably still exist. Increase of the F127 concentration only has a minor influence on the relaxation time.

In forthcoming publications, the effect of different co-solutes (which have different effects on the solvent quality of F127 solution and on the adsorption behaviour of F127 at interfaces) as well as the effect of pH on the stability and thinning of aqueous triblock copolymer films will be studied in order to establish which factors determine the behaviour of thin films formed from aqueous solution of PPO-PEO type polymeric surfactants.

References

1. J. N. Israelachvili, *Intermolecular and surface forces*. A. Press, Ed. (1992).
2. O. V. Elisseeva, N. A. M. Besseling, L. K. Koopal, M. A. Cohen Stuart, *Langmuir* **21**, 4954-4963 (2005).
3. D. Exerowa *et al.*, *Advances in Colloid and Interfaces Science* **104**, 1-24 (2003).
4. B. Diakova, D. Platikanov, R. Atanasov, M. Kaisheva, *Advances in Colloid and Interface Science* **104**, 25-36 (20.01.2005, 2003).
5. B. Diakova, M. Kaisheva, D. Platikanov, *Colloid and Surfaces A:Physicochem.Eng. Aspects* **190**, 61-70 (2001).
6. K. J. Mysels, M. N. Jones, *Discuss. Faraday Soc.* **42**, 42 (1966).
7. V. A. Shishin, Z. M. Zorin, N. V. Churaev, *Kolloidnyi Zhurnal (English transl.)* **39**, 351 (1977).
8. B. V. Derjaguin, Z. M. Zorin, N. V. Churaev, V. A. Shishin, J. F. P. (editor), *Wetting, Spreading and Adhesion* (Academic Press, London, 1977).
9. H. G. Tompkins, *A User's Guide to Ellipsometry* (Academic Press, Inc., San Diego, 1993).
10. D. Schmaljohann *et al.*, *Langmuir* **21**, 2317-2322 (2005).
11. G. Wanka, H. Hoffman, W. Ulbricht, *Macromolecules* **27**, 4145-4159 (1994).
12. P. Flory, *Principles of Polymer Chemistry* (Cornell University Press, 1956).
13. C. Monteux, C. E. Williams, J. Meunier, O. Anthony, V. Bergeron, *Langmuir* **20**, 57-63 (2004).
14. V. Bergeron, D. Langevin, A. Asnacios, *Langmuir* **12**, 1550-1556 (20.01.2005, 1996).
15. J. Van der Gucht, N. A. M. Besseling, *J. Phys. Condens. Matter* **15**, 6627 (2003).
16. M. Malmsten, B. Lindman, *Macromolecules* **25**, 5440-5445 (1992).

Chapter 4 Equilibrium and transient thicknesses of wetting films

ABSTRACT

We studied the time-dependent thickness of wetting films formed from aqueous solutions of NaCl on a silica surface modified with the block co-polymeric surfactant F127 (PEO₉₉PPO₆₅PEO₉₉). The drainage kinetics of these films was investigated by means of a film balance and an ellipsometer. It was found that the thickness of the films depends strongly on whether or not surfactant was applied over the entire substrate or only at a spot coinciding with the investigated wetting film. In the former case, the thickness shows a transient maximum, in the latter case, it equilibrates quickly. An interpretation of the transient thicknesses is given, and the equilibrium values are discussed.

1 Introduction

For draining wetting films, the thickness as a function of time, $h(t)$, is the most important quantity to be determined experimentally. When a thin film is formed from a solution (phase α) in air (phase β) it is initially thick. However, it thins under the driving force, $\Delta p = p^\beta - p^\alpha$. This pressure difference can be an externally created pressure difference (I). Draining films with liquid interfaces (foam, emulsion) are not always plane-parallel. The balance between the disjoining pressure, Π and capillary (or hydrodynamic) pressures determines the shape of the film. Non-equilibrium thicknesses of films can also occur if a bubble approaches a solid surface and a liquid film is formed between them. This film does not necessarily drain continuously: there are several distinct stages of the thinning process in wetting films (2). Since the drainage near the film border is initially faster than in the film centre, the thickness at the barrier rim quickly reaches a value close to the equilibrium one. Thus, a specific film profile known in the literature under the name of dimple is generated. This phenomenon is transient.

Here we describe observations on thicknesses of wetting films formed from aqueous solutions of NaCl at silica surfaces with a pre-adsorbed layer of surfactant. The emphasis is on the interpretation of the transient behaviour of wetting films. Under special conditions we observed thickness of films, which had a maximum (as a function of time). The incentive for carrying out the present set of experiments came from previous chapter 3, where we found an unexpected retarding effect of NaCl on the drainage of wetting films formed by aqueous solutions of a triblock copolymer surfactant, Pluronic F127 (3, 4). Pluronic F127 is the BASF trade name for an ABA block copolymer. It is composed of one hydrophobic polypropylene oxide block B (PPO) and two hydrophilic polyethylene oxide blocks A (PEO) and has an average molecular composition $\text{PEO}_{99}\text{PPO}_{65}\text{PEO}_{99}$.

In order to analyze the influence of NaCl on the kinetic behaviour of wetting films, we should have some information about the kinetics of adsorption of the triblock copolymer surfactant at the two interfaces of this film. Here we organize the results as follows: the adsorption data are given in the first section (3.1); transient and equilibrium film thicknesses are discussed in the second part (3.2); the last section (3.3) is devoted to the comparison of the equilibrium thicknesses of the films obtained via different thinning mechanisms.

2 Experimental

2.1 Materials

The polymeric surfactant (triblock copolymer) Pluronic F127 (average molecular composition $\text{PEO}_{99}\text{PPO}_{65}\text{PEO}_{99}$, Sigma-Aldrich CO., USA) was used without further purification. Pluronic F127 has a

number-average molar mass, M_n of 12600 and a PEO content of 70% by weight. Further in the text the term of *polymeric surfactant* or *surfactant* is used for the triblock copolymer F127. Aqueous solutions of surfactant were prepared by dissolving the surfactant in demineralised water under gentle agitation. Sodium chloride, NaCl, (J.T. Baker Chemicals B.V., Holland) was used without further purification.

The water used is purified using a two-stage deionization processes (ion exchanger/active carbon), supplied by a “Barnstead pure UV system” (USA). After deionization, the water is filtered through a 0.2-micron filter. It produces water with a resistivity of 18.3 Megohm-cm ($M\Omega\text{cm}$).

All measurements were carried out at $\text{pH} \approx 6$ and $T \approx 21\text{-}23^\circ\text{C}$.

2.2 Preparation and saturation of silica

Polished silicon wafers, Si (p-type, boron-doped, oriented <1-0-0>, resistivity 12-18 Ωcm) were purchased from Wafer Net, Germany. The thickness of the natural silicon oxide SiO_2 layer on the surface was about 2 nm, as determined by ellipsometry. Wafers were cut into small strips (3×1 cm) and boiled for 5 min at 80°C in a mixture of 25% NH_3 , 30% H_2O_2 and H_2O (1:1:5 by volume). The strips were then rinsed with water and ethanol (99.8%). They were kept in a closed container under water until use. Before the strips were placed in the cell, they were dried with a stream of nitrogen and treated for 30 seconds in a plasma cleaner (Harrick, Model PDC-32 G). A subsequent plasma treatment was performed with air (10 Pa). After cleaning, the contact angle of water was always lower than 8° , indicating the hydrophilic nature of the silicon oxide surface. The full silicon strips, or parts of them, were covered with the solution of polymer.

2.3 Formation and measurements of wetting films

2.3.1 Thin Film Balance (TFB)

The TFB technique was used to measure the thinning of films. This technique, based on the original design of Mysels and Jones (5), was developed and described for wetting films by Shishin and Derjaguin et al (6, 7). A drawing of the TFB and a detailed discussion of the measurements is given in our previous publications (3, 4). In figure 1 (see section 2.3.2) we show a very schematic picture of the film inside the porous disc: a porous glass disc (1) saturated in the NaCl solution is placed on the silica surface (2) covered with polymer solution. This is done in two different ways ((a) and (b)) which we discuss in the next section (2.3.2). A thin wetting film (3) is formed in the hole (diameter of 0.5 cm) drilled in the porous disc. The porous disc and the silica strip are placed inside a covered Plexiglas cell, which has narrow channels and grooves for the beams of the ellipsometer light.

2.3.2 Formation and manipulation of wetting film

The wetting film is formed on the silica surface once the porous disc, saturated in NaCl solution, is positioned on the surface and the hydrostatic pressure is applied. Manipulation of this pressure affects the

disjoining pressure, Π in the film. A positive disjoining pressure resists thinning, while a negative one promotes thinning. At equilibrium, Π is opposite in sign and equal in magnitude to the hydrostatic pressure difference Δp_H .

$$\Pi(h) + \Delta p_H = 0 \quad (1)$$

Hence, in this way the disjoining pressure can be measured. The hydrostatic pressure difference is given by $\Delta p_H = \rho g H$, where ρ is the liquid density, g is the gravitational acceleration and H the height difference between the silica surface and the reservoir. H has negative values as the level in the vessel is below the silica surface. It is measured with a cathetometer (Mitutoyo, Model AT11-N600, Japan).

It is necessary for the following discussion to stress the way of modification of the surface with the solution of surfactant. Two situations are shown in Figure 1.

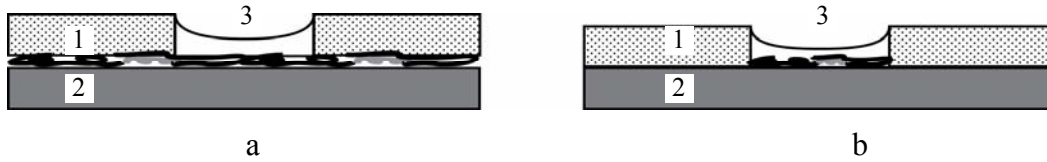


Figure 1 The formation of a film at fully (a) and partly (b) covered with the surfactant silica surface.

- Porous glass disc, 2 – silica, 3 – wetting film.

(a) - Surfactant is present between the disc and the silica surface

(b)- No surfactant is present between the disc and the silica surface.

In case (a) the silicon strip was immersed into the solution of surfactant (400 μM) for 1 hour, removed and dried in an oven at 50°C, cleaned with water and finally dried with air. Hence, in case (a) the entire surface of the strip is covered with a layer of polymeric surfactant, corresponding to saturated adsorption from water. In the second case (b) we covered only the part of the surface with the size of the diameter of the hole in the porous discs (~ 0.5 cm). We put a drop of 1 μl of the solution of surfactant in the centre of the strip. The spreading area of the drop was around 0.2 cm^2 , as the hole comprises only about 7% of the entire area (the area of the silicon strip is 3 cm^2). The area of the silica surface covered by polymeric surfactant was almost 15 times smaller for the case (b). In case (a) the film in the hole was in full contact with both the pores of the disc and the thin, surfactant containing, layer between the disc and silica, whereas in case (b) the contact was only with the pores.

Immediately, a pressure of -4.5 kPa was applied and thinning of the film was followed by ellipsometry.

2.3.3 Measurements of the thickness of wetting films

Ellipsometry measures changes in the polarization state of light reflected from interfaces. The experimental data are expressed in terms of the ellipsometric angles ψ (where $\tan \psi = |r^p|/|r^s|$ is the amplitude ratio of the parallel (p) and perpendicular (s) reflection coefficient) and Δ (the change in the phase difference that

occurs upon reflection). These are related to the Fresnel reflection coefficients r^p and r^s , for p- and s-polarized light as $r^p/r^s = \tan \psi e^{j\Delta}$. These coefficients are complex functions of the angle of incidence, the wavelength, the optical properties of the substrate, the ambient medium, and of the layers and the thickness of the layers. Details can be found elsewhere (8).

The ellipsometric angles were determined via *in situ* null ellipsometry. In null ellipsometry, the polarizing elements (polarizer, P and analyzer, A) are rotated until the signal at the photo-detector is minimized (“nulled”). A Multiskop instrument (Optrel Gbr, Berlin) was used for the measurements. The light source was a He-Ne laser with wavelength of 632.8 nm. Because of some differences between the available porous discs, we measured at angles of incidence varying between 65° and 70°, which is close to the Brewster angle for an air-silicon interface (75°). The ellipsometric angles were recorded as a function of time. A four-layer model {silicon/ silicon oxide/aqueous film/air} was considered for the computation of the film thickness. In the calculations of the film thickness (h_{film}), predetermined values for the refractive indices of silicon (3.85), silica (1.46), aqueous solution (n_{sol}) and air (1.00), as well as for the thickness of the silica layer (2 nm) were used. Furthermore, it was assumed that the aqueous film is homogeneous, and that the refractive index is the same as that in the aqueous bulk solution, n_{sol} , which was measured with an Abbe refractometer for each salt concentration (21° C, white light). More details are discussed in our previous publications (4).

It should be noted that the computation of the thickness of the wetting film is more accurate than that of the thicknesses of the surfactant layers at interfaces of the film. The way of measurements of the thicknesses of the surfactant layers is given in the next chapter (2.4). The obtained thicknesses depend sensitively on choice of the refractive indexes of the adsorbed layer. We used the value 1.38 for the refractive index of the adsorbed layers at interfaces. This value is an estimation based on literature data for similar systems and our own results (4, 9).

2.4 Ellipsometric measurements of layers adsorbed at the silica-water interface.

The kinetics of adsorption of surfactant on the silica-water interface was also studied by means of *in situ* null ellipsometry. In this case a silicon strip (with a silicon oxide layer) was placed in a Teflon cell with glass windows. The cell was filled with water/surfactant solution. After that a known amount of NaCl solution (if any) was added and stirred for one minute. Half minute after stirring was stopped, the measurement was started. The ellipsometric angles were recorded as functions of time until the parameters Δ and ψ reached stable values.

A four-layer model (silicon/silicon oxide/adsorbed surfactant layer/aqueous solution of NaCl) was used for the numerical evaluation of the refractive index n_{ads} , the mean thickness h_{ads} of adsorbed layer, and the surface concentration, Γ . In these calculations, the surface concentration, Γ on the silica-water interface was determined using the expression (10):

$$\Gamma = (n_{\text{ads}} - n_{\text{sol}}) h_{\text{ads}} / (dn_{\text{sol}}/dc) \quad [7]$$

Here n_{sol} is the refractive index of the solution; dn_{sol}/dc is the refractive index increment of aqueous solution. The refractive index of solution n_{sol} was measured with an Abbe refractometer (21 °C, white light), and the dn/dc of 0.1276 ml/g was obtained from the previous measurements was used.

2.5 Drop Tensiometry

The surface tension γ of a surfactant solution was studied using an automated drop tensiometer (ITCON-CEPT, Longessaigne, France), where γ is calculated from the profile of a drop. The drop was automatically formed at the tip of a capillary fitted to a syringe, inside which the pressure is measured by a transducer. The actual shape of the drop results from the balance between interfacial tension and gravity forces. The drop profile was processed according to the fundamental Laplace equation applied to the drop profile:

$$\frac{1}{x} \frac{d}{dx} (x \sin \theta) = \frac{2}{b} - cz$$

where x and z are the Cartesian coordinates at any point of the drop profile, b is the radius of curvature of the drop apex, θ is the angle of the tangent to the drop profile, and c is the capillarity constant. Several times per second the computer calculates three characteristic parameters of the drop: area, volume and interfacial tension. The measurements were started immediately after the drop is formed. Details are given by Benjamins et al (11).

3 Results and Discussion

3.1 NaCl effect on the kinetics of adsorption of surfactant at solid-water and air-water interfaces

In the absence of electrolyte, surfactant adsorbs both at the silica-water and the air-water interface, at the former as a thin layer, probably bound to the surface via the EO-moiety, at the latter with the PPO enriching the surface proper and the EO-tails essentially dangling into the solution (4, 12-15). It is known that addition of NaCl affects the adsorption of surfactant at the air-water and silica-water interfaces in a different way. In the former case, the adsorption increases (4), while in the later case it decreases (4, 13, 16).

Figure 2 compares the kinetics of adsorption of surfactant at the silica-water interfaces with and without 0.1 M NaCl.

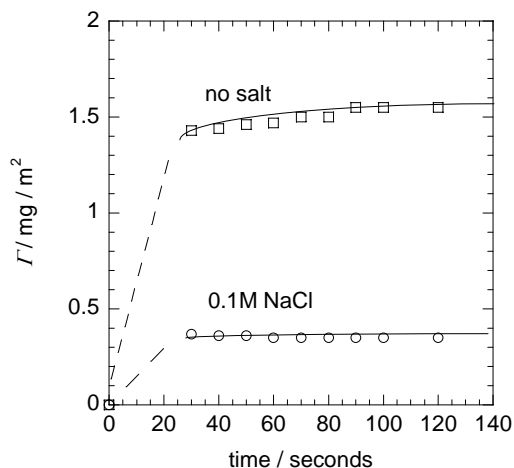


Figure 2 Surface concentration of surfactant adsorbed from 100 μM solutions at the silica-water interface versus time, obtained via ellipsometry at 22°C. The lines are made to guide the eye.

It should be noted that we have a gap in the first experimental observation of 30 seconds. It means that the range $0 < \text{time} < 30$ seconds Γ is unknown. In both cases adsorption occurs very quickly: after 30 seconds equilibrium is entirely (in 0.1 M NaCl) or almost (without NaCl) established. It is seen that NaCl leads to reduced adsorption of surfactant on the silica surface. The reason for less adsorption of the surfactant is probably similar to the effect of pH on the adsorption of PEO and PEO-containing non-ionic surfactants at the silica-water interface, which is described in the literature (17-20). Salt-induced desorption of surfactant (F127) from the silica-water interface has been investigated and discussed extensively (13, 16). The mechanism of desorption of PEO and PEO-containing surfactants (including F127) is probably the same, and determined by the cation Na^+ , which displaces the PEO segments from the silica surface. More information is given in refs (16, 17, 19, 21).

The adsorption of surfactant at the air-water interface also occurs relatively fast, as can be deduced from the drop in surface tension (Figure 3).

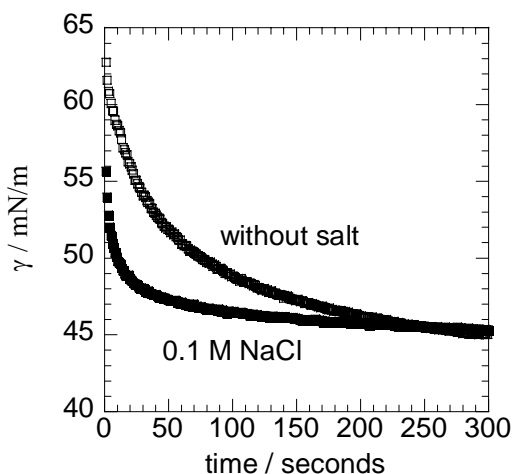


Figure 3 Surface tension γ of $4 \mu\text{M}$ solutions of surfactant measured by ADT at 22°C .

Notice that the concentrations of surfactant chosen for the kinetics studies at the air-water and silica-water interfaces are different: 4 and $100 \mu\text{M}$, respectively. Saturation of the surface (at $4 \mu\text{M}$) takes about 200 sec. in salt-free conditions and about 50 sec. in the presence of NaCl. For higher surfactant concentration ($100 \mu\text{M}$) it was impossible to see the effect of salt on the air-water interface with our set-up.

Figure 3 reflects that addition of NaCl up to 0.1 M increases the rate of adsorption of surfactant at the air-water interface: the equilibration time decreases by a factor of about four. Quick equilibration of adsorbate at the air-water interfaces is most likely due to decrease of the solvent quality, which is known to be determined by the nature of the anion.

3.2 Kinetics of wetting films: transient and equilibrium thicknesses

Figure 4 shows the $h(t)$ behaviour of films formed from aqueous solution without salt (open circles) and in the presence 0.01 M NaCl (black circles) at the silica surface, both fully covered with surfactant (case (a) of fig.1).

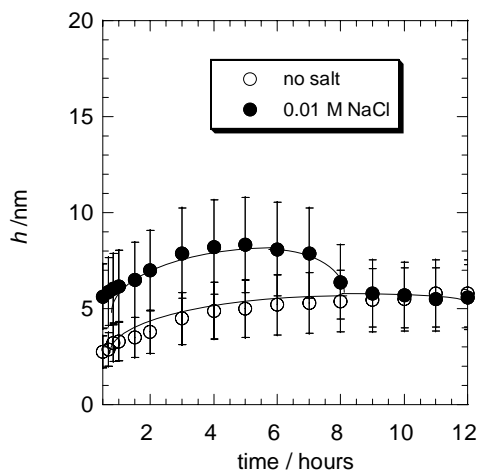


Figure 4 The thickness of films, h versus time formed on fully covered silica (fig. 1a), Δp_H of -4.5 kPa and 22°C .

The reproducibility of these curves is not perfect, but the trend is statistically significant: a transient thickening of the film formed in 0.01 M solution NaCl is clearly seen.

Obviously, a spontaneous thickening of the film cannot be explained in terms of drainage. To account for the transient maximum we supposed that surfactant desorption by the NaCl was at the origin. This desorption will take place inside the hole (fig.1a), and beyond it, under the porous ring. The extent of desorption inside the ring is faster than under the ring, so that a gradient of Γ ensures which leads to transport of surfactant from under the ring to the hole. The increased surfactant concentration inside the hole creates a transient osmotic pressure with respect to the fluid inside the plug, which leads to suction, and transient thickening of the film.

To underpin this osmotic pressure mechanism, two sets of experiments were carried out. In the first, the experiment was repeated in more concentrated NaCl. When the proposed mechanism applies, more pronounced and earlier maxima should be observed, because the extent of desorption is enhanced.

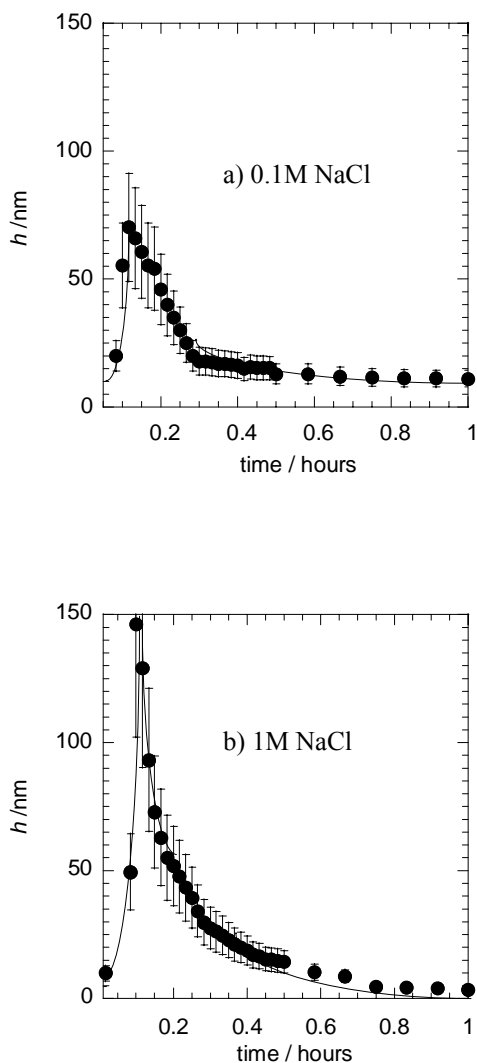


Figure 5 As fig.4, but now in the presence of 0.1 and 1 M NaCl, respectively.

As can be seen in fig.5 this is indeed the case. The time scale of the existence of the maxima decreases from a few hours (Fig. 4) to a few minutes (Fig.5) upon increasing the NaCl concentration from 0.01 to 1 M and the maxima become much more pronounced. We note that in 1 M NaCl films have a tendency to become unstable after one hour. Sometimes the film breaks. Eventually ($t \rightarrow \infty$) the films drain till their final values of about 5-8 nm.

The main point we want to stress is that the maxima in the drainage curves of the wetting film are the result of salt-induced desorption of adsorbate from the solid-liquid interface and the subsequent increase of the concentration of adsorbate leading to a (local) increase of the osmotic pressure. It seems essential that a

free surfactant concentration builds up *under the porous disc* and that drives the thickness increase in the wetting film in the hole.

This is supported by the data obtained for case (b). In this case the supply of surfactant from the large “bath” underneath the porous ring is blocked (fig. 1b). Indeed, in this case these maxima disappear. Figure 6 shows the $h(t)$ behaviour of films formed from 0.1 M NaCl at the surface partly covered with the surfactant. The surfactant desorption from the hole is only about 7% of that in the case (a) and not large enough to produce any substantial effect.

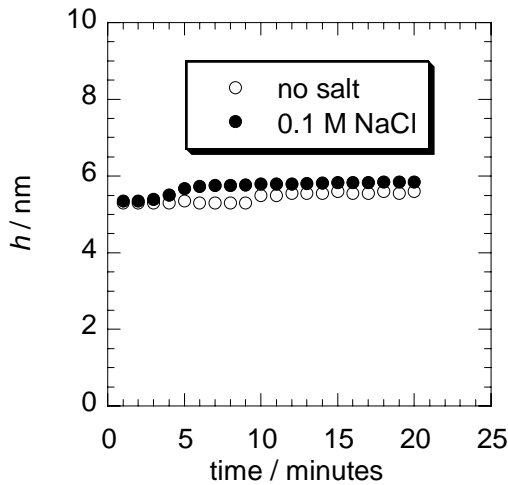


Figure 6 The thickness of films versus time formed on partly covered silica (fig. 1b), Δp_H of -4.5 kPa and 22°C .

If the increase of the concentration of the surfactant under the porous disc would not play a role and if desorption of the surfactant in the wetting film (the hole) were capable of driving the thickening phenomena, we should still observe a maximum in the $h(t)$ behaviour of films formed at silica partly covered with surfactant. This is not what we find. Indeed, this scenario is very unlikely as the desorbed surfactant in the hole can (and will) quickly adsorb to the nearby water-air surface, so that it is no longer free.

3.3 Comparison between final thicknesses of films attained with or without transient maxima.

In view of the complicated dynamic nature of the drainage process quantitative interpretation the $h(t)$ graphs is not simple. However, the thicknesses measured at steady state are precisely the ones obtained in measurements with solutions containing salt and surfactant (chapters 2, 3), which we interpret as the equilibrium film thicknesses. The only difference then, is that the use of surfactant-loaded surfaces surfactant-free electrolyte leads to much faster equilibration, particularly in case (b). In view of the

extremely long drainage times (up to days) found previously, there is an enormous advantage. Hence, we can now discuss the film thickness in terms of equilibrium.

We expect that the steric repulsion, which comes from the layers adsorbed at interfaces of the wetting film, plus the Van der Waals repulsion are the dominant contributions to the disjoining pressure. In figure 7 some of our previous disjoining pressure isotherms are shown for aqueous films on silica observed under various conditions.

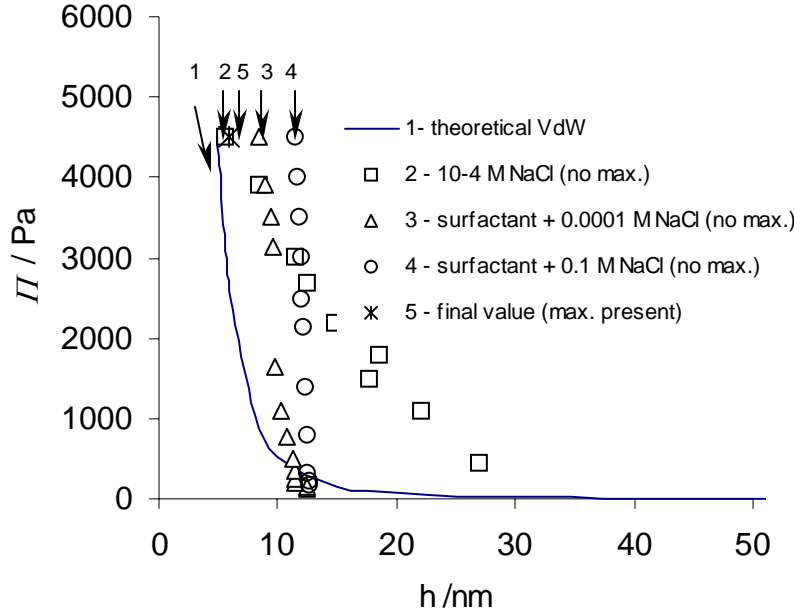


Figure 7 A comparison: $\Pi(h)$ isotherms of aqueous films at the silica surface observed under various conditions: curve 1 - the van der Waals isotherm calculated; curve 2 - 10^{-4} M NaCl; curve 3 - $50 \mu\text{M}$ F127 + 10^{-4} M NaCl; curve 4 - $50 \mu\text{M}$ F127 + 0.1 M NaCl point 5 – final thickness of films with a maxima in the drainage .

Curve 1

In fig.7 the Van der Waals isotherm for the system silica/water/air is plotted as a solid curve. The Van der Waals interaction (curve 1) is calculated from:

$$\Pi_{\text{VdW}} = -A/6\pi h^3 \quad (2)$$

Here A is the Hamaker constant ($A_{\text{silica/water/air}} = -10^{-20}$ J (22)), and h is the film thickness.

Note that the Van der Waals interaction is repulsive.

Curve 2

The squares in fig.7 give the $\Pi(h)$ data for the film formed from only 10^{-4} M NaCl, i.e., there is no pre-adsorbed surfactant. As this film does not contain any surfactant, the gradually decreasing repulsion

between the interfaces from 7 up to around 30 nm must be attributed electrostatics (DLVO theory). The decay should be exponential and this is indeed found. A decay length, κ^{-1} of 10 nm was so that an exponential decay, with a decay length equal to the Debye length is expected.

At short distances $\Pi(h)$ is dominated by its Van der Waals part.

In fig.7 we also give $\Pi(h)$ data for films formed from 50 μM of the solution of surfactant at 10^{-4} M and 0.1 M NaCl, respectively. Here we focus attention on the thicknesses of the films obtained at high pressures (> 4 kPa). Non-DLVO forces come into play and they must stem from the adsorbed layers of surfactant. From our previous studies (chapter 2) it follows that at 50 μM of surfactant (which is ~ 0.4 of critical micellization concentration (cmc)) the film interfaces are not fully saturated with the surfactant. The sum of the thicknesses of adsorbed surfactant layers at the two film surfaces was established to be around 7 nm for both concentrations of NaCl (4). At 4 kPa the films formed from surfactant in 10^{-4} and 0.1 M NaCl have thicknesses of 10 nm.

Point 5 - final thickness of films with a maximum in the drainage

There is a certain spread in the final thickness value. In the present work wetting films are formed from aqueous solutions of NaCl, which did not contain surfactant. The only surfactant present in the system is that pre-adsorbed at the silica-water interface, but there is some irreproducibility in the surfactant transport from the ring to the hole. As a result, we do not know the exact concentration of surfactant within the film. In previous works (3, 4) the films were formed from solutions of surfactant with known concentration. Different concentration of surfactant at interfaces of film might explain the difference between the final thickness of wetting films obtained in previous and present work. Accepting this spread, the final thicknesses of our present study may be taken as equilibrium values. They are determined by steric interactions.

A practical importance of the present findings is that final thicknesses can be obtained more rapidly. Earlier, we observed that the equilibration of the films contained surfactant and NaCl (the latter at concentrations higher than 0.1 M) took hours or even days. This makes the study of equilibrium film thickness very cumbersome, and possibly subject to additional problem (e.g. evaporation). Therefore, being able to reach equilibrium quickly is enormous advantage.

References

1. D. Platikanov, D. Exerowa, *Thin Liquid Films in Fundamentals of Interface and Colloid Science*. J. Lyklema, Ed., FICS (Elsevier, Amsterdam, 2005), vol. V, 6.1 - 6.91.
2. R. Tsekov, Letocart, P., Schulze, H. J., *Langmuir* **16**, 8206-8209 (2000).
3. O. V. Eliseeva, R. G. Fokkink, N. A. M. Besseling, L. K. Koopal, M. A. Cohen Stuart, *accepted for publication in J. Colloid Interface Sci.* (2006).
4. O. V. Eliseeva, N. A. M. Besseling, L. K. Koopal, M. A. Cohen Stuart, *Langmuir* **21**, 4954-4963 (2005).
5. K. J. Mysels, M. N. Jones, *Discuss. Faraday Soc.* **42**, 42 (1966).
6. V. A. Shishin, Z. M. Zorin, N. V. Churaev, *Kolloidnyi Zhurnal (English transl.)* **39**, 351 (1977).
7. B. V. Derjaguin, Z. M. Zorin, N. V. Churaev, V. A. Shishin, *Wetting, Spreading and Adhesion*. J. F. Padday, Ed. (Academic Press, London, 1977).
8. H. G. Tompkins, *A User's Guide to Ellipsometry* (Academic Press, Inc., San Diego, 1993).
9. B. Rippner, K. Boschkova, P. M. Claesson, T. Arnebrant, *Langmuir* **18**, 5213-5221 (2002).
10. J. A. De Fieter, J. Benjamins, F. A. Veer, *Biopolymers* **17**, 1759-1772 (1978).
11. J. Benjamins, A. Cagna, E. H. Lucassen-Reynders, *Colloid and Surfaces* **114**, 245-254 (1996).
12. K. Khristov, B. Jachimska, K. Malysa, D. Exerowa, *Colloid and Surfaces A: Physicochem. Eng. Aspects* **186**, 93-101 (20.01.2005, 2001).
13. M. Malmsten, P. Linse, T. Cosgrove, *Macromolecules*, 2474-2481 (1992).
14. R. Sedev, *Colloids and Surfaces* **156**, 65-70 (1999).
15. R. Sedev, R. Steitz, G. H. Findenegg, *Physica B* **315**, 267-272 (2002).
16. O. V. Eliseeva, N. A. M. Besseling, L. K. Koopal, M. A. Cohen Stuart, *submitted to CCA*.
17. T. Van Den Boomgaard, T. F. Tadros, J. Lyklema, *Journal of Colloid and Interface Science* **116**, 8-16 (1986).
18. G. P. Van der Beek, M. A. Cohen Stuart, *J. Phys. (Paris)* **49**, 1449 (1988).
19. G. P. Van der Beek, M. A. Cohen Stuart, T. Cosgrove, *Langmuir* **7**, 327 - 334 (1991).
20. F. Tiberg, University of Lund (1994).
21. M. Malmsten, B. Lindman, *Macromolecules* **25**, 5440-5445 (1992).
22. J. Lyklema, *Fundamentals of Interfaces and Colloid Science*, FICS (Academic press, London, 1991), vol. I, A 9.4.

Chapter 5 Effects of pH and additives on aqueous wetting films stabilized by a triblock copolymer

Abstract

Effects of pH and additives (NaCl, Na₂SO₄, NaSCN and urea) on the adsorption of an ABA triblock copolymer (F127) with polyethylene oxide (PEO) as the A blocks and polypropylene oxide (PPO) as the B blocks, at the interfaces of wetting films, on film drainage and on the interaction forces in these films are examined using ellipsometer and a thin film balance technique. The main findings are that all additives reduce the adsorption at the silica surface and retard the film drainage. Moreover, high pH values (~ 10) destabilize the wetting film if 0.1 M NaCl is present. The reduction of the adsorbed amount appears to be correlated to a dramatic slow down of film drainage. The slow drainage as well as the destabilization of the film is attributed to bridging attraction between a densely covered air-water interface and a very sparsely covered silica-water interface.

1 Introduction

The problem of wetting film stability on a solid is important in numerous technical processes, such as cleaning and mineral flotation, and products like windows and textile fibers. We consider here the stability of aqueous wetting films on silica. In simple cases, the main forces controlling the stability of aqueous wetting films are repulsive electrostatic and Van der Waals forces. Since the potential of the clean air-water interface is negative ($\Psi_1 = -35$ mV) (1) and also the silica-water interface is at neutral pH-value negatively charged ($\Psi_1 = -30$ mV) (2) the electrostatic interaction between the solid-liquid and liquid/gas interfaces is clearly repulsive. Moreover, the Van der Waals force is also necessarily repulsive (Hamaker constant $A_{\text{silica/water/air}} = -10^{-20}$ J (3)). In addition, it may occur that there are attractive hydrophobic forces between the solid-water and air-water interface (4, 5). If the film forms from an aqueous polymer solution, an important contribution comes from the polymer-induced forces: steric, bridging and depletion forces (6, 7). When the polymer adsorbs, the properties of the adsorbed layers become crucial. The total force induced by such polymer layers results from a balance between several interactions (7). When the polymer is in a good solvent, the force between the interfaces has a repulsive component due to the excluded volume repulsion between the two adsorbed layers, but also an attractive component due to the formation of bridges between the two surfaces. If the adsorption is irreversible, and the surfaces of the film are saturated with polymer, the osmotic excluded volume interaction is dominant and polymer layers induce repulsion between the interfaces and thus stabilization of the film. If the interfaces are not saturated with polymer, bridging attraction may become dominant and the polymers can induce a destabilization of the film. Stabilization is therefore favoured if the repulsive osmotic interaction is stronger than the attractive bridging interaction.

The effect of polymers on the forces between two identical surfaces has been amply studied. The case of wetting films is more complicated due to the asymmetry of this system. Only a few publications and reviews on wetting films formed by aqueous solutions of polymers are available (4, 5, 8-12). In our previous studies we observed an unexpected effect of NaCl on the thickness and drainage of aqueous wetting films, stabilized by the triblock copolymer Pluronic F127 (11, 13). We attributed this effect to changes in the solubility of the triblock copolymer, which becomes worse upon addition of electrolyte. In theoretical treatments the behaviour of polymers at an interface is usually characterized by two interaction parameters, one for the free energy of mixing polymer and solvent (χ), and one for the free energy associated with the formation of polymer-surface contacts and concomitant breaking of surface-solvent contacts (χ_s) (14). For our system of PEO-PPO-PEO triblock copolymers adsorbing from water onto two different surfaces (silica/water and air/water) we have two χ parameters ($\chi_{\text{PEO/water}}$ and $\chi_{\text{PPO/water}}$) and four χ_s parameters (one for each monomer/interface combination). Changing pH or adding of additives to aqueous solutions may change any of these parameters, thereby affecting the thickness and wetting behaviour of the film.

It is the purpose of the present investigation to assess the role of polymer-mediated surface forces on the stability and thickness of wetting films on silica. We therefore studied the effect of pH and additives on i) the adsorption of the polymer F127 at silica-water and at water-air interfaces, and on ii) the polymer-induced interactions in aqueous wetting films on silica. In particular, we address the question of how the nature of the interfaces influences the adsorption and how the adsorption, in turn, modifies the surface interactions. Accordingly, we consider: 1) effects of additives on the behavior of F127 in aqueous solution; 2) effects of pH and additives on the adsorption of F127 at silica-water and air-water interfaces; 3) effects of pH and additives on wetting films: polymer-induced forces, drainage and wetting behavior.

2 Experimental

2.1 Materials

The polymeric surfactant (triblock copolymer) Pluronic F127 (average molecular structure $\text{PEO}_{99}\text{PPO}_{65}\text{PEO}_{99}$, Sigma-Aldrich CO., USA) was used without further purification. Pluronic F127 has a number average molar mass, M_n of 12600 and a PEO content of 70% by weight. Aqueous solutions of F127 were prepared by dissolving the polymer in demineralised water under gentle agitation. Sodium chloride, NaCl, sodium sulfate, Na_2SO_4 , sodium thiocyanate, NaSCN and urea, $(\text{NH}_2)_2\text{CO}$ (purity min 99.99% supplied by J.T. Baker Chemicals B.V., Holland) were used without further purification. The water used was purified using UV light (Barnstead EASY pure UV, USA). It uses a three-stage deionization process combined with 0.2-micron filter to polish pretreated water (distilled, deionized, or reverse osmosis) to produce water with a resistivity of 18 M Ω cm.

Polished silicon plates, Si (p-type, boron-doped, oriented $\langle 1-0-0 \rangle$, resistivity 12-18 Ω cm) were purchased from Wafer Net, Germany. The thickness of the natural silicon oxide SiO_2 layer on the surface was about 2 nm, as determined by ellipsometry. Wafers were cut into small strips and boiled for 5 min at 80°C in a mixture of 25% NH_3 , 30% H_2O_2 and H_2O (1:1:5 by volume). The strips were then rinsed with water and ethanol (99.8%). They were kept in a closed container under water until use. Before the slices were placed in the cell, they were dried with a stream of nitrogen and treated for 30 seconds in a plasma cleaner (Harrick, Model PDC-32 G). The plasma treatment was performed with air (10 Pa). After cleaning, the contact angle of water was always lower than 8°, indicating the hydrophilic nature of the silicon oxide surface. Measurements were carried out at pH 6 and T 21-23°C unless stated otherwise.

2.2 Thin Film Balance (TFB)

The TFB technique based on the original design of Mysels and Jones (15), is developed and described for wetting films by Shishin and Derjaguin et al (16, 17). A schematic drawing of the TFB used in the current study is given in Figure 1. A thin liquid film is formed on a silica surface (1), in a hole of 0.5 cm drilled in a porous glass disc (2) (Robu, Germany, pore size 4 μ m), which is fused to the end of a glass tube (3). The latter is connected to a glass vessel (4), via a polyvinylchloride (Rauclair) tube (5). The film holder

is placed inside a covered plexiglas cell (6). The Plexiglas cover and the porous discs have narrow channels and grooves for the incident and reflected light beams of the ellipsometer. Some elements of the ellipsometer are shown in fig. 1. P stands for polarizer and A stands for analyzer. Details of the ellipsometric data acquisition and processing are given in the ellipsometry section, below. The silica plates and porous glass disc were saturated for a night in a F127 solution before the TFB measurements.

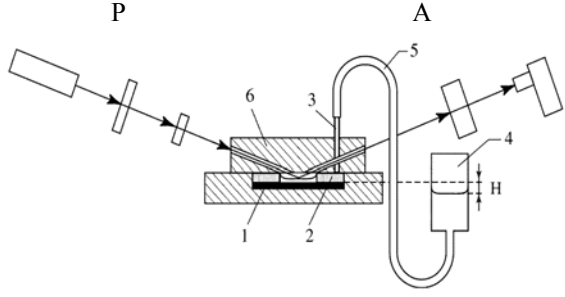


Figure 1 Thin-Film Balance. (1) Silica strip (2) porous glass disc, (3) glass tube, (4) glass vessel, (5) polyvinylchloride (Rauclair) tube, (6) plexiglas cell. Arrows indicate the light beam; (A) analyzer, (P) polarizer.

Manipulation of the hydrostatic pressure, by changing the height difference (H) between the silica surface and the liquid in reservoir (4), will affect the pressure, Π in the film. At equilibrium, Π is the disjoining pressure; it is opposite in sign and equal in magnitude to the hydrostatic pressure difference Δp_H .

$$\Pi(h) + \Delta p_H = 0 \quad (1)$$

The hydrostatic pressure difference is given by $\Delta p_H = \rho g H$, where ρ is the liquid density, g is the gravitational acceleration and H the height difference between the silica surface (1) and the reservoir (4). H has negative values as the level in the vessel is below the silica surface, and is measured with a cathetometer (Mitutoyo, Model AT11-N600, Japan). In the film drainage experiments a pressure of -4.5 kPa was applied after which thinning of the film was followed by ellipsometry.

2.3 Ellipsometry

Ellipsometry measures variations of the polarization state of light reflected from interfaces. The experimental data are expressed in terms of the ellipsometrical angles ψ (where $\tan \psi = |r^p|/|r^s|$ is the amplitude of the ratio of the parallel (p) and perpendicular (s) reflection coefficient) and Δ (the change in the phase difference that occurs upon reflection). These are related to the Fresnel reflection coefficients r^p and r^s , for p- and s-polarized light as $r^p/r^s = \tan \psi e^{i\Delta}$. These coefficients are complex functions of the angle of incidence, the wavelength, the optical properties of the substrate, the ambient medium, and of the layers and the thickness of the layers. Details can be found elsewhere (18).

The ellipsometric angles were determined via *in situ* null ellipsometry. In null ellipsometry, the polarizing elements (polarizer, P and analyzer, A) are rotated until the signal at the photo-detector is minimized ("nulled"). A Multiskop instrument (Optrel Gbr, Berlin) controlled by a computer was used for

the measurements. The light source was a He-Ne laser with wavelength of 632.8 nm. Because of some differences between the available porous discs, we measured at angles of incidence varying between 65° and 70°, which is close to the Brewster angle for an air-silicon interface (75°). The ellipsometric angles were recorded as a function of time. A four-layer model {silicon/ silicon oxide/aqueous film/air} was considered for the computation of the film thickness. In the calculations of the film thickness (h_{film}), predetermined values for the refractive indices of silicon (3.85), silica (1.46), aqueous solution (1.333) and air (1.00), as well as for the thickness of the silica layer (2 nm) were used. Furthermore, it was assumed that the aqueous film is homogeneous, and that the refractive index is the same as that in the aqueous bulk solution, n_{sol} . Although the accuracy of the calculated sample parameters such as the adsorbed layer thickness (h_{ads}) or the film thickness (h_{film}) as well as the refractive index (n_{ads} or n_{film} , respectively) depends on the correctness of the assumed model, trends in these parameters are less sensitive to the model. Correction of the film thickness to account for an internal structure with adsorbed layers at the interfaces, e.g., F127 adsorbed layer at the silica-water interface / aqueous film core / F127 adsorbed layer at the air-water interface (11) does not significantly alter the results. The disjoining pressure curves determined this way are always very smooth, but their absolute position on the h -axis may have an uncertainty (at most) 10-15 %. Adsorption measurements are also monitored via ellispometry. Details are given in our previous work (11).

2.4 Static Light scattering

Static light scattering (SLS) was used for the characterization of the F127 in solution. The light source was an argon ion laser (Lexel, Palo Alto, CA) emitting vertically polarized light at a wavelength of 514.5nm. Light scattering measurements were carried out with the static/dynamic compact goniometer system an ALV/DLS/SLS-5000 (Langen, Germany). The scattering angle was 90°. Solutions were contained in a cell thermostatted at 22°C.

2.5 Contact angle goniometry

A drop of liquid was placed on the silica surface and the image of this drop was investigated with a Contact Angle Meter G-1 (Goniometer), Erma Optical works, Ltd., Tokyo, Japan at T=22°C. The contact angle of water was always lower than 8°, indicating the hydrophilic nature of the silicon oxide surface.

3 Result and discussion

3.1 Effects of additives on the properties of the surfactant in aqueous solutions

It is known that block copolymers form aggregates of different kinds, depending on the molar mass, block sizes, the solvent composition, and the temperature. The effect of various additives on the aggregation of F127 in aqueous solution has been studied in detail (11, 19, 20). Alexandridis et al. have correlated the effect of salts on micellization of the triblock copolymer with the ionic radius and the heat of

solvation of the salts (21). Because F127 is rather polydisperse (the M_w/M_n ratio is around 1.3 as measured with gel permeation chromatography (GPC) by Nelson et al (22)), it is not easy to obtain a sharp cmc value. It is probable that some lower molar mass diblock PEO-PPO is present in the sample (22). In the present study we used static light scattering (SLS) in order to measure the influence of different types of additives on micellization (cmc) of F127. Upon increasing the concentration of F127 the scattering intensity was found to display a rapid increase at a given concentration. The values of the critical micellization concentration were obtained from the intersection point between linear regressions for the two distinct regions in the intensity-concentration plot. The results are summarized in Table 1.

Table 1 The cmc as found by SLS of F127 in 0.1 M additive at pH = 6 and T = 22° C.

0.1 M additive	cmc / μ M
Na ₂ SO ₄	400
NaCl	800
No additive	1400
Urea	1800
NaSCN	2500

We can see that Na₂SO₄ and NaCl both shift the cmc to lower values, while urea and NaSCN shift it to higher concentrations. Like others (21, 23, 24), we attribute these effects to changes in the χ - parameters (solvent quality) for PEO and PPO blocks, as follows: i) NaCl and Na₂SO₄ decrease the solubility (increase χ) of the copolymer in water (salting-out), ii) NaSCN and urea have the opposite effect (salting-in). The salting-out effect of the anions at a given concentration follows the so-called Hofmeister series: $SO_4^{2-} > Cl^- > SCN^-$. Anions with a strong structure-making tendency decrease the cmc. This may arise from the repulsive interactions between PPO or PEO on the one hand, and salt ions on the other, leading to a salt-deficit zone around the monomers and competition for hydration water (25-27). The increase of the cmc in the presence of urea or SCN⁻ probably comes from the enhanced solubility of the surfactant's hydrophobic moiety PPO. The PPO can be affected by urea either 1) by breaking the water "structure", or 2) replacement of water molecules and hydrogen bonding to urea molecules. Which mechanism is dominant is not very clear. A more extensive discussion is given by Alexandridis et al (26).

3.2 Effects of pH and additives on the adsorption of the surfactant at silica-water and air-water interfaces

Having some overview of the effect of additives on the behaviour of F127 in aqueous solution, we turn our attention to the effect of these additives as well as that of pH on the adsorption behaviour of F127 at the silica-water and air-water interfaces, respectively.

Whether or not adsorption of a given polymer at an interface will occur depends on $-\chi_s$, that is the difference between the Gibbs energy (in units kT) of monomer/surface contacts and that of solvent/surface contacts. If this difference is sufficiently negative (χ_s is positive) adsorption will occur. Adsorbed polymer chains at an interface are often thought to be composed of three types of subchains: trains, which have all their segments in contact with the substrate, loops, which have no contact with the surface and connect two trains, and tails which are non-adsorbed chain ends. The conformation of a polymer on a surface depends on the polymer concentration, the solvent quality, χ_s and the density and distribution of the active sites. An extensive discussion is given in (7, 14). In our previous work we studied the effect of the polymer concentration on the adsorption of F127 at silica-water and air-water interfaces (11). For both interfaces a clear increase in the adsorbed amount (Γ) was measured upon increasing the polymer concentration. The commonly found very steep initial rise, followed by a plateau, i.e., a high-affinity adsorption isotherm, was observed for both interfaces. However, the plateau values at the silica-water interface were reached at a lower concentration of polymer ($\sim 200 \mu\text{M}$) than those at the air-water interface ($\sim 600 \mu\text{M}$). Most likely, F127 adsorbs at the air-water interface via hydrophobic PPO groups, the PEO-moieties dangling into the solution. At silica phase boundary the polymer presumably binds via the EO-parts (the ether oxygen of PEO forms H-bonds with silanol groups), forming either some sort of flat structure (at low concentration) or an adsorbed micellar or bilayer structure, driven by hydrophobic interactions between PPO-parts (at higher concentration).

In general, additives may have two effects on polymer adsorption: 1) they may change $\chi_{\text{PEO/water}}$ and $\chi_{\text{PPO/water}}$ and 2) they may modify $\chi_{s, \text{PEO}}$ and $\chi_{s, \text{PPO}}$ for both surfaces. With increasing χ water becomes a poorer solvent for PEO, leading to a higher adsorbed amount (7). The higher adsorption in poor solvents comes from the fact that the weaker effective lateral repulsion between segments makes the accumulation at the surface easier. The effect of additives on χ_s is less obvious. For the water/air interface, where hydrophobic desolvation is an important driving force, the effect most probably parallels that of the solvency effect: higher adsorption from a poorer solvent. For the silica/water interface, however, additives may take a role as competitor, which displace monomer units from the surface. In addition, the adsorption may be affected by surface charging, because this leads to a changing number of active surface sites. One example of that effect is the decrease in adsorption of PEO homopolymer on silica with increasing pH (7).

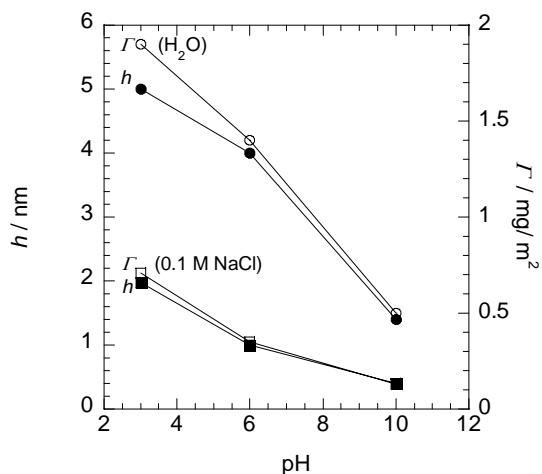


Figure 2 Influence of pH on ellipsometric thickness h and the adsorbed amount Γ of surfactant at the silica-water interface in water and 0.1 M NaCl. $c_{F127} = 100 \mu\text{M}$, $T = 22^\circ\text{C}$.

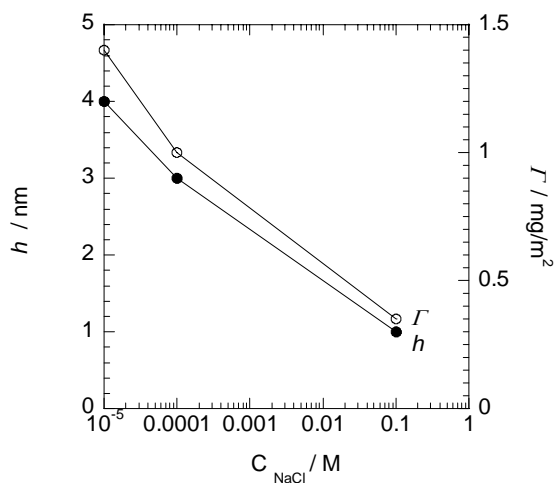


Figure 3 Influence of NaCl on ellipsometric thickness h and the adsorbed amount Γ of surfactant at the silica-water interface. $c_{F127} = 100 \mu\text{M}$, $\text{pH} = 6$, $T = 22^\circ\text{C}$.

Indeed, a decrease of the adsorbed amount of F127 at the silica-water interface was detected upon increasing the pH (see fig.2). Between pH 3 and 10, Γ drops by a factor of five. A similar decrease in the adsorbed amount was measured when increasing the salt concentration at fixed pH (Fig. 3). Moreover, almost no adsorption occurs at high pH in 0.1 M NaCl (Fig. 2). The same trend is found by others for PEO homo- and block-copolymers (28, 29). We adopt here the explanation that the isolated silanol groups which most likely provide the best adsorption sides, act as proton donors in a hydrogen bond to ether oxygens, i.e. $-\text{SiOH} \cdots \text{O}-(\text{CH}_2-\text{CH}_2)-$ (28). Similarly, the PPO groups might be also bound to the silica via hydrogen

bonds (i.e. $\text{SiOH}\cdots\text{O}-(\text{CH}_2(\text{CH}_3)-\text{CH}_2)-$), but whether or not this occurs is not very clear. Given the hydrophilic nature of silica and the fact that PPO is a hydrophobic block due to the presence of the pendant methyl group it is likely that PEO dominates the surface layer. With increasing pH, the silica surface is progressively deprotonated leading to a decrease in the amount of adsorption sites and adsorbed amount of polymer. A similar mechanism might occur upon increasing NaCl concentration. Na^+ ions accumulate as counter ions at the silica surface, acting as “displacers” competing with PEO segments of the polymer (14, 30). In order to check this hypothesis, the effect of other salts with the same counter ion (Na_2SO_4 , NaSCN) on the adsorption behaviour of F127 at the silica- water interface was studied, and compared with the effect of the non-electrolyte urea ($\text{NH}_2)_2\text{CO}$.

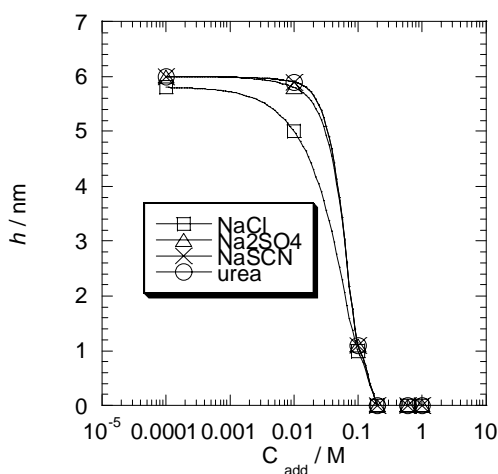


Figure 4 Influence of additives (shown in the picture) on the ellipsometric thickness h at the silica-water interface.

$c_{\text{F127}} = 400 \mu\text{M}$, $\text{pH} = 6$, $T = 22^\circ\text{C}$.

Indeed, a decrease of the adsorbed amount of F127 ($400 \mu\text{M}$) at the silica-water interface was clearly detected upon increasing the concentration of salts (Fig. 4).

A very similar trend was found upon increasing the concentration of urea. At first sight, this may seem puzzling, as urea is not an electrolyte. However, urea has a proton accepting carbonyl- group, by which it will adsorb from the aqueous solution on proton-donating silanol groups, so that it is also capable to displace the polymer from the interface.

An opposite trend was found at the air-water interface: we measured an increase of the adsorbed amount with increasing electrolyte concentration (Figure 5).

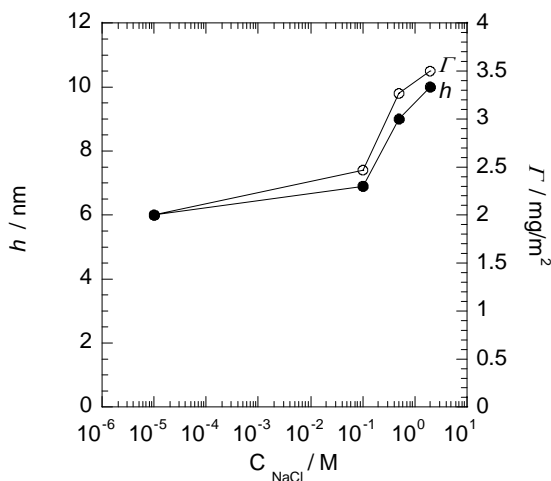


Figure 5 Influence of NaCl on ellipsometric thickness h and the adsorbed amount Γ of F127 at the air-water interface. $c_{\text{F127}} = 100 \mu\text{M}$, $\text{pH} = 6$, $T = 22^\circ\text{C}$.

Of course, the different behaviour of F127 at the air-water and silica-water interfaces comes from different mechanisms of adsorption. At the air-water-interface triblock copolymer molecules adsorb with their hydrophobic moiety, namely PPO towards air, and the hydrophilic PEO moiety protruding into water. With increasing NaCl concentration the lateral repulsion between PEO-moieties becomes smaller, leading to shrinking and a higher adsorption of polymer at the interface, whereas the anchoring affinity (χ_s) is not significantly affected. We expect the same trend for an increasing concentration of Na_2SO_4 . Because the opposite effect of NaSCN and urea on the solvent quality for F127 (compared with the effects of NaCl and Na_2SO_4) has been found, we expect the adsorption of F127 at the air-water interface to slightly decrease in the presence of these additives. Alexandridis et al have measured that the surface pressure (on water) of a similar triblock copolymer, Pluronic P105 ($\text{PEO}_{37}\text{PPO}_{56}\text{PEO}_{37}$) increases in the presence of urea (26).

To summarize: a clear decrease in the F127 adsorption at the silica-water interface upon increasing the pH or the concentration of additive, (or both) is very likely dominated by the cation as a displacer, whereas at the air-water interface an increase in the adsorbed amount of PEO-PPO block copolymer on raising the NaCl concentration is most likely governed by the decreasing solvent quality, and determined by the anion.

3.3 Effects of pH and additives in wetting films: polymer-induced forces and drainage behavior

3.3.1 Polymer-induced forces in wetting films

When polymer-covered surfaces of a wetting film approach each other, they interact by two mechanisms: 1) steric repulsion and 2) bridging attraction. The former case 1) dominates at high interfacial coverage and

provides the stability of films. The latter mechanism 2) becomes important at low coverage and leads to unstable films. The formation of bridges leads to an attraction. If the surface coverage changes, a system can switch between a sterically stabilized and bridging-destabilized case.

Figure 6 shows the effect of adsorbed layers of F127 in dilute (10^{-4} M) NaCl on the $\Pi(h)$ curves at a concentration of the polymeric surfactant below the cmc (400 μ M). At this concentration the silica-water interface has a saturated F127 layer, while the air-water interface has not yet reached a plateau value (11).

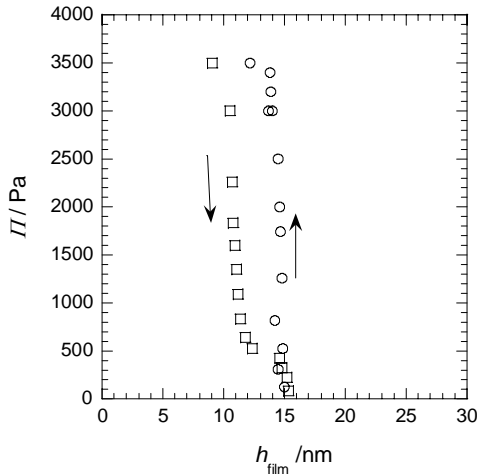


Figure 6 Reversibility of $\Pi(h)$ isotherm: (○ - Δp_H increases, □ - Δp_H decreases). The waiting time between each point is 15 minutes. $c_{F127} = 400 \mu\text{M}$, $pH=6$, $c_{NaCl}=10^{-4}$ M, $T=22^\circ\text{C}$.

Films are stable in the range of pressure studied (0 - 4 kPa), indicating that there is repulsion between the interfaces within the film. In order to check the reversibility, $\Pi(h)$ isotherms are measured in two ways: first by increasing the pressure difference Δp_H down to - 4 kPa, followed by bringing it back to 0 Pa (Fig.6). The arrows in fig.6 indicate the way in which this cycle was completed. The film thicknesses obtained in the first part of the cycle are slightly higher than those obtained on the way back. However, both lead to the same thickness of ~ 15 nm at the end of the pressure cycle (increase/ decrease) at $\Pi \sim 0$: the films behave (almost) reversibly. Probably, a longer time (> 15 minutes) is required to reach an equilibrium thickness when increasing the Π .

The steep $\Pi(h)$ dependence is characteristic for strong steric repulsion between adsorbed layers: the thickness of the film at high pressure is consistent with the sum of the thickness of the two layers adsorbed at the interfaces of the wetting films (11).

In order to compare the total thickness of the adsorbed layers of polymer $h_{ads.layers} = h_{air-water} + h_{silica-water}$ with the film thickness h_{film} , we plot the $h_{ads.layers}$ (measured by ellipsometry) versus the h_{film} measured at $\Pi = 4.5$ kPa for different concentrations of F127 (Figure 7, c_{F127} shown in μM).

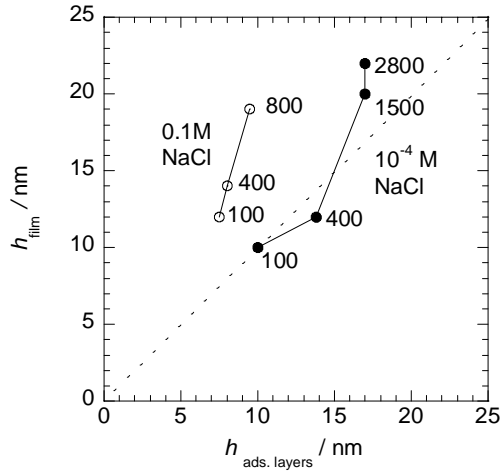


Figure 7 Equilibrium film thickness h_{film} (at $\Delta p_H = -4.5$ kPa) versus thickness of adsorbed layers $h_{ads.layers}$ at pH=6, $T=22^\circ\text{C}$.

The dashed line in Figure 7 represents the case $h_{film} = h_{ads.layers}$ for 10^{-4} M NaCl. The two lines in fig. 7 refer to low (10^{-4} M) and high (0.1 M) NaCl concentrations, respectively. In 10^{-4} M NaCl the h_{film} has almost the same values as the $h_{ads.layers}$ for the studied concentrations of polymer. The slope increases somewhat with the concentration of F127, showing that h_{film} is slightly higher than the $h_{ads.layers}$ for the concentrations of F127 around the cmc. We should keep in mind that for films of a few nm, ellipsometric readings are rather insensitive to the film thickness (adsorbed amounts are determined more accurately from ellipsometry). The thickness depends on the film model used for the calculation: for example, the refractive index (of the adsorbed layer n_{ads} or the film n_{film} , which have different values) is a rather important parameter. Therefore, it is not surprising that the h_{film} has not exactly the same values as the $h_{ads.layers}$.

In 0.1 M NaCl h_{film} clearly deviates from $h_{ads.layers}$: at given $h_{ads.layers}$ the h_{film} is higher. In 0.1 M NaCl the film thickness is almost twice the total thickness of the adsorbed layers. This seems unexpected: NaCl causes a shrinkage and mutual attraction of the polymer molecules so that one anticipates a lower h_{film} . Possibly, we are dealing here with a laterally inhomogeneous layer containing ‘lumps’ of polymer which extend further out from the surface and are responsible for the disjoining pressure. In our previous work we reported ellipsometric images of the film and observed that the film is highly heterogeneous in 0.1 M NaCl(13).

In Figures 8 and 9 we compare the effect of the pH (fig.8) and 0.1 M additives (fig.9) on the interaction forces in wetting films of F127. Stable films are seen for all pH; moreover, pH has a negligible effect on h_{film} .

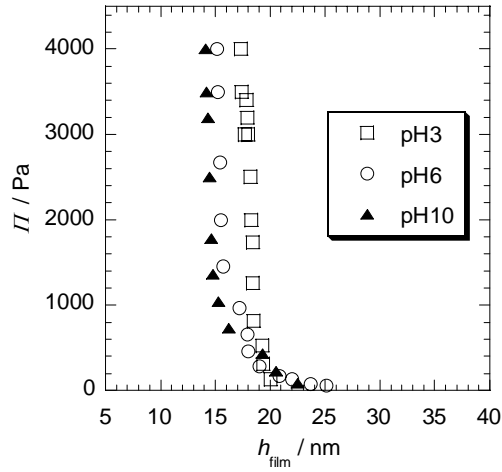


Figure 8 the effect of pH on $\Pi(h)$ isotherms at $C_{F127} = 400 \mu\text{M}$, $C_{\text{NaCl}} = 10^{-4} \text{ M}$, $T = 22^\circ\text{C}$.

Most likely the steep repulsion comes from the steric effects driven by the adsorbed layers. Since the ionic strength is low, electrostatic effects might play a role as well ($\kappa^{-1} \approx 30 \text{ nm}$ for 10^{-4} M NaCl). Besides, it is generally accepted that the potential of the clean air-water interface is negative ($\Psi_1 = -35 \text{ mV}$) (1) and also the silica-water interface is at neutral pH-value negatively charged ($\Psi_1 = -30 \text{ mV}$) (2). If this is the case, the range of the thickness should be higher for higher pH. However, the opposite trend is observed: a higher thickness at lower pH. Apparently, the increase of the adsorbed amount at the silica-water interface (Fig.2) is more important. However, the gradual repulsion between 23 and 15 nm shows that electrostatics might play role at pH 10 and below 700 Pa.

Stable films are also obtained with different additives at pH=6 (Fig. 9). The thickness of these films was measured after the drainage had completed.

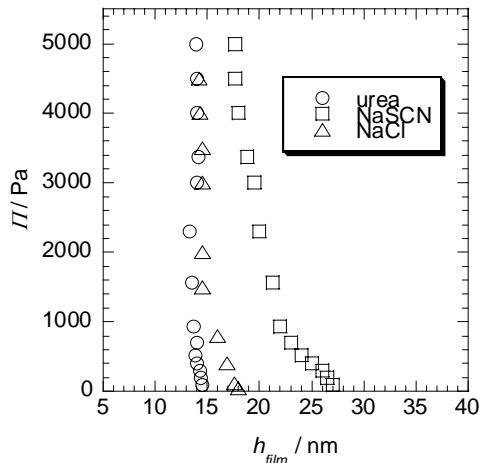


Figure 9 The effect of 0.1 M additives on $\Pi(h)$ isotherms at $c_{F127} = 400 \mu\text{M}$, $\text{pH} = 6$, $T = 22^\circ\text{C}$.

A thickness of 14-15 nm taken from the steep part of the isotherm is found for both 0.1 NaCl and urea. In 0.1 M NaSCN the h_{film} has a slightly higher value of 18 nm. It is most likely that the PEO-chains swell more in NaSCN solution.

3.3.2 Effects of pH and additives on drainage of wetting films

In our previous paper, we demonstrated that films made of F127 in the presence of a lot of NaCl (0.1 M or more) tend to drain very slowly. We reproduce one example here (fig.10). The thickness of the film h is plotted versus time on a semilogarithmic scale.

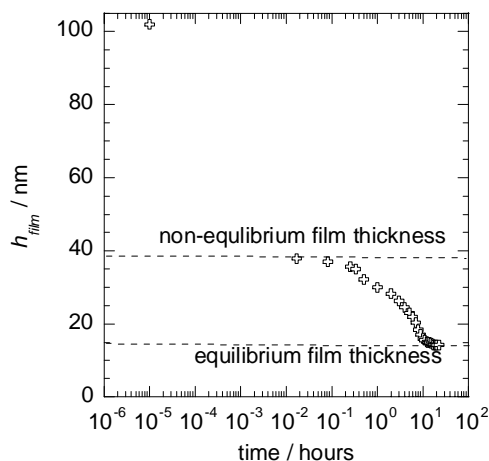


Figure 10 Film drainage in 0.1 M NaCl at a fixed $\Delta p_H = -4.5 \text{ kPa}$, $c_{F127} = 400 \mu\text{M}$, $\text{pH} = 6$, $T = 22^\circ\text{C}$.

Fast drainage is observed during the first minutes, where the thickness changes from 100 down to 40 nm. Beyond 40 nm one sees that the drainage slows down markedly and the thickness changes from 40 down to 20 nm in 15 hours. After 15 hours the thickness changes only slightly. Below we refer to films that undergo this kind of slow thinning as ‘non-equilibrium films’. One of the explanations given for the slow drainage was an increase of the local concentration of F127 within the film, followed by gelation of F127 under the influence of NaCl (13). Considering that an increase of the pH i) decreases the adsorption of F127 at the silica-water interface (Figs. 2- 4) and ii) has no effect on the solvent quality for F127, we studied the rate of drainage of films for different pH; if our explanation makes sense, there should be no pH effect on the rate of drainage. In Figure 11 the drainage for different pH is shown.

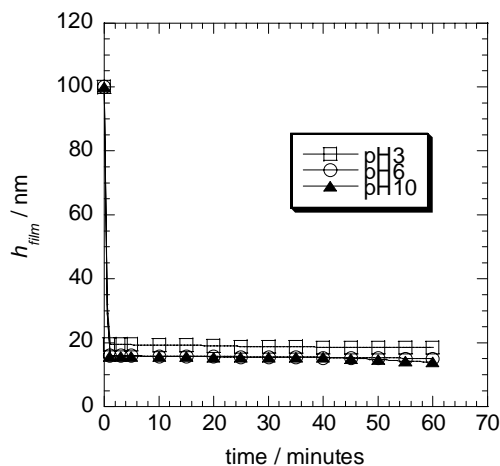


Figure 11 Influence of the pH on the film drainage at $\Delta p_H = -4.5$ kPa, $c_{F127} = 400 \mu\text{M}$, $c_{\text{NaCl}} = 10^{-4}$ M, $T = 22^\circ\text{C}$.

It is clear that the slow regime is indeed not seen at any pH: all these films drain very quickly. This seems to hold generally as long as the additive concentration is low. However, an increase of pH from 6 to 10 in the presence of 0.1 M NaCl leads to unstable films. Moreover, the drainage slows down dramatically in 0.1 M NaCl. Supposing that the reason of the slow drainage is the solvent quality of water for F127, which depends on the temperature and the nature of additives, one wonders how the other additives affect drainage. We have seen that water becomes a better solvent for the PEO blocks if urea or NaSCN is present in the solution (salting-in effect) (19, 26) and the cmc was shown to increase (table 1). On the basis of the arguments above one expects that these additives would not slow down drainage. To check this, we have studied the effect of urea and NaSCN on the drainage of films (Figure 12).

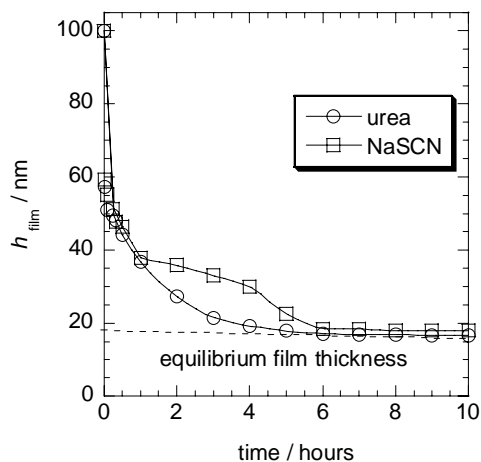


Figure 12 Influence of 0.1 M additives on film relaxation at a fixed $\Delta p_H = -4.5$ kPa, $c_{F127} = 400 \mu\text{M}$, $pH = 6$, $T = 22^\circ\text{C}$.

In Fig. 12 we observe, surprisingly, a similar trend as in 0.1 M NaCl (Fig. 10): a slow drainage regime. The films drain a little quicker: after 5-6 hours film drainage is almost completed, whereas for NaCl this was 15 hours. Taking into account that the NaSCN displaces the gel region as well as the cloud point of F127 to a higher concentration (19), gel formation cannot explain the slow drainage of these films. Two things stand out from the data: i) all additives have a strong retarding effect on drainage and on desorption from the solid surface; ii) the retarding effects of NaCl and Na₂SO₄ are larger than those of NaSCN and urea.

Since all additives slow down drainage and reduce the adsorption on silica we propose that these two observations are coupled. Liquid films under external pressure will usually develop a lateral thickness profile. This is because there is a hydrodynamic pressure gradient in the radial direction. The rate at which a thick film drains is therefore largely determined by the thickness at which the perimeter stabilizes: a very thin perimeter acts as a ‘bottleneck’, which retards drainage strongly. Desorption of F127 from the silica-water interface under the influence of additives might lead to weak bridging of polymers between the interfaces of film. If this happens, even if the film remains stable, liquid flow is very much impeded. The gelation effect seems to be secondary: NaCl and Na₂SO₄ enhance the drainage time by a factor of 4 or more, but the other two additives also induce a slowing down which cannot be attributed to solvency effects. Note that in 0.1 M electrolyte the electrostatic effects are screened and the deviation of films from the plane-parallel shape under the bridging attraction of polymer might indeed occur.

The shapes of curves in urea and NaSCN are different: more gradual relaxation is seen in 0.1 M urea. Probably, the electrostatic repulsion between interfaces of the film (which is not suppressed as compared with 0.1 M electrolyte) might resist the bridging attraction and therefore keep the film plane-parallel.

To summarize, the rate of drainage is controlled by the (thin) periphery of the film. We have seen that all additives reduce the adsorption at the silica surface, and that an increase in pH in the presence of these additives eventually destabilizes the films. We concluded that destabilization must be due to bridging attraction. We therefore propose that bridges are also present at lower pH and 0.1 M additive, although the bridging force is not strong enough to cause film destabilization under these conditions. If bridges are indeed present, they must have a major retarding effect on solvent flow along the midplane of the film. In a way, bridges lead to a kind of polymer network straddling the solvent film (Fig. 13b).



Figure 13 a) $c_{\text{NaCl}} \leq 10^{-4}$ M: plane-parallel film; quick drainage.

b) $c_{\text{NaCl}} > 10^{-4}$ M: deflection of film from the plane-parallel shape due to bridging, slow drainage

This would have a major effect on film drainage slow down. An additional effect comes from the reduction in solvency caused by NaCl and Na₂SO₄, which give the adsorbed layer a gel-like character, thus further retarding drainage. This latter effect is noticeable, but not as important as the bridging effect. One

might object that at high pH we observed low Γ at the silica-water interface (fig.2) and yet fast drainage of films (fig. 11). Probably, electrostatics prevents bridging in this case (by keeping the film plane-parallel).

3.3.3 Wetting

In order to assess the polymer contribution to the stability/instability of wetting films formed by aqueous solution of F127 (see 3.3.1.), contact angles at the silica interface were measured for different concentrations of NaCl at a given polymer concentration. The results are summarized in Table 2.

Table 2. Contact angle of aqueous solution of F127 (100 μ M) at silica surface.

$C_{\text{NaCl}} / \text{M}$	$\theta / ^\circ$
0	< 8
10^{-4}	< 8
0.1	10
1	12
2	13

Contact angles give us an idea about the interaction forces in wetting films. If the repulsive forces in wetting films are strongly dominant over the attractive ones, we expect complete wetting, while in the opposite situation we expect a finite contact angle. The slight increase of the contact angle upon raising the concentration of NaCl suggests that the bridging attraction might indeed occur.

4 Conclusions

The main results of this paper are that additives used in this study: 1) reduce the adsorption of F127 at the silica-water interface; 2) destabilize films at high pH; 3) slow down drainage of films. We think that reduction of adsorption and retardation of drainage is coupled. We propose that bridges, which occur under the influence of additives, impede liquid flow (fig. 13 b). Moreover, we suggest that destabilization comes from the attractive contribution, which most likely is also driven by polymer bridging. Electrostatic repulsion might give extra stabilizing effect in films at pH 10 and low salt concentration.

References

1. D. Exerowa, P. Kruglyakov, *Foam and Foam Films* (Elsevier, 1998).
2. K. Stöckelhuber, A. Werner, *Eur. Phys. J.* **E12**, 431-435 (2003).
3. J. Lyklema, *Fundamentals of Interfaces and Colloid Science*, FICS (Academic press, London, 1991), vol. I, A 9.4.
4. N. V. Churaev, *Colloid Journal* **65**, 263-274 (20.01.2005, 2002).
5. N. V. Churaev, *Colloid Journal* **62**, 517-525 (21.01.2005, 2000).
6. D. H. Napper, *Polymeric stabilization of colloidal dispersions* (Academic Press, London, 1983).
7. G. J. Fleer, M. A. Cohen Stuart, J. M. H. M. Scheutjens, T. Cosgrove, B. Vincent, *Polymers at interfaces* (Chapman & Hall, London, UK, 1993).
8. B. Diakova, C. Filiatre, D. Platikanov, A. Foissy, M. Kaisheva, *Advances in Colloid and Interface Science* **96**, 193-211 (20.01.2005, 2002).
9. B. Diakova, M. Kaisheva, D. Platikanov, *Colloids and Surfaces A:Physicochem.Eng. Aspects* **190**, 61-70 (2001).
10. B. Diakova, D. Platikanov, R. Atanasov, M. Kaisheva, *Advances in Colloid and Interface Science* **104**, 25-36 (20.01.2005, 2003).
11. O. V. Eliseeva, N. A. M. Besseling, L. K. Koopal, M. A. Cohen Stuart, *Langmuir* **21**, 4954-4963 (2005).
12. N. E. Esipova, S. V. Itskov, N. V. Churaev, *Colloid Journal* **64**, 699-705 (2002).
13. O. V. Eliseeva, R. G. Fokkink, N. A. M. Besseling, L. K. Koopal, M. A. Cohen Stuart, *accepted for publication in J. Colloid Interface Sci.* (2006).
14. M. A. Cohen Stuart, G. J. Fleer, H. M. Scheutjens, *Journal of Colloid and Interfaces Science* **97**, 515-535 (1984).
15. K. J. Mysels, M. N. Jones, *Discuss. Faraday Soc.* **42**, 42 (1966).
16. V. A. Shishin, Z. M. Zorin, N. V. Churaev, *Kolloidnyi Zhurnal (English transl.)* **39**, 351 (1977).
17. B. V. Derjaguin, Z. M. Zorin, N. V. Churaev, V. A. Shishin, *Wetting, Spreading and Adhesion*. J. F. Padday, Ed. (Academic Press, London, 1977).
18. H. G. Tompkins, *A User's Guide to Ellipsometry* (Academic Press, Inc., San Diego, 1993).
19. M. Malmsten, B. Lindman, *Macromolecules* **25**, 5440-5445 (1992).
20. G. Wanka, H. Hoffman, W. Ulbricht, *Macromolecules* **27**, 4145-4159 (1994).
21. P. Alexandridis, J. F. Holzwarth, *Langmuir* **13**, 6074-6082 (1997).
22. A. Nelson, T. Cosgrove, *Langmuir* **21**, 9176-9182 (2005).
23. K. D. Collins, M. W. Washabaugh, *Q. Rev. Biophys.* **18**, 323-422 (1985).
24. A. Kabalnov, U. Olsson, H. Wennerström, *J. Phys. Chem.* **99**, 6220-6230 (1995).
25. E. Florin, R. Kjellander, J. C. Eriksson, *J. Chem. Soc. Faraday Trans.* **80**, 2889 (1984).
26. P. Alexandridis, V. Athanassiou, T. A. Hatton, *Langmuir*, 2442-2450 (1995).

27. T. Boomgaard, J. Lyklema, *Langmuir* **5**, 245 (1989).
28. J. Rubio, J. A. Kitchener, *J. Colloid Interface Sci.* **57**, 132-142 (1976).
29. M. Malmsten, P. Linse, T. Cosgrove, *Macromolecules*, 2474-2481 (1992).
30. T. Van Den Boomgaard, T. F. Tadros, J. Lyklema, *Journal of Colloid and Interface Science* **116**, 8-16 (1986).

Chapter 6 Interaction forces between surfaces immersed in solutions of a polyethylene oxide-polypropylene oxide copolymer

Abstract

The interaction between two silica surfaces, immersed in solutions of a surfactant is studied by colloidal probe atomic force microscopy (CP-AFM). The surfactant used is Pluronic F127, which is an ABA block copolymer, composed of hydrophobic polypropylene oxide B block (PPO) and two hydrophilic polyethylene oxide A blocks (PEO). It has an average molecular composition $\text{PEO}_{99}\text{PPO}_{65}\text{PEO}_{99}$. Hydrophilic and hydrophobized silica surfaces are used. Long ranged attractive forces are found between bare hydrophobic and hydrophilic surfaces in aqueous solutions. In the presence of surfactant the attraction disappears, and only repulsive forces are observed. Repulsive forces are also measured in the solution of surfactant between two hydrophilic surfaces. The repulsion becomes shorter ranged when electrolyte is added in increasing amounts. A weak adhesion between a hydrophobic and a hydrophilic surface is measured in the presence of F127 in 0.1 M NaCl. This attraction is attributed to bridging of polymer between a densely covered hydrophobic surface and a sparsely covered hydrophilic surface. This is consistent with the behavior of wetting films (air/ aqueous film/ silica), which in some case destabilize in the presence of NaCl due to the formation of polymer bridges.

1 Introduction

Interaction forces between adsorbed layers of ABA polymeric surfactants (composed of a propylene oxide anchoring block (B block) and polyethylene oxide buoy block (A block)) onto hydrophobic and hydrophilic surfaces have been studied in polymer-free electrolyte solutions (1-3). The reason for the interest in these systems is the wide use of these surfactants as colloidal stabilizers, in e.g., paints, drug formulations, mineral flotation and other areas. In addition, they are also commonly used as stabilizers of thin films, including wetting films. One of the interesting properties of the triblock copolymers is the different solubility of the PEO and PPO blocks, which results, for example, in adsorption at both hydrophilic and hydrophobic surfaces.

By measuring interactions between adsorbed layers of polymers at colloidal particles or surfaces, information about the ranges and the types of forces acting between surfaces can be obtained. By knowing the forces, the stabilizing ability of these surfactants can be predicted, tuned and used in practice.

Colloidal probe atomic force microscopy (CP-AFM) can be used to study the interaction forces between a spherical probe attached to the AFM cantilever and a surface. This technique is quite young (AFM has been developed in 1986 (4)) but also very successful. The reasons for the widespread use of the AFM method are coming from the facts that i) it is considerably easy to use than the surface force apparatus, and ii) it is not limited to mica as a substrate. Detailed overviews of colloidal probe CP-AFM are given elsewhere (1, 5, 6). This technique is also used in the present work.

The motivation to carry out the present study comes from our previous investigations of wetting films (7, 8), where we studied the interactions in thin films formed from aqueous solutions of surfactant { triblock copolymer Pluronic F127 ($\text{PEO}_{99}\text{PPO}_{65}\text{PEO}_{99}$) } onto silica. An interesting finding was that in the presence of additives such as e.g., NaCl the drainage of the films decreased dramatically. We attributed this effect to bridging attraction between a densely covered air-water interface and a very sparsely covered silica-water interface. Bridging was correlated with the reduction of the adsorbed amount on silica, which occurred upon increasing the concentration of the additives.

On the basis of these measurements we expected to find attractive forces between hydrophobic and hydrophilic surfaces in the solution of surfactant, when the concentration of electrolyte would be sufficiently high.

In recent work of McLean et al. (3), a weak attractive force is measured between two hydrophilic silica surfaces bearing triblock copolymer ($\text{PEO}_{122}\text{PPO}_{56}\text{PEO}_{122}$) layers in 0.15 M NaCl. These authors also studied the forces between adsorbed layers on hydrophobized silica. In the latter case only a repulsive force is measured. In recent studies (1, 2) Luckham also describes repulsive forces between ABA copolymers

adsorbed onto hydrophobic surfaces. However, the effect of the electrolyte concentration and the interactions between different surfaces in the solution of block copolymer was not studied.

The effect of electrolytes on the interaction between polyethylene oxide (PEO) -covered silica surfaces was studied by Giesbers et al. (5, 6). Under some conditions a strong adhesion was observed and attributed to bridging of PEO between two silica surfaces. In Table 1 we summarize the information, published so far (as obtained by CP-AFM) about the interactions between surfaces in the presence of water-soluble polyethers. To distinguish various cases, we will use the abbreviations: phil/phil, phob/phob and phob/phil indicating the nature of the interacting pairs: both hydrophilic, both hydrophobic, and the asymmetric case with one hydrophilic and one hydrophobic surface, respectively.

Table 1 Reported (or to be reported) systems on the interactions between polymer bearing surfaces, obtained (or to be obtained) by colloidal probe AFM

Surfaces Polymers	Phil/Phil	Phob/Phob	Phil/Phob
PEO-PPO-PEO	McLean et al. (3) Present study	McLean et al. (3), Luckham et al. (1, 2)	Present study
PEO	Giesbers et al. (5, 6)	-	-

The present study focuses on the block copolymeric surfactant and on the asymmetric case (phob/phil), with some attention for phil/phil as a reference case.

2 Experimental

2.1 Apparatus

The force measurements are done using the MultiMode PicoForce, which is operated by a NanoScope IIIa (Digital Instruments) controller. The MultiMode PicoForce microscope is equipped with a standard liquid cell and a PicoForce scanner. Because of the sensitivity of the AFM to thermal drifts and external vibrations, the apparatus is located in a thermostatted room in a part of the building (basement) where vibrations are weak.

2.2 Materials

The water used is purified using a “Barnstead pure UV” system (USA). The important purification steps are: a pre-treatment by ion-exchanger, an UV system (to remove/ breakdown organic molecules), an active carbon column, and a filtration through a 0.2-micron filter. It produces water with a resistivity of 18.3 Megohm-cm ($M\Omega\text{cm}$).

The polymeric surfactant (triblock copolymer) Pluronic F127 (average molecular composition PEO₉₉PPO₆₅PEO₉₉, Sigma-Aldrich CO., USA) is used without further purification. Pluronic F127 has a number-average molar mass, M_n of 12600 and a PEO content of 70% by weight. Aqueous solutions of F127 are prepared by dissolving the polymer in demineralised water under gentle agitation. Further in the text the terms ‘surfactant’ or ‘F127’ are used for the triblock copolymer F127.

Solutions of NaCl are used as the continuous medium. Sodium chloride, NaCl, supplied by Baker Chemicals (Holland), is used without further purification.

All measurements were carried out at pH~6 and T~ 294-296 K.

Hydrophilic surfaces

Polished silicon wafers, Si (p-type, boron-doped, oriented <1-0-0>, resistivity 12-18 Ωcm) are purchased from Wafer Net, Germany. The thickness of the natural silicon oxide SiO₂ layer on the surface is about 2 nm, as determined by ellipsometry. Wafers are cut into small strips (1×1 cm) and boiled for 5 min at 80°C in a mixture of 25% NH₃, 30% H₂O₂ and H₂O (1:1:5 by volume). The strips are then rinsed with water and ethanol (99.8%). They were kept in a closed container under water until use. Before the strips are placed in the cell, they were dried with a stream of nitrogen and treated for 30 seconds in a plasma cleaner (Harrick, Model PDC-32 G). The plasma treatment is performed with air (10 Pa). After cleaning, the contact angle of water is always lower than 8°, indicating the hydrophilic nature of the silicon oxide surface.

Hydrophobic surfaces

Cleaned silica strips are placed under hexamethyldisilazane (HMDS) vapour overnight. The silica coated with HMDS has a contact angle of 90°, which changes to 80° after more than two hours of immersion in water. The characteristics of HMDS- coated silica have been reported in detail by Maccarini et al. (9).

2.3 Technique and Procedure

2.3.1 Colloidal probe AFM

Butt (10) and Ducker (11) are the pioneers in the measurements of colloidal interactions using AFM. They attached a colloidal particle to the end of a cantilever and measured the forces between a silica particle and a silica plate. In this mode of operation, the bending of the cantilever with a probe is monitored as a function of the probe/plate distance. Displacements of the particle toward or away from the surface are achieved by applying a voltage to a piezoelectric element, and the deflection of the cantilever is monitored by means of a reflected laser beam, which is picked up by a position-sensitive photodiode (1). An experiment consists of simply applying a constant ramp voltage from a function generator to the piezo element: changing the frequency changes the approach rate, whilst changing the amplitude changes the amount of compression (1). By knowing how much the surfaces move for a given voltage on the piezo (this can be obtained by calibration prior to the experiment) and by knowing the spring constant of the cantilever) the force-distance profile between the particle and surface can be obtained (1). Two assumptions have to be made: 1) the force at large separation, where the cantilever is undeflected, is assumed to be zero,

and 2) the separation, where the constant compliance region is observed, is assumed to be zero. The first assumption is generally valid, but the second one is frequently incorrect when a thin film of adsorbed material with very low compressibility is present between the two surfaces (1). This is the main disadvantage of the AFM operated as a surface force apparatus.

2.3.2 Procedure

Before setting up the CP-AFM measurements, we glued a silica sphere with a diameter of 6 μm to an AFM cantilever using the method of Giesbers (5, 12). The cantilevers used have a spring constant of around 0.06 N/m. The spring constant of the cantilevers is determined using the Nanoscope IIIa and applying the thermal noise method (13). In this method the power spectrum of the thermal vibrations of a freely oscillating cantilever (no driving oscillation, tip far away from the surface) is analyzed (13).

The cantilever with the silica sphere (treated for 30 seconds in a plasma cleaner) is placed into the liquid cell, and the silica strip is positioned on the scanner. The liquid cell is closed with an O-ring and filled with the solution studied. The surfaces are left for around 20 minutes to equilibrate before starting the measurement. An approach/ retract rate of around 200 nm/s is used in all experiments. The data are collected using a commercial software package called *Nanoscope 6.12*. Finally, the data were processed using Excel 2000.

3 Results

3.1 Hydrophilic silica surface and silica probe (phil/phil).

In order to establish whether the surfactant had adsorbed onto the surfaces, we first have to determine the interactions between bare surfaces. The force profile of phil/phil surfaces is given in Fig.1

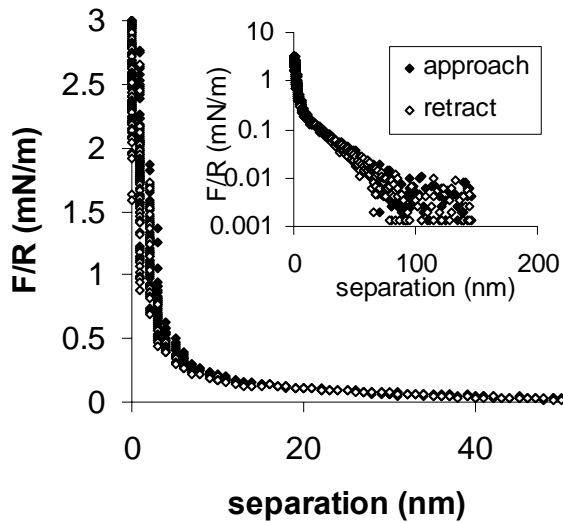


Figure 1 Force distance interaction profiles between hydrophilic silica strip and hydrophilic silica probe immersed in water. Inset: force distance interaction profiles on a semi-logarithmic scale.

Almost no difference is seen between the forces on separation and approach. No interaction between the surfaces is observed until they are around 40 nm from contact. Upon further approach an increasing repulsive force is observed, which is most likely electrostatic in nature. Since such electrostatic forces are known to decay exponentially with distance, we plot the data on a semi-logarithmic scale (inset). A linear decay between 5 and 50 nm seems to be consistent with the data, with a decay length of 20 nm, which would imply an ionic strength of 3×10^{-4} M, possibly coming from traces of electrolyte in the cell.

In Fig. 2 we present a comparison of the force profiles for the phil/phil surfaces immersed in water (filled symbols) and in surfactant (open symbols) solution, respectively.

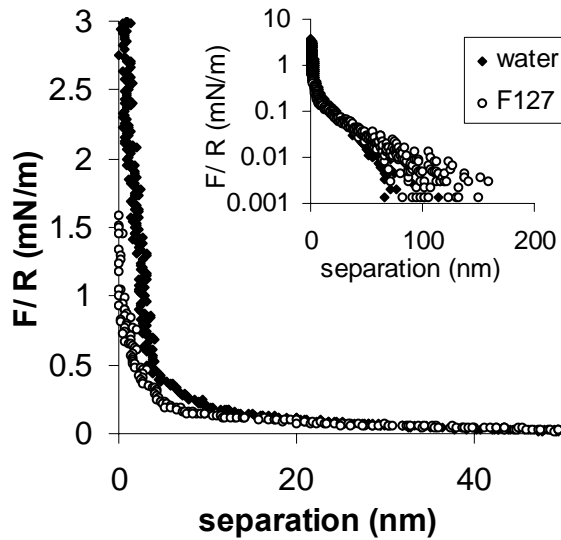


Figure 2 Force distance interaction profiles (upon retraction only) between hydrophilic silica strip and a hydrophilic probe immersed in water and in 400 μ M F127 solution, respectively.

Inset: force distance interaction profiles on a semi-logarithmic scale.

The characteristic feature is the same as for the previous figure: there is no interaction between the surfaces until they are around 40 nm from contact where a repulsive force comes up for both cases. The decay length is around 60 nm (inset), which is similar to interactions obtained in water. When we compare the two cases it can be seen that the interaction profile in water is shifted as compared to that in the surfactant solution. This indicates that some (weak) attractive component is present in the force profile when surfactant is present.

The short-ranged repulsive force is most likely due to steric overlap of the adsorbed layers. Note that the zero of separation is almost certainly different for the two curves, as the adsorbed polymer layer is hardly compressible (see introduction).

The effect of electrolyte on the interaction profiles for F127 solution (400 μM) is shown in Figs. 3a,b.

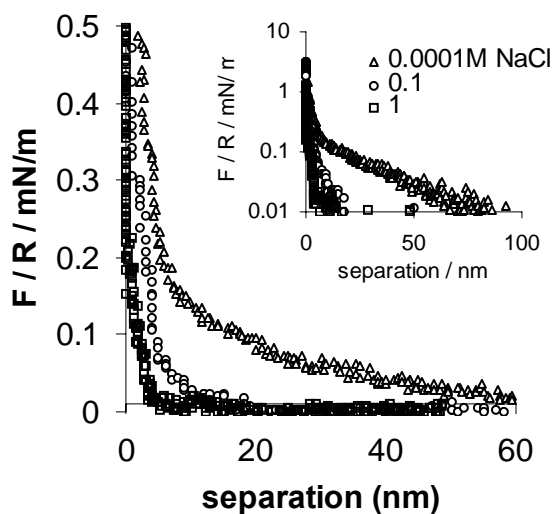


Figure 3a Effect of NaCl on force distance interaction profiles (upon retraction) between a hydrophilic silica strip and a hydrophilic probe immersed in 400 μM F127 solutions.

Inset: force distance interaction profiles on a semi-logarithmic scale.

From fig. 3a, it is clearly seen that electrostatic interactions are screened so that the decay lengths of the repulsive force are decreased upon increasing the concentration of salt. A linear decay between 5 and 50 nm seems to be consistent with a decay length expected for the concentrations of electrolytes.

In Fig. 3b the force between phil/phil surfaces at a separation of 15 nm (obtained upon approach and retraction) is plotted versus the logarithm of the concentration of NaCl.

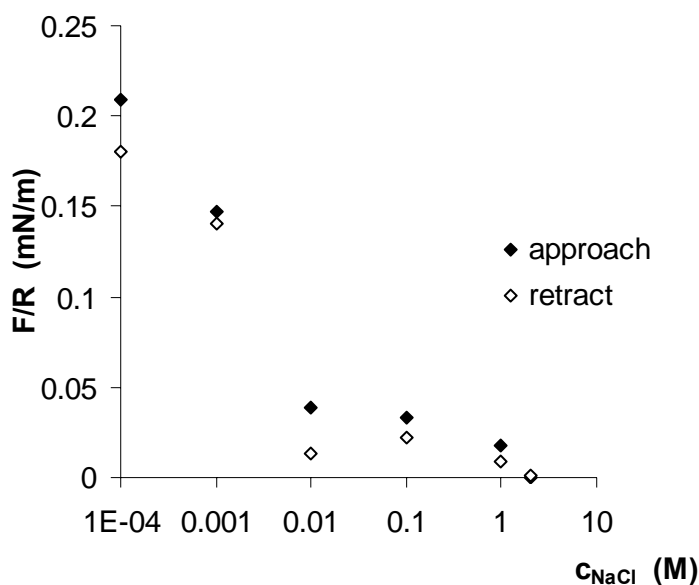


Figure 3b Force at separation 15 nm between phil/phil surfaces in 400 μ M F127 versus the concentration of NaCl

A clear decrease of the force with the electrolyte concentration is observed, which levels off at around 0.5 M. This feature reveals the suppression of electrostatic repulsion for approach and retraction curves. Note, however, that the force remains repulsive; no attractive contribution can be detected. We can also see that the force on retraction is slightly smaller than that on approach. This holds for all force profiles studied.

In Fig. 4 we present one of the force profiles for the phil/phil interactions in the presence of F127 (400 μ M) in 1 M NaCl.

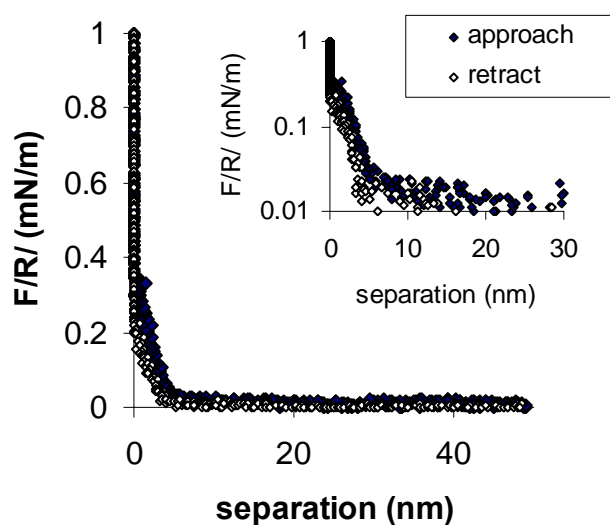


Figure 4 Force distance interaction profiles between phil/phill surfaces immersed in 400 μ M F127 + 1 M NaCl. Inset: force distance interaction profiles on a semi-logarithmic scale.

We can see that the forces are still entirely repulsive. A careful look of the data reveals that the forces upon retraction are slightly weaker than those on approach. This effect can be attributed either to hydrodynamic effects or can be ascribed to very weak polymer bridging. This effect is more pronounced for the interactions between phob/phil surfaces, which are presented in the next section (3.2).

3.2 Hydrophobized silica surface and hydrophilic silica probe (phob/phil).

As before, we first consider the bare surfaces. The interactions between phob/ phil surfaces in water are shown in Figure 5.

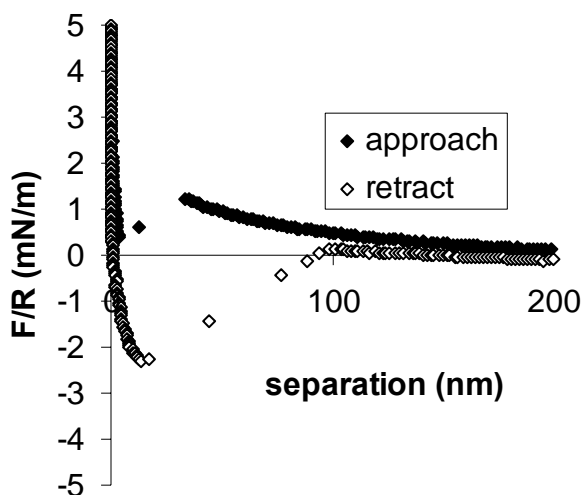


Figure 5 Force distance interaction profile between hydrophobized silica and a hydrophilic silica probe immersed in water.

No interactions between surfaces are observed until they are some 100 nm from contact. Upon further approach, a repulsion is observed, which exponentially increases until the surfaces are about 25 nm apart. At this point an attractive interaction is experienced and the surfaces jump into the contact. On separation, a strong adhesion is observed, which we tentatively attribute to capillary bridge formation (see discussion).

In Fig. 6 we compare the force profiles between phob/phil surfaces in water and in surfactant solution. For the sake of clarity we only show the 'retract' force profiles.

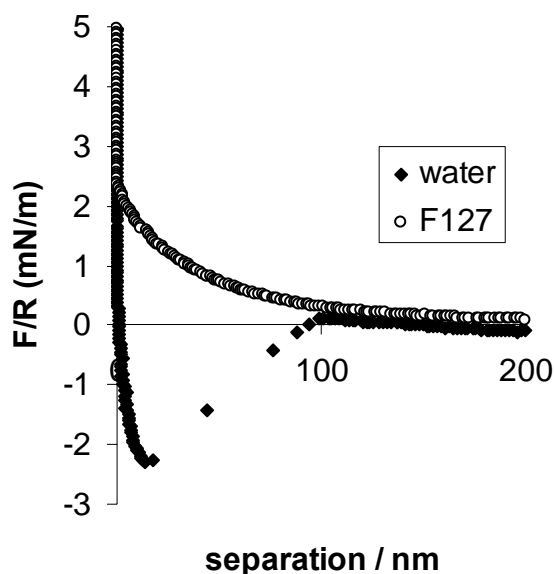


Figure 6 Force distance interaction profiles (upon retraction) between hydrophobized silica and a hydrophilic silica probe immersed in water and 400 μ M F127 solutions.

As can be seen from fig. 6 the long ranged attractive interactions displayed by the bare surfaces have disappeared in the presence of polymer. There is no interaction until the surfaces are some 100 nm apart where a repulsive increasing force is observed. This repulsion is attributed to both electrostatic and a steric interaction (i.e. osmotic repulsion due to an increased polymer concentration between the surfaces). The data, obtained in the present of surfactant and plotted on a semi-logarithmic scale, show a decay length of 50 nm, indicating that again electrostatic forces might be indeed present. This is similar to results obtained for phil/phil surfaces (figs. 1,2).

Figures 7a,b reflect the effect of electrolyte on the phob/phil interaction profiles (upon retraction) for F127 solution (400 μ M). To some extent, the results are similar to those of phil/phil surfaces: upon increasing the concentration of salt the range of the force becomes smaller.

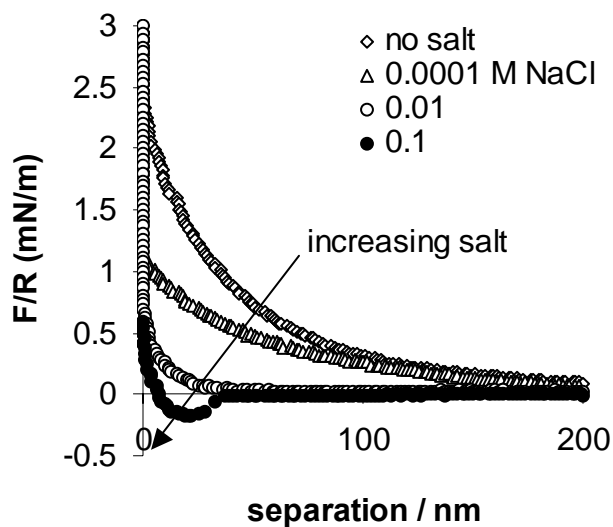


Figure 7a Effect of NaCl on force distance interaction profiles (upon retraction) between hydrophobized silica and a hydrophilic silica probe immersed in 400 μ M F127 solutions.

However, there is also a new feature: an adhesive force is observed in 0.1 M NaCl (Fig. 7a). Good agreement exists between our phil/phob forces profiles in F127 in 0.01 M NaCl (fig. 7a), and those of Musoke and Luckham (2) obtained between hydrophobic glass surfaces bearing an adsorbed layer of PEO/P108 immersed in 0.01 M Na_2SO_4 . A steric interaction is proposed to govern this repulsion. We will return to fig. 7a in the discussion.

As for the phil/phil surfaces we have again plotted the force for the phob/phil surfaces at separation of 15 nm (obtained upon approach and retraction) versus the concentration of NaCl (Fig. 7b).

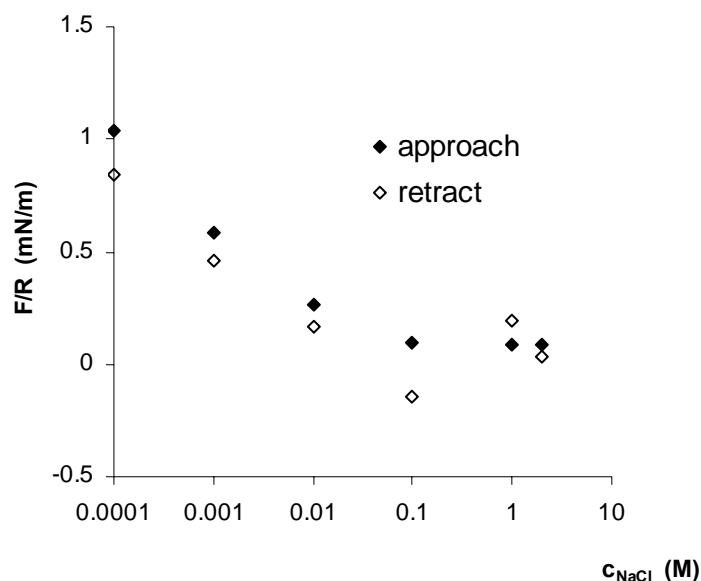


Figure 7b Force (upon retraction) at separation 15 nm between hydrophobized silica and a hydrophilic silica probe immersed in 400 μM F127 solutions versus the concentration of NaCl.

In contrast with the data of fig. 3b, in fig. 7b we observe here a (weak) attractive minimum at 0.1 M NaCl. Since we know from adsorption studies that the polymer remains strongly attached to the hydrophobic surface, the attraction occurring between bare surfaces (fig. 6) must be ruled out. Hence, this minimum can only be attributed to the polymer, that is, to polymer bridging between the hydrophilic and the hydrophobic surface.

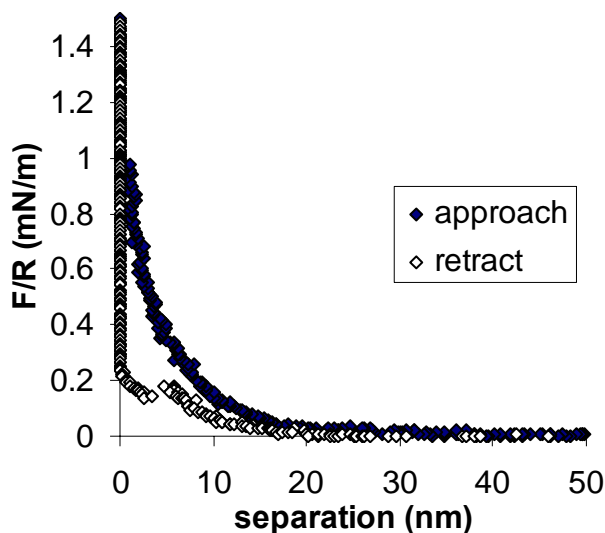


Figure 8 Force distance interaction profiles between phob/phil surfaces immersed in 400 μ M F127 + 1 M NaCl.

As may be expected for bridging, hysteresis in the interaction profiles is more pronounced between the phob/phil surfaces (fig. 8) as compared to that of the phil/phil ones (fig. 4). It should be also noted that upon increasing the concentration of salt, hysteresis becomes more marked as well.

4 Discussion

4.1 F127 adsorption and adsorbed layer thicknesses at hydrophilic and hydrophobic surfaces.

The adsorption of non-ionic surfactants (including triblock copolymers) onto hydrophilic and hydrophobized silica surfaces has been well studied (14-20). Triblock copolymers adsorb both at the hydrophilic and hydrophobic surfaces; at the former they adsorb as a thin layer, probably bound via the EO-moiety, at the latter with the PPO enriching the surface proper and the EO-tails essentially dangling into the solution. In previous studies (20) we have also studied the adsorption of F127 onto silica-water and air-water interfaces as a function of concentration, by means of ellipsometry. The commonly found very steep initial rise is followed by a plateau at $\sim 200 \mu$ M and $\sim 800 \mu$ M for silica-water and air-water interfaces, respectively. Plateau levels of adsorption were 2.5 mg/m^2 (adsorbed layer thickness, $h_{\text{ads}} \sim 7 \text{ nm}$) and 3 mg/m^2 ($h_{\text{ads}} \sim 9 \text{ nm}$) for silica-water and air-water interfaces, respectively (8, 20).

We have also studied the effect of electrolytes on the adsorption of F127 at the silica-water interface. A pronounced decrease of the adsorbed amount was detected upon increasing the NaCl concentration.

4.2 Interactions between *phil/phil* surfaces

Comparison of the interactions between *phil/phil* surfaces immersed in water and in the solution of F127 shows a similar feature: the long ranged repulsion commencing at around 40 nm from contact. This repulsion is most likely dominated by electrostatic repulsion between silica surfaces (Figure 2). The measured forces decay exponentially at large separation. Only when the surfaces come closer (< 20 nm), an attractive component decreases slightly the repulsive force in the solution of F127.

Giesbers et al (5) obtained similar interaction features on approach of two PEO-covered silica surfaces in aqueous solution. They attributed this attractive component to bridging. Taking into account that the PEO moiety of F127 most likely dominates the surface layer of hydrophilic silica (8, 16, 20), some sort of bridging as observed by Giesbers might perhaps occur. The attachment of PEO to the silica surface occurs via hydrogen bonding, which at low surface coverage leads to flat or “pancake” conformation of F127 at silica surface (similar to the PEO). At high coverage a micellar or bi-layer structure, resulting from hydrophobic interaction between PPO, might be formed at silica (20). The latter structure at silica surface is most probable for 400 μ M surfactant. Such structures could be heterogeneous: micellar structures might co-exist with flat conformations of polymers. Upon approach, reconformations of the polymer layers might take place, and additional adsorption of PEO segments is perhaps possible. Some of them might form bridging contacts of PEO with two silica surfaces. Giesbers’ result also shows a clear adhesive force on separation of the surfaces, which is further evidence of bridging; this does not occur in our system. Hence, bridging interaction, if any, is extremely weak.

A long ranged shallow attractive force followed by steric repulsion is also measured by Mclean et al (3) between Pluronic F108 (PEO₁₂₂-PPO₅₆- PEO₁₂₂) layers adsorbed on hydrophilic silica in 0.15 M NaCl. However, the range of attraction is smaller than that observed for PEO and attributed to the van der Waals attraction, probably wrongly. The authors suggest that the presence of the adsorbed polymer layer increases the attractive van der Waals force slightly. At the same time, they do not exclude that the weak attraction could also be due to polymer bridging taking into account the low surface coverage of Pluronic F108 when adsorbed onto silica.

The system studied by Mclean is similar to our system in figs.3 (a, b). However, we did not observe adhesion in the solution of F127 between *phil/phil* surfaces, whereas Mclean observed very weak attraction. One of the slight differences between our force profiles and those of Mclean and of Giesbers could be the different density of polymer at surfaces. Our interaction profiles between *phil/phil* surfaces were measured after 20 minutes of equilibration of in the presence of F127 solution. Note that adsorption occurs very quickly: after a few seconds equilibrium is established (21). Mclean and Giesbers used surfaces with pre-adsorbed polymer, but flushed the polymer solution out with 0.15 M NaCl. Taking into account that the adsorption and, as a result of it, the surface density of triblock copolymer at silica surface decreases in the presence of electrolyte, bridging formation might indeed be more pronounced in case of pre-adsorbed surfaces.

4.3 Interactions between *phob/phil* surfaces

What is interesting and new (to the best of our knowledge) is that a clear attraction is observed between hydrophobic and hydrophilic surfaces (*phob/phil*) in water (Figure 5). Capillary bridges can explain the observed adhesion on approach of bare surfaces. The attraction range on separation is too large to be attributed to the van der Waals attraction. Long ranged attractive forces between hydrophobic surfaces have been reported in similar measurements (2, 22, 23). The proposed explanation in these cases was the following: on separation between surfaces a nano-bubble is formed which is capable of holding the surfaces together before they are finally being released. Taking into account that one of the surfaces in our study is hydrophobic, we propose that capillary bridging can also govern the attraction. Note that bridging can occur only if the hydrophilic surface has a non-zero contact angle. Previously we have measured the contact angle at silica (8); it is small but definitely non-zero ($\sim 8^\circ$).

If the origin of the attraction is bubble formation on the hydrophobic surfaces then this attraction is expected to disappear in the presence of adsorbing polymer. Indeed, only repulsive interactions are observed when the surfaces coming into contact in the solution of F127 (Fig. 6). This is not surprising, keeping in mind that the adsorbed F127 renders the hydrophobic silica more hydrophilic, thus suppressing bubble formation, while the degree of hydrophilicity of the hydrophilic surface changes only slightly.

The long ranged repulsive force, observed in the presence of polymer (fig.6), can be explained by electrostatic repulsion between surfaces. In agreement with electrostatics, the repulsive forces are suppressed upon increasing the salt concentration (fig.7a). This is similar to the profiles of interaction between hydrophilic surfaces (fig. 3a).

It seems likely that bridging between surfaces in the solution of polymer also plays a role when increasing the concentration of electrolyte. Upon increasing the concentration of NaCl more and more molecules of F127 adsorbed at hydrophilic silica will detach from the surface, leaving some “free” sites for attachments of molecules from the hydrophobic surface. Upon approaching the surfaces, the PEO-moiety of F127 from the hydrophobic surface can then bridge with the hydrophilic surface. Upon increasing the concentration of electrolyte, binding of PEO at the silica surface becomes progressively weaker, and so does the repulsion (which is essentially due to trapping of polymer between surfaces). Meanwhile, the bridging force (which requires accessibility of the hydrophilic surface) increases.

In line with the bridging phenomenon, increasing hysteresis in the interaction profiles between *phil/phob* surfaces was observed in the solution of polymer upon increasing the salt concentration (fig. 8). Hysteresis is indeed more pronounced between *phil/phob* surfaces as compared to that of *phil/phil* ones. Finally, we note that at sufficiently high salt concentration (1M), the PEO bridging affinity on silica becomes so weak, that the bridging force vanishes again. This is also borne out by the data in fig. 7.

5 Conclusions

We have measured interaction forces between two hydrophilic silica surfaces, and hydrophilic and hydrophobized silica surfaces immersed in aqueous solutions of Pluronic F127 surfactant. Attraction

occurs between a hydrophobic and a hydrophilic surface in water, which most likely due to capillary bridges. Purely repulsive interactions are measured between all pairs of surfaces immersed in salt-free solution of surfactant. This repulsion is attributed partly to the action of electrostatic double layer forces (long ranged) and partly to steric forces (short ranged). Upon increasing the concentration of electrolyte the repulsive force becomes less pronounced. The decrease in the repulsion is primarily attributed to the suppression of double-layer repulsion and emerging polymer bridging. An attractive force is measured between a hydrophilic and a hydrophobic surfaces immersed in aqueous solution of F127 in the presence of 0.1 M NaCl. It is very likely that bridging rules this attraction. There is a slight hysteresis in the interactions between hydrophilic surfaces, immersed in the solution of surfactant, which becomes more pronounced for the case of hydrophilic plus hydrophobic surfaces. This effect was also attributed to polymer bridging. The present work supports our previous results on wetting films stabilized by F127, where bridging attraction was also proposed as interpretation, in order to account for extremely slow drainage effects (see chapter 5).

References

1. P. Luckham, *Advances in Colloid and Interface Science* **11**, 29 - 47 (2004).
2. M. Musoke, P. Luckham, *Jornal of Colloid and Interfaces Science* **277**, 62-70 (2004).
3. S. C. McLean, H. Lioe, L. Meagher, V. S. J. Craig, M. L. Gee, *Langmuir* **21**, 2199-2208 (2005).
4. G. Binnig, C. F. Quate, C. Gerber, *Phys. Rev. Lett.* **56**, 930 (1986).
5. M. Giesbers, J. M. Kleijn, G. J. Fleer, M. A. Cohen Stuart, *Colloid and Surfaces A:Physicochem.Eng. Aspects* **142**, 343 (1998).
6. M. Giesbers, Wageningen University (2001).
7. O. V. Eliseeva, R. G. Fokkink, N. A. M. Besseling, L. K. Koopal, M. A. Cohen Stuart, *accepted for publication in J. Colloid Interface Sci.* (2006).
8. O. V. Eliseeva, N. A. M. Besseling, L. K. Koopal, M. A. Cohen Stuart, *submitted to CCA*.
9. M. Maccarini, M. Himmelhaus, S. Stoycheva, M. Grunze, *Applied Surface Science* **252**, 1941-1946 (2005).
10. H. J. Butt, *Biophys. J.* **60**, 1438 (1991).
11. W. A. Ducker, T. J. Senden, R. M. Pashley, *Nature (Lond.)* **353**, 239 (1991).
12. M. Gisbers, Wageningen (2001).
13. W. K. Wijting, W. Knoben, N. A. M. Besseling, F. Leermakers, M. A. Cohen Stuart, *Phys. Chem. Chem. Phys.* **1**, 1-9 (2004).
14. S. Partuka, S. Zaini, M. Lindeheimer, B. Bruin, *Colloid and Surfaces* **12**, 255-270 (1984).
15. T. Van Den Boomgaard, T. F. Tadros, J. Lyklema, *Journal of Colloid and Interface Science* **116**, 8-16 (1986).
16. M. Malmsten, P. Linse, T. Cosgrove, *Macromolecules*, 2474-2481 (1992).
17. F. Tiberg, University of Lund (1994).
18. R. Sedev, *Colloids and Surfaces* **156**, 65-70 (1999).
19. R. Sedev, R. Steitz, G. H. Findenegg, *Physica B* **315**, 267-272 (2002).
20. O. V. Eliseeva, N. A. M. Besseling, L. K. Koopal, M. A. Cohen Stuart, *Langmuir* **21**, 4954-4963 (2005).
21. *not published* (our experimental data).
22. P. Attard, J. L. Parker, P. M. Claesson, *J. Phys. Chem.* **98**, 8468 (1994).
23. J. Wood, R. Sharma, *Langmuir* **11**, 4797 (1994).

Summary

Thin aqueous films formed on a solid surface play an important role in adhesion, spreading, and colloidal stability. These phenomena are all relevant for paint systems. Measuring surface forces in these films is an experimental challenge, and over the years several techniques have been developed to measure the interaction forces as a function of the thickness of the film, the so-called disjoining pressure isotherms. A thin film balance technique (TFB) in combination with an ellipsometer offers the possibility to study the surface forces in aqueous films formed at a silica surface.

The aim of this project was twofold. Firstly, we wanted to set up the technique and test it by investigating interaction forces in thin aqueous films formed between an air interface and a solid interface (air/aqueous film/silica). Secondly, we intended to apply this technique for investigating interaction forces in aqueous films formed between an oil interface and a solid interface (oil/ aqueous film/ silica). As happens so often in research, we were ‘immersed’ in the first system, and as a result of it, we did not reach the second aim. Hence, this thesis deals with the experimental investigations of the interaction forces in thin aqueous films formed between an air phase and a solid phase. A non-ionic polymeric surfactant is used as a stabilizer of these films. In addition, we have also used colloidal probe atomic force microscopy (CP-AFM) in order to see if phenomena similar to those in wetting films might occur in the interactions between two silica surfaces, immersed in solutions of the surfactant.

In **chapter 1** an introduction is given to wetting films, to the surfactant used and to the technique used in the present study. A short overview of the interaction forces in wetting films and the drainage of these films is presented. As foam films, which are aqueous films between two air phases (air/ aqueous film/ air), have much more extensively been studied than wetting films, we also discussed drainage of foam films, and an interesting finding in foam films stabilized by similar surfactants.

In **chapter 2** the solution behaviour of the surfactant and its adsorption on silica-water and air-water interfaces is studied using light scattering, surface tensiometry and ellipsometry. Interaction forces in wetting films stabilized by the surfactant are measured and are interpreted in terms of a disjoining pressure as a function of a thickness of the film. Parameters of the systems are the concentration of the surfactant and the concentration of NaCl. The main findings are that addition of NaCl lowers the cmc, diminishes adsorption of the surfactant on silica, and increases the thickness of the wetting film stabilized by the surfactant.

In **chapter 3** we investigate the thinning of wetting films formed from aqueous solution of the surfactant on silica using a TFB and an ellipsometer. In addition, imaging ellipsometry is used to visualize the film structures at subsequent stages of their development. The main findings are that the thick films observed in chapter 2 are metastable. The time required for the formation of steady films strongly increases with the concentration of electrolyte. For sufficiently large amounts of salt, two characteristic relaxation regimes can be clearly identified: after initial quick thinning, further thinning slows down enormously. The

interpretation we give of the observed features is that these typical kinetic regimes are the result of coupled dependencies of the bulk and interfacial properties of the surfactant on salt concentration.

In **chapter 4** the time-dependent thickness of wetting films formed from aqueous solutions of NaCl on a silica surface modified with the surfactant is revisited, because of a rather surprising finding: the thickness as a function of time could go through a maximum. It turned out that the thickness of the films depends strongly on whether or not the surfactant was applied over the entire substrate or only at a spot coinciding with the investigated wetting film. In the former case, the thickness shows a transient thickness maximum, in the latter case, it equilibrates quickly. A possible interpretation of the transient thicknesses is given, and the equilibrium values of the thickness are discussed.

In **chapter 5** the effects of pH and different additives (NaCl, Na₂SO₄, NaSCN and urea) on the adsorption of the surfactant at the interfaces of wetting films, on film drainage and on the interaction forces in these films are examined using an ellipsometer and a TFB. These additives reduce the adsorption of the surfactant on silica and all retard the drainage of the films stabilized by the surfactant. Moreover, the film destabilizes at high pH values if 0.1 M NaCl is present. The reduction of the adsorbed amount is correlated to a dramatic slow down of film drainage. We conclude that these effects must be attributed to bridging attraction between a densely covered air-water interface and a very sparsely covered silica-water interface.

In **chapter 6** the interactions between two silica surfaces, immersed in solutions of the surfactant is studied by CP-AFM. The main findings are that (i) there are long ranged attractive forces between bare hydrophobic and hydrophilic surfaces in aqueous solution; and that (ii) a weak adhesion occurs between a hydrophobic and a hydrophilic surface in the presence of the surfactant in 0.1 M NaCl. Results (i) can be attributed to capillary bridging and (ii) to bridging of the polymeric surfactant between a densely covered hydrophobic surface and a sparsely covered hydrophilic surface, thus confirming the effect found in chapter 5.

Samenvatting

Dit proefschrift gaat over waterige bevochtigingsfilms die door triblock-copolymeer gestabiliseerd worden. De krachten in de films en de drainage van de films worden via de dunne-film-balans techniek in combinatie met de ellipsometer gemeten.

In hoofdstuk een wordt een inleiding gegeven over bevochtigingsfilms en waarom ze belangrijk zijn om te bestuderen. Vervolgens gaat dit hoofdstuk over de niet-ionogene surfactants (triblock copolymers) die in dit proefschrift worden gebruikt. Verder worden de krachten die een rol spelen in bevochtigingsfilms besproken. De drainage van de bevochtigingsfilms wordt vergeleken met de drainage van schuimfilms.

In hoofdstuk twee worden metingen van het gedrag van het triblock-copolymeer (Pluronic F-127) in waterige oplossing, aan lucht-water en aan silica-water grensvlakken, en in de bevochtigingsfilms gepresenteerd. Een onverwacht effect van zout op dunne films die gestabiliseerd worden door niet-ionogene surfactants is gevonden. In sommige gevallen is de dikte van de films groter dan was verwacht.

In hoofdstuk drie wordt de drainage beschreven van bevochtigingsfilms die gestabiliseerd worden door de bovengenoemde polymeren. Wij hebben gevonden dat de tijd die nodig is om stabiele films te krijgen afhangt van de zoutconcentratie. Wij concluderen dat de dikke films die in hoofdstuk twee gepresenteerd werden, metastabiel zijn.

In hoofdstuk vier is de drainage van waterige films gevormd op met triblock-copolymeer bedekte silica onderzocht. De dikte van de films als de functie van de tijd bleek soms via een maximum gaan. De verklaring van het verschijnsel is besproken.

In hoofdstuk vijf kijken wij naar de gevolgen van de pH en de additieven op i) de adsorptie van de triblock copolymers aan de lucht-water en silica-water grensvlakken van de bevochtigingsfilms, ii) de krachten in de films en iii) de drainage van de films. Brugvorming door triblock-copolymeer tussen de lucht-water en silica-water grensvlakken is voorgesteld als verklaring voor vertraagde drainage.

In hoofdstuk zes werd brugvorming tussen een silica deeltje en een silica oppervlak onderzocht met AFM. Zowel in waterige oplossingen zonder het triblock-copolymeer als in aanwezigheid van het polymeer en 0.1 M NaCl werd aantrekkingskracht tussen een hydrofoob en een hydrofiel oppervlak gemeten.

Краткое содержание для всех

Книжка, которую вы держите в руке, посвящена тоненьким, тонюсеньким, тончайшим **пленочкам**.

Вы, читатель, наверняка играли в детстве (а может и до сих пор играете!) с мыльными пузырями (рисунки 1 и 2).



Рисунок 1. Мыльный пузырь.



Рисунок 2. Девочка-эльф на мыльном пузыре.

Мыльный пузырь – это шарик (а точнее сфера!), образованный тонкой, тоненькой, тонюсенькой, тончайшей **пленочкой** жидкости и заполненный воздухом (газом), и снаружи также окруженный воздухом. Толщина этой **пленочки** ну очень, очень маленькая (где-то между несколькими нано- и микрометрами, а это 10^{-9} - 10^{-6} метра). Следовательно, **пленочка** эта очень легко рвется (ведь где тонко, там и .. рвется)! Сами видели, как пузырьки быстро лопаются! Состоит такая **пленочка** из слоя воды окруженного двумя слоями специфических молекул (*поверхностно-активных веществ*) (рисунки 3).

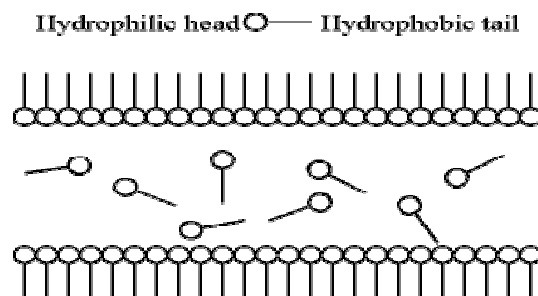


Рисунок 3. Состав мыльной пленочки.

Важный вопрос: где можно встретить **тоненькие пленочки**? Ответ: в любой коллоидной системе, когда две частички этой системы подходят очень близко друг к другу (расстояние между частичками = толщине **пленочки**). Для любопытных – определение *коллоидной системы*, а так же и *коллоидной химии* (область химии, в которой специализировался автор этой книжечки, написано в самом низу!). Следовательно, тонкие **пленочки** можно найти *в крови, в пиве, шампанском, красках, чернилах, мыльных растворах и так далее*. “Тонкие **пленки** имеют важное значение для зарождения и существования жизни!! Их специфические физико-химические свойства играют решающую роль во многих биологических процессах. Например, *биологические мембраны* (Рисунок 4) можно рассматривать, как **тонкие пленочки** сложной структуры.

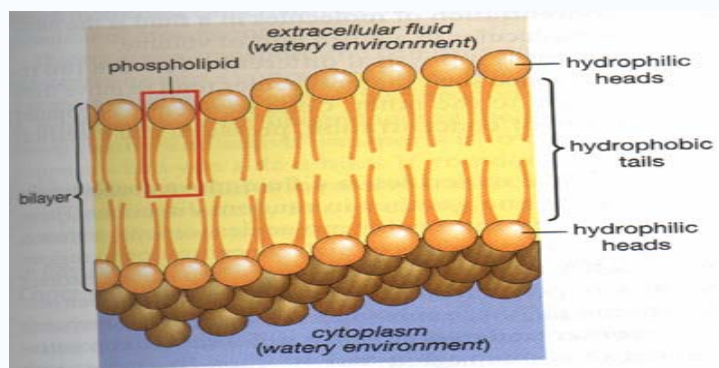


Рисунок 4. Биологическая мембрана

Другими типичными примерами являются *слезные пленки, альвеолярный выстилающий слой, смачивающие пленки в биомеханических суставах, жидкие пленки между клетками* и т. д. “Итак, измерением толщин **тоненьких, тонюсеньких, тончайших пленочках**, а так же измерением сил в этих **пленочках** занимался автор. Маленькая деталь: **пленки** формировали на твердой поверхности стекла {а точнее оксида силикона (SiO_2)!}. Жидкость, из которой образовывалась пленка, хорошо смачивала поверхность, отсюда и название: **смачивающая пленка**. ‘Наша’ **пленочка** на поверхности стекла {а точнее оксид силикона (SiO_2)!} показана на рисунке 5.



Рисунок 5. Смачивающая пленка изучаемая в данной книжке.

Устойчивость **смачивающих пленочек** имеет важное значение, например, для флотации {Флотация (франц.) это способ обогащения руд полезных ископаемых, основанный на различной смачиваемости частиц рудных минералов (полезного ископаемого) и пустой породы}.

Другое применение, из которого берет начало эта книжка (!), это краски и их промышленность. Нам уже понятно (!), что краска это очень сложная система (*дисперсная*), состоящая из пигментов (*дисперсная фаза*), особого вещества (*связующего*), различных добавок и растворителя (*дисперсионная среда*). Главные вопросы в красочной промышленности – это стабильность такой системе и формирование пленок (здесь уже не пленочек!!) на твердой поверхности. А стабильность такой системы (а именно, краски в банке) зависит от стабильности опять-таки **тонких пленочек**, разделяющих маленькие-малюсенькие {опять-таки от микро- до нано-метров (10^{-6} - 10^{-9} метра)} частички (*дисперсионные*), находящиеся внутри краски. Итак, изучение устойчивости таких **тоненьких смачивающих пленочек** – очень, очень важно (!).

Смачивающая пленочка, изучаемая в данной книжке, состояла из растворенного в воде **полимера**, обладающего специфическими, интересными свойствами (одна часть полимера “любит” воду, а другая – “не любит”). А что такое полимер написано в самом низу этой главы! Было интересно узнать (и мы кое-что узнали!), как этот полимер ведет себя на поверхности вода-воздух, стекло-воздух, а так же в наших **тонких пленочках**. Мы меняли концентрацию полимера, различных солей, и pH. Интересно было узнать при каких условиях **пленочка** рвется {(при увеличении pH в присутствии соли (см. главу 2) + некоторые специфические случаи главы 4)}, а при каких – нет {во всех остальных задаваемых условиях (см. главы 2, 3, 4, 5)}. Основными исследовательскими игрушками были 1) прибор для формирования тонкой пленки (специальная ячейка с пористым диском) и 2) прибор для измерения тонкой пленочки (элипсометр). А самой интересной игрушкой для меня был 3) атомный силовой микроскоп. С помощью этого микроскопа можно 1) увеличивать маленькие поверхности и видеть их фото (!!) на компьютере, 2) а так же измерять силы между мельчайшими частичками (размером от микро- до нанометров!!). Последняя глава 6 этой книжки посвящена измерению сил взаимодействия между микро-частичкой и поверхностью силики в растворе изучаемого полимера с помощью атомного силового микроскопа.

Сделали ли мы интересные, великие открытия?? Великие – конечно, нет, а интересные для нас, маленькие открытия в узкой пленочной области – да!!

Некоторые определения слов и терминов:

Коллоидная химия возникла в середине XIX века. В 1861 г. известный английский химик Т. Грэм изучал диффузию различных веществ в водных растворах. Он обнаружил, что некоторые вещества (желатин, агар-агар и т.п.) диффундируют в воде во много раз медленнее, чем, например, соли и кислоты. Кроме того, эти вещества при пересыщении растворов не кристаллизовались, а формировали студнеобразную клейкую массу. *По-древнегречески клей называется "колла", и эти "особые" вещества Грэм назвал "коллоидами"*. Так появилось название науки - коллоидная химия.

Дисперсная система - это смесь, состоящая из минимум двух веществ, которые совершенно или практически не смешиваются друг с другом и не реагируют друг с другом химически. Первое из веществ (**дисперсная фаза**) мелко распределено во втором (**дисперсионная среда, диспергатор**). Фазы можно отделить друг от друга физическим способом (центрифугировать, сепарировать). Обычно дисперсные системы - это коллоидные растворы, золи.

Виды дисперсных систем. В зависимости от агрегатного состояния обеих фаз различают следующие виды дисперсий:

Вид	Диспергатор	Дисперсная фаза	Пример
Жидкий аэрозоль	газ	жидкость	туман
Твёрдый аэрозоль	газ	твёрдое тело	дым
Эмульсия	жидкость	жидкость	молоко, крем
Пена	жидкость	газ	пена
Гель	растворитель	макромолекулы	гель, клей
Ассоциированный коллоид	жидкость	агрегаты	мыло, краска
Биофлюид	жидкость	эритроцит	кровь
Биоколлоид	коллаген	апатит	кость

Полимер — это сложная большая молекула с большой молекулярной массой (от нескольких тысяч до нескольких миллионов), в которой атомы, соединенные химическими связями, образуют линейные или разветвленные цепи, а также пространственные трехмерные структуры. Часто в его строении можно выделить повторяющийся структурный фрагмент, включающий несколько атомов. К полимерам относятся *белки, нуклеиновые кислоты, полисахариды, каучук* и другие вещества.

Acknowledgements

The book is written. The work is done.
Natuurlijk heb ik het niet alleen gedaan.

I want to thank people, who were around, who supported, helped and cooperated with me during this 5 special years.

Klaas, thank you for the help, for the meetings and for the discussions of my work. You had always time for me in your schedule! Indeed, my English was (and still is..) not very perfect, but I hope you noticed that it progressively improved from day to day (or year to year).. **Luuk**, thanks for the intensive discussions of my results and for the Wednesday meetings. You were always willing to discuss and give some estimation of the results! And not always I had ‘a space’ to say something.. I want to thank my promoter - **Martien Cohen Stuart**. Martien, talks and discussions with you were always inspired me for the further work. You are incredibly quick in generating ideas and in understanding the main point of the problem! I learnt a lot from you! **Hans Lyklema**, I am happy that I had a chance to work with you. I did always enjoy our discussions, which were not only about science! Thank you for your encouragement advises and help! I hope that you, Petya and Marat will keep up with your Russian.

Jan Knuiman, thank you for the re-orientation back to chemistry, and your suggestion to do a PhD! **Remco**, without you my ellipsometrical measurements would never be so beautiful! Thank you very much! **Gert Buurman**, your drawings in my book are fully yours, eventhough they look like they are fully mine..! Thank you very much! **Ronald, Jansen, Petya, Marat**, thanks a lot for giving me PC support! My thanks to **Jan** and **Jan-William Benjamins** for ellipsometry and BAM. **Wout** and **Joris**, thanks a lot for helping me with a very special creature: so-called AFM! **Marcel Giesbers**, thank you for the beautiful explanation and help with attaching the micro-beestjes to the AFM cantilever. **Wouter**, thanks for providing me with the information about the bio-AFM! **Ilja, Wiebe, Saskia, Bart** and **Maarten**, it was super-nice with all of you in Berlin! **Pascal and Bas**, I enjoyed our ‘book’ discussions a lot! **Diane, Guido, Erika, Henk, Aernout**, it was always nice to have a chat with you! Good luck to each of you with your promotion! **Natalie, Mireille**, and **Renate**, it was gezellig (!!) with you in room K130! **Renate**, thanks a lot for your support (!!) and good luck with your promotion (30 is a nice number!)! **Wim**, bedankt voor je hulp met de “heксе” spullen en voor de gezellige praatjes! **Luuk** en **Els**, bedankt voor de gezellige dinnertjes in jullie huis. **Luben**, thanks for the experiments on foam stability and the AFM. Unfortunately, foam was not very stable.. **Jasper**, thanks for the tricks concerning the ellipsometrical cell and the tricks about finding a job! **Rene**, hartelijk bedankt voor de osmosis experimenten. Helaas heb ik ze niet gebruikt in mijn proefschrift.. **Geraard Fleer**, I always enjoyed the Friday meetings, thanks! **Frans**, thanks for your ideas and suggestion to do some calculations on my system! Unfortunately ‘your’ SF box still remains black to me.. **Richard**, my application letters should be beautiful now. Thanks! **Anita**, thanks for your help with tricky issues (money, money, money.. IND, and some others)! **William Noorde**, thanks for providing me with the information about the bio-labs! **Anneke** en **Roda**, bedankt voor mijn stralende kamertje and voor de gezellige praatjes! **Bert**, bedankt voor je hulp met de leesversie! **Willy**, thanks for the quick delivering me to the Gelderse Vallei once. **Yun Yan**, thanks for the nice chats and for the Chinese dinners! I wish that your dreams would come true one day (preferably very soon!!)!

FYSCO crew, thanks for the nice atmosphere! I will miss you..

Dick Legger, thank you for proposing the MSc study, eventhough it was not perfectly suitable for me! I am still here in Holland and happy with my “old love” – chemistry! **Carla Haenen**, thanks a lot for your help with a lot of things in quite a difficult time for me. Dear **Jane**, your adventurous spirit helps me to challenge my life. Thank you and good luck with your beautiful English course!! **Anna and Christophe**,

thank you for your help in the special time. I wish you will catch the light and keep this light in your arms among French mountains! **Krisztina**, thanks a lot for cheering me up in some moments and for the fun we had together!! Good luck with your promotion, your new life in Rotterdam and your new work! **Rink** of the lord (or lord of the rinks..), thanks for the nice chats we had! Good luck with your future! **Hafida**, bedankt voor de oppas met mijn kleintje! Succes in je toekomst in alle richtingen!! **Paola**, bijzonder veel dank aan jou! Jij hebt een ‘groot’ hart! Bedankt voor alles!! **Radhika**, thank you very much for your help! You, like not many people, can simply feel the life.. Thanks a lot! I wish you a beautiful life in Rotterdam!! **Erik** en **Bernadette**, hartelijk bedankt voor de leuke tijden, die Angelika en ik bij jullie hebben gehad! Thanks for your support. **Daisy**, **Bernado**, **Karoly**, **Tamas**, thanks for the nice time and fun we had together! I wish each of you good luck with your promotion and strength in your future!! **Petra**, bedankt voor de oppas en de gezellige tijden. Kleine **Richard**, bedankt voor de leuke spelletjes met mijn kleine droppeltje!! **Denisse**, I believe that difficulties are temporary: one day they will end, and beautiful times will take their place..!

Dear **Katka**, your help was unbeatable! You gave me your hands and support in the time I needed it the most.. Besides, we had a lot of fun together! Thank you very much!! I wish you pure happiness in your life! **Josie**, your cheerful and strong personality can make everyone stronger! Your love towards people is amazing. Thanks for the support, for the will to listen, for cheering me up, and, of course, for the English support. You are indeed a FYSCO queen!! One day you must be crowned..! I wish you will be cautious with your energy supply and that you will always have beautiful people around!! My next flat/house will definitely have a lift!

Ellen and Ton, you are very unique to me.. Thank you millions of times for the support, for the hospitality, for the fun we had, for the moment I have met you and for your love. You were like my family in this country. Thank you and I am wishing you only happiness, joy and a beautiful life in your houses!!

Ханс, так помогают только настоящие друзья! Спасибо за Вашу помощь! Здоровья и силы Вам!

Марина, спасибо за выходные с моей малышкой и за болтовню. **Петька**, спасибо за твою помощь и готовность всегда помочь! “Двойная” защита должна обязательно состояться! Обязательно!!

Марат, спасибо за помощь с компьютером, с компьютерным телефоном и моей обложкой!! Спасибо!! Будь героем на своей защите! **Сашка**, успехов тебе в Вахенингене! **Лия**, желаю тебе веселой жизни в голландской деревеньке и уверена, что скоро ты будешь учить маму и папу голландскому (хи-хи..)! Доктор **Ленка Шурова**, **Галина Денискина**, **Витька Урываев**, **Сашка Любин**, **Ольга Гафонова**, доктор **Ольга Купцова**, спасибо за веселые разговоры и письма!!

Лолочка, спасибо за рассказы о твоих приключениях. Самые интересные еще впереди!!

Катька, спасибо что ты “болела” за меня. Будь сильной: мальчишкам нужна сильная мама!

Оксанка, ты моя “наистарейшая” подруга. Спасибо, что ты у меня есть, и что ты в моей команде. Пора тебе ко мне приехать вместе с Вовкой и детенышами!

Евгения Павловна, Ваши письма всегда давали и дают мне “пищу” к размышлениям. Спасибо за письма, за поддержку, за виртуальные разговоры, за обмен мнениями, за Ваше понимание! Желаю Вам красоты и интересной жизни в далекой-далекой американской стороне! Не знаю почему, но мне кажется, что мы с Вами обязательно увидимся!

Лариса Аркадьевна, спасибо за Ваши письма и за то, что я Вас знаю. Я уверена что Лешке бы понравилось, что мы общаемся... Эту книжку я посвящаю ему. Он, когда-то давным-давно, привел меня в Универ. **Лешка**, спасибо тебе..

Алексей Митрофанович, мой спортивный отец, спасибо Вам за мой характер, за поддержку и за Ваше неугасаемое чувство юмора! Таблетки от головной боли уже на подходе к Вам..А может все-таки йог?

Таня, спасибо Вам за Вашу поддержку. Ваши советы и разговоры “спасали” меня миллион раз. Вы понимали и знали ситуацию, как никто другой. Спасибо огромное!! Желаю, чтобы судьба Вам чаще улыбалась и удивляла только хорошими сюрпризами!

Светка, твой боевой и геройский дух всегда держал меня в ‘спортивной’ форме. Спасибо за твою поддержку, за то, что ты такая и не другая. Очень горжусь дружбой с тобой, и желаю тебе, наконец познакомиться с тем чего хочешь (пора мой друг пора..)!

Иринка Веселовская - моя “старая” подружка – спасибо тебе за твое понимание. Ты одна из тех, которым не надо все объяснять. Все понимаешь с полуслова.. Ты даже чувствуешь, когда надо пропасть, а когда вновь объявиться (хи-хи)..Энергии и радости тебе в твоём уютном доме и с твоей любимой игрушкой - наукой! **Степка Николаевич**, не прошло и сто лет, как Гордейкина закончила учиться.. Спасибо за уроки английского когда-то сто лет назад (помнишь??), на лавочке у Макдоналдса!

Леночка, Андрюшка, Машунька, Евгений и Аленчик, спасибо Вам за то, что вы есть. Именно здесь, в Европейской, уютной, плоской и гладко-причесанной стране я почувствовала, как безумно важна семья...Наверное, только ради этого чувства стоило так далеко заехать..Целую, обнимаю и люблю вас всех!

Мамочка и папочка, ваша любовь может сдвинуть горы.. Вы так в меня верите, и так меня любите, что мне ничего не остается, как просто двигаться вперед по накатанной дорожке любви. Вы вместе – это тот фундамент, на котором я держусь.. Спасибо за вашу веру и за вашу любовь!! Вы – самые лучшие родители в мире!

Анжеличка, ты мой маленький и самый любимый человечек в этом мире, милая, добрая и чистая капелька жизни. С твоим появлением вся моя жизнь перевернулась и помчалась в новом, но очень интересном направлении. Я так мало уделяю тебе времени, и знаю, как ты ждешь меня (очень, очень сильно!!)..Обещаю проводить с тобой больше времени (все, эта книжка написана!), потому что я тебе должна еще столько рассказать и показать, а может и научить, и просто, потому что с тобой безумно интересно!

Ольга Июль 2006

List of publications

1. Abramov, A.A., Elisseeva, O.V., Iofa, B.Z. *Prognosis of physical-chemical constants of francium, radium, and actinium. **Radiochemistry**, 1998 (40), 4, 292-295 (in Russian).*
2. Abramov, A.A. Elisseeva, O.V. Volkova, S.V. *The role of temperature upon suppression of extraction of one metal by the others. **Vestnik of MSU**, 2000(2) (chemistry), 41, 3, 212-214 (in Russian).*
3. Elisseeva, O.V., Besseling, N.A.M., Koopal, L.K., Cohen Stuart, M. A. *Influence of NaCl on the behavior of PEO-PPO-PEO triblock copolymers in solution, at interfaces, and in asymmetric liquid film,. **Langmuir**, 2005, 21, 4954-4963.*
4. Elisseeva, O.V., Fokkink, R.G., Besseling, N.A.M., Koopal, L.K., Cohen Stuart, M. A. *Thinning of wetting films formed from aqueous solutions of non-ionic surfactant. **JCIS**, 2006, 301, 210-216.*
5. Elisseeva, O.V. Besseling, N.A.M., Koopal, L.K., Cohen Stuart, M.A. *Effects of pH and additives in aqueous wetting films stabilized by a triblock copolymer. **submitted to CCA**, June 2006*
6. Elisseeva, O.V, Besseling, N.A.M., Koopal, L.K., Cohen Stuart, M. A.. *Interaction forces between surfaces immersed in solutions of a polyethylene oxide-polypropylene oxide copolymer. **to be submitted**.*

Curriculum vitae

Olga Eliseeva was born the 7th August 1971 in Niesjnie Tagil, a big industrial city in Russia. In September 1991 she started studying chemistry at the Moscow State University. In June 1996, she obtained her diploma as a chemical engineer. In August 2000 she arrived in the Netherlands where she has remained until now. Since April 1 2001 until October 1 2006 she was a PhD student in the laboratory of Physical Chemistry and Colloid Science of Wageningen University. The results of her PhD research are presented in this book.

Printed by Universal Press-Veennendaal